ib

Revista Mexicana de Ingeniería Biomédica

Modalidad de publicación

Publicación continua:
una vez que se acepta y prepara un
manuscrito, se publicará en línea

Publication Modality

Continuous publication:
once a manuscript is accepted and
prepared, it will be released online

Sociedad Mexicana de Ingeniería Biomédica

La Mesa Directiva de la Sociedad Mexicana de Ingeniería Biomédica hace una extensa invitación a las personas interesadas en participar, colaborar y pertenecer como Socio Activo de la SOMIB. La SOMIB reúne a profesionistas que se desarrollan en áreas de Ingeniería Biomédica, principalmente ingenieros biomédicos, así como otros profesionistas afines con el desarrollo de tecnología para la salud.

Membresía Estudiante
$1,400.00 *PESOS MXN*
15% de descuento para grupos de 5 o más personas.

Membresía Profesionista
$2,400.00 *PESOS MXN*
15% de descuento para grupos de 5 o más personas.

Membresía Institucional
$11,600.00 *PESOS MXN*
No aplica descuento.

Membresía Empresarial
$20,000.00 *PESOS MXN*
No aplica descuento.

EL PAGO CUBRE UN AÑO DE CUOTA. EN CASO DE REQUERIR FACTURA
FAVOR DE SOLICITARLA, ADJUNTANDO COMPROBANTE DE PAGO Y ESPECIFICANDO CONCEPTO,
AL CORREO ELECTRÓNICO: *gerencia@somib.org.mx*

Para ser socio

› Realiza el pago de derechos, de acuerdo a la categoría que te corresponde.

› Ingresa a *www.somib.org.mx/ membresias* y elige el tipo de membresía por el cual realizaste el pago de derechos.

› Completa el formulario correspondiente y envíalo.

› Se emitirá carta de aceptación y número de socio por parte de la mesa directiva (aprobada la solicitud).

› Para mayor información sobre beneficios, ingresa a *www.somib.org.mx*; o escribe a *gerencia@somib.org.mx.*

Datos bancarios

› **Beneficiario:** *Sociedad Mexicana de Ingeniería Biomédica A. C.*

› **Banco:** *Scotiabank*

› **Referencia:** *1000000333*

› **Cuenta:** *11006665861*

› **CLABE Interbancaria:** *044770110066658614*

AUTORES

Los trabajos a publicar en la RMIB, deben ser originales, inéditos y de excelencia. Los costos de publicación para autores son los siguientes:

NO SOCIOS:	**$5,000** *PESOS MEXICANOS*
SOCIOS:	**$4,000** *PESOS MEXICANOS*

PUBLICIDAD

A las empresas e instituciones interesadas en publicitar su marca o productos en la RMIB, los costos por número son los siguientes:

MEDIA PLANA:	**$4,999.00** *PESOS MXN (INCLUYE I.V.A.)*
UNA PLANA:	**$6,799.00** *PESOS MXN (INCLUYE I.V.A.)*
CONTRAPORTADA:	**$7,799.00** *PESOS MXN (INCLUYE I.V.A.)*
FORROS INTERIORES:	**$7,799.00** *PESOS MXN (INCLUYE I.V.A.)*

DESCUENTO DEL **20%** AL CONTRATAR PUBLICIDAD EN DOS O MÁS NÚMEROS.

INFORMES

Juan Vázquez de Mella #481,
Polanco I Sección,
Alc. Miguel Hidalgo, C. P. 11510,
Ciudad de México, México,
(555) 574-4505
rib.somib@gmail.com

Revista Mexicana de Ingeniería Biomédica

MESA DIRECTIVA

Dra. Norma Patricia Puente Ramírez

PRESIDENTA

Mtro. Edgar Del Hierro

VICEPRESIDENTE

Ing. Christopher Bricio

TESORERO

Mtro. David Palomo

SECRETARÍA GENERAL

Dra. Dora-Luz Flores

EDITORA EN JEFE DE RMIB

Afiliada a:

International Federation of Medical and Biological Engineering (IFMB-IUPSM-ICSU)

Federación de Sociedades Científicas de México, A.C. (FESOCIME)

Consejo Regional de Ingeniería Biomédica para América Latina (CORAL)

SOMIB

Juan Vázquez de Mella #481, Polanco I Sección, Alc. Miguel Hidalgo, C. P. 11510, Ciudad de México, México (555) 574-4505

www.somib.org.mx

Disponible en línea:

www.rmib.mx

CONTENTS
CONTENIDO

Preventive Detection of Driver Drowsiness from EEG Signals using Fuzzy Expert Systems

Detección Preventiva de la Somnolencia del Conductor a partir de Señales EEG Mediante Sistemas Expertos Difusos

Análisis Matemático no Lineal Relacionado a un Modelo de Insulina-Células Pancreáticas en Presencia de Epinefrina

Nonlinear Mathematical Analysis based on an Insulin-Pancreatic Cells Model in the Presence of Epinephrine

Study of the Length of time Window in Emotion Recognition based on EEG Signals

Estudio de la Longitud de Ventana de Tiempo en el Reconocimiento de Emociones Basado en Señales EEG

Use of Biomedical Engineering for Rehabilitation of Patients with Disability Caused by Guillain-Barré Syndrome: a Systematic Review

Uso de la Ingeniería Biomédica para Rehabilitación de Pacientes con Discapacidad Causada por el Síndrome de Guillain-Barré: Una Revisión Sistemática

Preventive Detection of Driver Drowsiness from EEG Signals using Fuzzy Expert Systems

Detección Preventiva de la Somnolencia del Conductor a partir de Señales EEG Mediante Sistemas Expertos Difusos

Rony Almirón[1] , Bruno Adolfo Castillo[1] , Andrés Montoya Angulo[1] , Elvis Supo[1] ,
Jesús José Fortunato Talavera Suarez[1] , Daniel Domingo Yanyachi Aco Cardenas[1] .

[1]Universidad Nacional de San Agustín de Arequipa - Perú

ABSTRACT

Currently, the percentage of traffic accidents has increased, and according to statistics, this percentage will continue to increase every year, so it is necessary to develop new technologies to prevent this kind of accidents. This paper presents a drowsiness detection system based on electroencephalogram (EEG) signals using a pair of channels (Fp1 and Fp2) applied to drivers before entering their vehicles. First, this model detects the relationship between the area under the curve (AUC) of alpha brain waves, an effective parameter for detecting drowsiness. Then, the extracted information is passed to a fuzzy expert system (FES) that classifies the subject's state as "alert" or "sleepy"; the criterion used was a threshold and training with subjective levels. The proposed system was compared with neural network models, such as support vector machine (SVM), K nearest neighbors (KNN), and random forest (RF). Measurements of one hundred and twenty minutes were performed on each of the ten drivers for two days to test the system. The tests confirm that this system is suitable for preventive measures and that the fuzzy system is superior to traditional neural network methods.

KEYWORDS: drive drowsiness, electroencephalogram, expert systems, sleepiness detection

RESUMEN

Actualmente, el porcentaje de accidentes de tráfico ha aumentado, y según las estadísticas, este porcentaje seguirá aumentando cada año, por lo que es necesario desarrollar nuevas tecnologías para prevenir este tipo de accidentes. Este trabajo presenta un sistema de detección de somnolencia basado en señales de electroencefalograma (EEG) utilizando un par de canales (Fp1 y Fp2) aplicado a los conductores antes de entrar en sus vehículos. En primer lugar, este modelo detecta la relación entre el área bajo la curva (AUC) de las ondas cerebrales alfa, un parámetro eficaz para detectar la somnolencia. A continuación, la información extraída se pasa a un sistema experto difuso (FES) que clasifica el estado del sujeto como "alerta" o "somnoliento"; el criterio utilizado fue un umbral y el entrenamiento con niveles subjetivos. El sistema propuesto se comparó con modelos de redes neuronales, como la máquina de vectores de soporte (SVM), K vecinos más cercanos (KNN) y el bosque aleatorio (RF). Se realizaron mediciones de ciento veinte minutos en cada uno de los diez conductores durante dos días para probar el sistema. Las pruebas confirman que este sistema es adecuado para las medidas preventivas y que el sistema difuso es superior a los métodos tradicionales de redes neuronales.

PALABRAS CLAVE: electroencefalograma, detección de somnolencia, sistemas expertos, somnolencia en la conducción

Corresponding author

TO: Rony Almirón

INSTITUTION: Universidad Nacional de San Agustín de Arequipa

ADDRESS: Santa Catalina 117, Arequipa, Arequipa, Perú.

CORREO ELECTRÓNICO: ralmirona@unsa.edu.pe

INTRODUCTION

According to data provided by the World Health Organization (WHO) in the Report on the Global Situation of Road Safety 2018, the number of deaths due to traffic accidents amounted to 1.35 million, being the leading cause of death among people aged 5 - 29 years (more than 300,000 deaths), and the eighth leading cause of death for all age groups[1]. According to the World Report on the Prevention of Injuries Caused by Traffic of the Pan American Health Organization (PAHO) for the year 2020, if road safety actions are not taken, deaths caused by traffic will rise worldwide to 2.34 million, representing 3.4 % of all deaths and road traffic injuries will rank sixth on the list of leading causes of death in the world and third on the list of causes of loss of physical abilities[2].

In Peru, the National Institute of Statistics and Informatics (INEI, by its acronym in Spanish) registered 2,826 fatal victims of traffic accidents in 2017, with more than 2,487 homicide victims[3]. In addition, INEI recorded 174 fatal accidents in the department of Arequipa in the same year and 188 accidents in 2018[3]. Recently, Dr. Helmer Huerta, a public health specialist, wrote that the statistics from the Ministry of Transport and Communications (MTC) of Peru revealed that, after a record of 3,531 deaths on the roads in 2011, 2,965 deaths had been registered in the 2015 and 3,245 deaths in 2018[4]. That is, nine Peruvians die daily in a traffic accident, having one of the highest mortality rates from road accidents in the region, a rate of 10.1 out of every 100,000 inhabitants, exceeding the deaths due to citizen insecurity[5]. This information is supported by the latest calculation of death rates from traffic accidents in 180 countries, made by the WHO in 2018; the average death rate for developed countries is 9.3 deaths per year per 100 thousand inhabitants, while in middle-income countries, the figure doubles, being 18.4 per 100 thousand inhabitants[5]. It is estimated that up to 30 % of road accidents are caused by driver fatigue and drowsiness[6].

To avoid traffic accidents, the driver's drowsiness should be controlled before the accident occurs. In the literature, the most used methods to detect drowsiness are subjective, physiological, vehicle-based, and driver behavior measurements. The subjective measures monitor the subject's state of drowsiness through self-perception. They place scores according to a set range[7], the most widely used being the "Karolinska Sleepiness Scale" (KSS)[8][9]. Physiological measurements are based on the use of signals; the most used are: Electrocardiogram (ECG), Electroencephalogram (EEG), Electrooculogram (EOG), and Electromyogram (EMG)[10][11]. Vehicle-based measurements require constant monitoring; any variation could be a sign of drowsiness[12][13]; some examples are: steering wheel movement, the difference in pedal pressure, deviation of the vehicle's position with respect to the road, etcetera[14]. Driver behavior measurements use a camera to detect drowsiness, which is detected by blinking of the eyes, rolling of the head, yawning, etcetera[15][16]. Some of us work, for example, that of Tayyaba Azima[17], determine the state of drowsiness of the driver through video cameras installed in the vehicle and a fuzzy expert system that manages to classify between a state of drowsiness and non-drowsiness. These measurements are good, but they determine the driver's drowsiness when it happens, so they do not have time to react to a possible disaster.

Much of the previous work focuses on detecting driver yawning, prolonged eye closures, eyebrow shape, and cameras that invade privacy and tend to make the driver uncomfortable, in addition to the large amount of data required to implement sleep identification algorithms for each system configuration and driver environment, e.g., different vehicles, different lighting, distance to sensor and driver physiology. Another group of works alerts when the driver presents evident drowsiness symptoms, giving a very short time between the correct identification of drowsiness and the alert to the driver in case of a possible traffic accident.

To solve these problems, in this research, we present a novel system for detecting driver drowsiness before getting into the vehicle in order not to disturb the driver while driving, and requiring a reduced database to make the algorithm feasible to train in both new system configurations and new environments where an extensive database is commonly not available. The porposed system is based on fuzzy expert systems for drowsiness classification, using data obtained by EEG. For simplicity, the generated interface shows the classification in only two states: not sleepy (alert) and sleepy. The results obtained by the drowsiness detection system from the EEG signals of the driver before entering the vehicle are contrasted with the driver's drowsiness record while driving. Finally, a success rate analysis of the tests is performed.

The rest of the document is structured as follows: Section 2 presents the works related to our research. Section 3 presents the materials used to perform the data acquisition. Section 4 presents the methods used for the classification of sleepiness. Section 5 shows the results obtained and their respective discussion. Finally, Section 6 contains the conclusions of this document and the projection of future work.

Related work

There are several notable studies that focus on detecting the state of drowsiness in drivers. Some of these studies make use of artificial vision systems, which is a non-intrusive method, to detect patterns in drivers that show the presence of drowsiness; the most used patterns are: yawning, angle of inclination of the eyes, continuous blinking, nodding, drooping of the eyelids, etc. To solve these problems, in this research, we present a novel system for detecting driver drowsiness before getting into the vehicle in order not to disturb the driver while driving, and requiring a reduced database to make it feasible to train the algorithm in both new system configurations and new environments where an extensive database is commonly not available. The system is based on fuzzy

expert systems for drowsiness classification, using data obtained by EEG. For simplicity, the generated interface shows the classification in only two states: not sleepy (alert) and sleepy. The results obtained by the drowsiness detection system from the EEG signals of the driver before entering the vehicle are contrasted with the driver's drowsiness record while driving. Finally, a success rate analysis of the tests is performed.

Tayyaba Azima, Arfan Jaffar, and Anwar M. Mirza[17] in their article describe a fatigue detection system based on video analysis of drivers. Their system uses two parameters to classify the state of drowsiness: Duration of ocular closure and yawning. The face is located in that system using the Viola-Jones face detection method. Then, they extract a window from the mouth region; simultaneously, they detect the pupils and their inclination angle. Monitored information from the eyes and mouth is sent to a fuzzy expert system (FES) that classifies the driver's drowsy state. The system shows that it is good at detecting and classifying the level of fatigue. Furthermore, the fuzzy expert system has proved to perform well for a sleepiness classification system.

Vineetha Vijayan and Elizabeth Sherly[18] also propose an architecture based on the measurement of facial movements such as eye blinking, yawning and head rolling, through RGB video and deep neural networks. They successfully compare three neural models, ResNet50, VGG16 and InceptionV3, and a fused architecture of the three models (FFA).

Boon-Giin L., Boon-Leng L. and W. Chung[19] present a sleep detection system with mobile devices, using 8-channel EEG signal and driver's breath. First, they extract the EEG characteristics with the wave packet transform (WPT) method to separate the signals into four frequency bands: alpha, beta, theta, and delta. A mutual information (MI) technique selects the most descriptive characteristics to perform a classification with a support vector machine (SVM). The classification

processing is carried out on a mobile device, verifying that this system requires very little computational cost, unlike other similar methods.

Yingying Jiaoa, Yini Denga, Yun Luoa, and Bao-Liang Lu[20][21] propose a model that detects driver drowsiness based on EEG and EOG signals. This model can track the change in alpha waves and differentiate the alpha-related phenomena: the alpha-blocking phenomenon and the fading-disappearing phenomenon. The LSTM (Long-Short Term Memory) network is used to manage the temporal information of the EEG and EOG signals.

Additionally, the Generative Adversary Network (GAN) is used in this paper to augment the training data set. The results show that their model has great precision when classifying the driver's condition. The same authors[22] also wrote another article in which they checked the phenomena of alpha. They used alpha's power spectrum density (PSD) to determine the phenomenon visually. Furthermore, it is observed that the attenuation-disappearance phenomenon takes a short time to appear, around ten seconds.

Another author who does an article on alpha-related phenomena is Arcady Putilov. Putilov associates the alpha attenuation-disappearance with drowsiness. In addition, he indicates in his document that this phenomenon appears when the participant closes his eyes and keeps them closed[23].

MATERIALS AND METHODS

Measuring devices

The tests were carried out on real vehicles, Figure 1 shows the instruments inside the vehicles of "San Cristóbal del Sur" company and "Transportes Libertad" company respectively.

EEG brain signals were recorded with the InteraXon Muse electroencephalogram. This device has four channels, uses Bluetooth to send data and has dry electrodes in order to be less invasive in data collection. According to the international convention for the placement of electrodes[24], the Muse electrodes are located at Fp1, Pp2, A1 and A2, with A2 being the reference electrode used, see Figure 2.
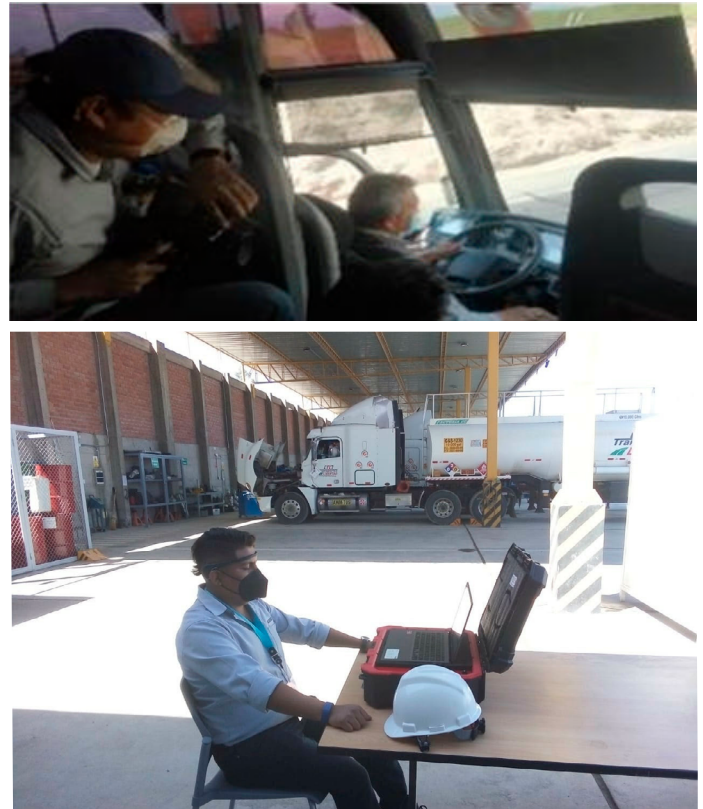
FIGURE 1. **Tests carried out on real vehicles. a) San Cristóbal del Sur company b) Transportes Libertad company.**

Data register

EEG signals recorded by the two selected channels, with a sampling rate of 256 Hz, were subjected to low-pass and high-pass filters (0.5 and 40 Hz, respectively), sampled, and stored in .csv files. The raw signals are visualized in real-time with a Python graphical interface (see Figure 3). All statistical analyses and data preprocessing were performed in Python with their respective scientific library.

Alpha wave

Alpha waves originate in the occipital lobe and are seen in relaxed wakefulness during eye closure[25].

These waves correspond to the frequency range between 8 - 12 Hz[26]. In[27], it is mentioned that the range of the waves is generally between 0.5 and 100uV, in addition, in the literature it has been shown that there is an amplitude difference between the normal state and the drowsy state in alpha waves[28].
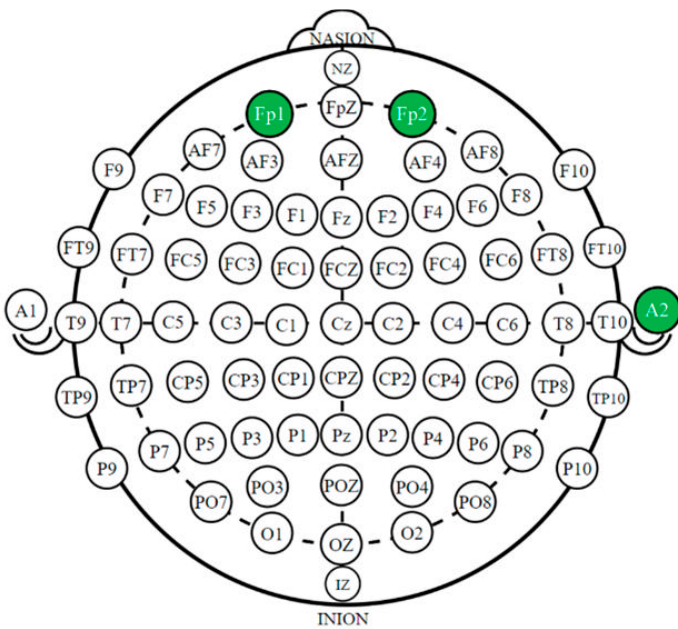
FIGURE 2. **Location of the electrodes on the head.**

Alpha blocking phenomenon

Alpha waves are produced when the eyes are closed in relaxed wakefulness and quickly fade when the eyes are reopened[20]. This phenomenon, known as alpha-blocking, indicates that the person has no trace of drowsiness[21]; for this reason, it serves as an indicator that the person is in an alert state.

Phenomenon of attenuation-disappearance of alpha waves

The attenuation of the alpha rhythm serves as a reliable EEG marker of sleep onset[20][29][30][31], it is considered the most valuable marker of sleep on-set during sleep[21]. Furthermore, objective assessment of sleepiness in permanently awake individuals could be facilitated by probing for alpha attenuation immediately after closing the eyes[32]. In this way, EEG tests can be performed in closed eyes for one minute.
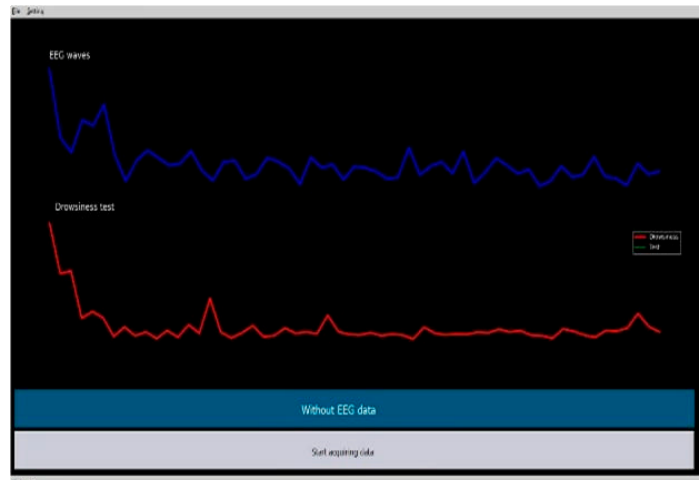
FIGURE 3. **Graphical interface showing measurements.**

Experimental procedure

A total of 10 volunteer subjects were evaluated. The age of the seven men ranged from 22 to 34 years (28 ± 6), and the three women ranged from 20 to 29 years (24.5 ± 4.5). All participants are heavy vehicle transport workers with at least one year of experience. The study volunteers did not report any mental or physical health problems and had no history of psychiatric or sleep disorders. The participants were evaluated at the beginning of their duties so that each one had at least eight hours of sleep, and it was ensured that none of them had ingested caffeinated beverages, medicines, or any food that could induce drowsiness. Written informed consent was obtained from each participant in the study.

Pre-test preparation

Before each EEG recording session, the participants were asked to use the modified Karolinska scale to indicate their level of alertness/sleepiness[7], this modification of the scale consisted of discarding the even levels, leaving the new scale as follows:

(1) Very alert.
(2) Alert.
(3) Neither drowsy nor Alert.
(4) Sleepy, easy to stay awake.
(5) Sleepy, great difficulty staying awake.

After registering the data, it is recorded that there were no level 1 values, so this scale was discarded, leaving levels 3, 5, 7 and 9. The classification of alertness/sleepiness is represented in Figure 4:
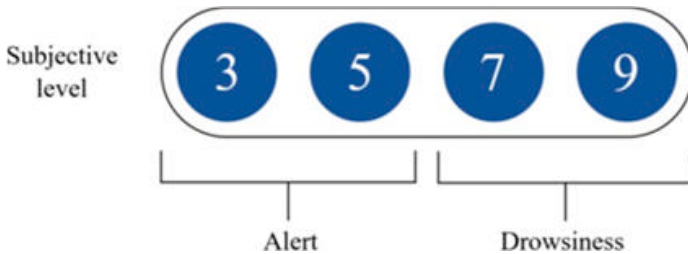
FIGURE 4. **Modified Karolinska scale.**

These subjective values were used as references of the real state of drowsiness of the participants, the precision values were obtained by comparing them with the value extracted from the system.

Open-closed-open eyes experiment

To visualize the phenomenon of alpha attenuation-disappearance, a comparison was made between measurements of 15 seconds with eyes open (reference), 1 minute with eyes closed (detection test), and finally, measurements of 15 seconds with eyes open (reference). See Figure 5.
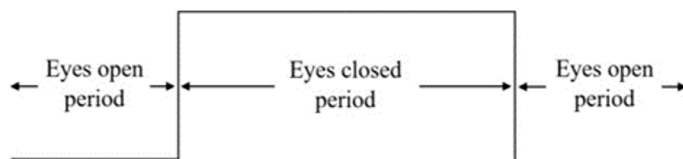
FIGURE 5. **Alpha attenuation-disappearance phenomenon.**

For data collection, the participants were in comfortable chairs, and a supervisor asked them to avoid any movement or distraction during the experiment. In addition, they indicated to the participants the exact moments when to close or open their eyes and not to blink during periods with eyes open. See Figure 6.

FIGURE 6. **Environment for driving tests**.

Test drive after analysis

After conducting the evaluation, the drivers began their working day (accompanied by a copilot for greater safety). Whether or not the driver showed drowsiness was recorded for a later analysis of the success rate of the tests. This test demonstrates the success of prevention of the level of drowsiness.

Methods

When the two phenomena related to alpha waves are observed, two different patterns are distinguished; the key to detecting if the driver is in a state of acute drowsiness is to distinguish which of these two phenomena is most closely related to the measurements. Therefore, the proposed model compares the alpha waves measured to the conductors with the waves that served as training for the model. The eye closure point (P1) is recognized as the point used to compare both samples. Figure 7 shows the flow diagram that the model follows in order to recognize an acute level of drowsiness (KSS = 9).

The following algorithms show the primary step sequences used in the model. First, Welch's method is applied to calculate the Alpha power spectrum (Algorithm 1)[33]. Then, it passes a filter to separate the wave by epoch, improving the model's precision. Then,

the strategy to detect the beginning and end of the alpha wave when closing and opening the eyes, respectively, is presented. Finally, the fuzzy expert system (FES) used in this model is described.
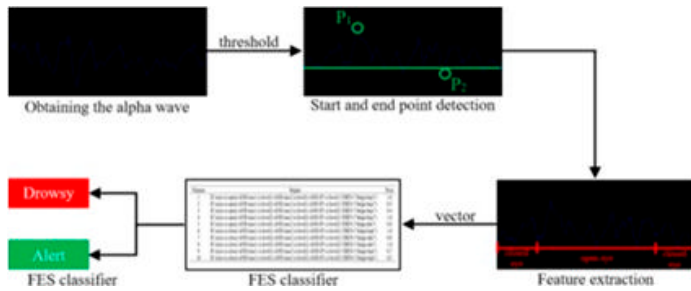
FIGURE 7. Proposed System flow diagram.

Obtaining the alpha wave energy threshold

We will start by estimating the power spectral density to calculate the absolute power in the alpha band. The most widely used method to do this is the Welch periogram[34]. Welch's method makes it possible to drastically reduce the variations produced by the constant variation of the spectral content of EEG signals[35]. Frequency resolution is defined by:

$$F_{res} = \frac{F_s}{N} = \frac{F_s}{t * F_s} = \frac{1}{t} = \frac{1}{60} \qquad (1)$$

Where Fs is the signal sampling frequency, N is the total number of samples and t is the duration, in seconds.

Algorithm 1 shows the procedure used to determine the alpha power using the "scipy" library.

Separation of energy in epochs

By having a length of the data (1 minute = 60 seconds), the final frequency resolution would be: 1/60 = 0.0167 Hz, which is 60 frequency bits per Hertz. A window long enough is taken to span at least two complete cycles of the lowest frequency of interest[36]. In this case, the lowest frequency of interest corresponding to the alpha band (8 Hz to 12 Hz) is 8 Hz, so it is chosen a window of 2/8 = 0.25 seconds, see the Algorithm 2.

ALGORITHM 1. Calculation of the potency of alpha.

```
0:   procedure POWER_ALPHA (data, sf,
     window=None, relative=False)
1:       from scipy.signal import welch
2:       from scipy.integrate import simps
3:       import numpy as np
4:       low ← 8
5:       high ← 12
6:       if window == None then
7:           npersg ← window * sf
8:       else
9:           npersg ← (2 / low) * sf
10:      end if
11:      freqs, psd ← welch(data, sf,
         npersg=npersg)
12:      freq_res ← freqs[1] - freqs[0]
13:      idx_band ← np.logical_and(freqs >=
                                   low,
                              freqs <= high)
14:      bp ← simps(psd[idx_band], dx=freq_res)
15:      if relative then
16:          bp /← simps(psd, dx=freq_res)
17:      end if
18:      return bp
```

Before calculating the absolute alpha band power (average), it is necessary to find the frequency intervals that intersect the Alpha range. For this purpose, it is defined the upper and lower frequency limits corresponding to this band (8 Hz to 12 Hz). Normalized measurements are used at all times to ensure that any sample is outside the range. The formula used is:

$$Alpha_{normalized} = \frac{Alpha - Alpha_{min}}{Alpha_{max} - Alpha_{min}} \qquad (2)$$

These calculated alpha values will be used to obtain the ratio of the area under the curve (AUC), see Algorithm 3.

Classification of levels using FES

The purpose of this classifier is to determine the starting point of eye closure, the point that initiates the phenomenon of fading-disappearance of alpha waves.

ALGORITHM 2. Calculation of the potency of alpha.

```
0:    procedure EPOCHS(data, sf, sliding, seg)
1:       from scipy.signal import welch
2:       import numpy as np
3:       low ← 8
4:       high ← 12
5:       win ← sliding * sf
6:       alpha_abs ← np.array([])
7:       i ← 0
8:       j ← sf * seg
9:       for v = 0, 1, …, 60 do
10:         epoch ← data[i:j]
11:         b ← np.greater(epoch, 500)
12:         c ← np.less(epoch, -500)
13:         if b = True or c = True then
14:            freqs, psd ← welch(epoch, sf,
                            nperseg=win)
15:            idx_a ← np.logical_and(freqs >= low,
                            freqs <= high)
16:            freq_res ← freqs[1] - freqs[0]
17:            alpha_power ← simps(psd[idx_a],
                            dx=freq_res)
18:            alpha_abs ← np.append(alpha_abs,
                            [al-
        pha_power])
             end if
         end for
19:  i ← i + sf *2
20:  j ← j + sf *2
21:  return alpha_abs
```

For this, the model must autonomously recognize when this phenomenon starts in the measurements made.

Feature extraction

Feature extraction algorithms are an important element in all machine learning models. The first step in developing this fatigue detection system is to determine the number of variables or characteristics involved, according to the criteria of the experts. The algorithm extracts the characteristics of the measurement during the test minute; the values of the measurements with the eyes open serve as a reference to have knowledge of the low alpha values of each individual. The characteristics chosen after conducting

an adequate study of our system are: Initial point ratio (P1), End point ratio (P2), Eye condition, Area under curve 1 (AUC1), Area under curve 2 (AUC2) and fatigue level. Table 1 shows the characteristics and associated linguistic terms.

ALGORITHM 3. Calculation of AUC.

```
0:    procedure AUC_CALCULATION(alfa_abs)
1:       import numpy as np
2:       from scipy.integrate import simps
3:       media ← np.mean(alfa_abs)
4:       d_st ← np.std(alfa_abs)
5:       index ← np.array([])
6:       for k = len(alfa_abs) do
7:          z ← (alfa_abs[k] - media) / d_st
8:          index ← np.append(index, [z])
9:       end for
10:      ventana ← 3
11:      b ← np.ones(ventana) * (1 / ventana)
12:      normal ← []
13:      x ← np.arange(0, len(index))
14:      freqs, psd ← welch(data, sf,
         npersg=npersg)
15:      for i = len(index) do
16:         normal.append(index[i] - min(index)) /
                            (max(index) -
                            min(index))
17:      end for
18:      area1 ← simps(normal[0:29], x[0:29])
19:      area2 ← simps(normal[30:59], x[30:59])
20:      return area1, area2
```

TABLE 1. Details of the input and output variables used by the expert system.

Variable	Type	Range	Linguistic Terms
Ratio P1	Input	X	Level A1, level A2
Ratio P2	Input	X	Level A1, level A2
Eye condition	Output	[0 - 1]	Open, closed
AUC 1	Input	X	Level B1, level B2
AUC 2	Input	X	Level B1, level B2
Fatigue level	Output	[0 - 1]	Low, high

The area under curve 1 is taken from the first 30 seconds of the closed-eye tests, while AUC2 is taken

from the remaining 30 seconds. Because the system is proposed as adaptive (to any gender, ethnicity, etc.), A1, A2, B1 and B2 levels of the input characteristics are determined according to the alpha values obtained during the first 15 seconds of the tests with open eyes.
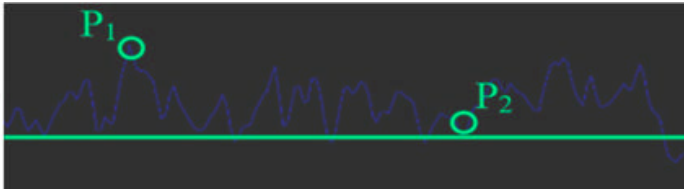
Detection of start and end points of alpha wave

As can be seen in Figure 8, to obtain the alpha energy value curve, it is applied the Welch periodogram, then a sharp change between two consecutive signals was detected. The largest in the entire measurement marks the point P1; then this information is passed to the trained model to make its classification.

FES classifier

FES uses fuzzy logic through functions and rules instead of Boolean logic to reason about input data. These systems can be seen as an attempt to formalize two human capacities[17]. Fuzzy logic intends to solve a problem relying on IF X AND Y THEN Z to solve a control problem instead of trying to obtain a mathematical model of the process. The model is empirically based on the operator's experience rather than his technical comprehension of the underlying system[37]. One of the most significant advantages of FES is that it generally does not require an extensive training set[17]. Since there is not a large amount of data to train, this classifier was chosen.

In this step, it is determined whether the driver's state of drowsiness is acute. If the fatigue level value is higher than 0.55, the system informs with a message ("with drowsiness") that indicates the driver is not fit to drive. The system can detect drowsiness regardless of the driver's ethnicity, gender, etc. Hence, the system

takes the first 15 seconds of measurement (during the eye-open portion of the test) to determine the range of the alpha-level input. Based on the selected variables, rules have been declared to express the behavior of the system in a comprehensible and logical way. Different rules are enunciated to express the behavior that the system follows from the variables mentioned in section 4.3.1.

We got a total of 18 understandable rules. According to these rules, the state of the eyes and the level of the characteristics play a significant role in detecting the state of the driver. Of the set of rules, ten are listed in Table 2, and the rest follow a similar pattern. In addition, the rules follow a hierarchy (added weight) according to their relevance when the system classifies.

TABLE 2. **Rules for the expert system.**

Number	Rules	Weight
1	IF (eyes is open) AND (auc1 is level1) AND (auc2 is level1) AND (P1 is level1) THEN ("low fatigue")	1.0
2	IF (eyes is open) AND (auc1 is level2) AND (auc2 is level1) AND (P1 is level1) THEN ("low fatigue")	0.5
3	IF (eyes is open) AND (auc1 is level2) AND (auc2 is level1) AND (P1 is level2) THEN ("low fatigue")	0.4
4	IF (eyes is open) AND (auc1 is level2) AND (auc2 is level2) AND (P1 is level1) THEN ("low fatigue")	1.0
5	IF (eyes is open) AND (auc1 is level2) AND (auc2 is level2) AND (P1 is level2) THEN ("high fatigue")	0.8
6	IF (eyes is close) AND (auc1 is level1) AND (auc2 is level1) AND (P1 is level1) THEN ("low fatigue")	1.0
7	IF (eyes is close) AND (auc1 is level2) AND (auc2 is level1) AND (P1 is level1) THEN ("high fatigue")	0.8
8	IF (eyes is close) AND (auc1 is level2) AND (auc2 is level1) AND (P1 is level2) THEN ("high fatigue")	1.0
9	IF (eyes is close) AND (auc1 is level1) AND (auc2 is level2) AND (P1 is level1) THEN ("low fatigue")	0.7
10	IF (eyes is close) AND (auc1 is level1) AND (auc2 is level2) AND (P1 is level2) THEN ("low fatigue")	0.5

The variables and rules were declared correctly, for this reason, now the fuzzy expert system process can follow the following steps[17]:

(1)   Return sharp input values to fuzzy
(2)   Evaluation of all If-Then rules in parallel.
(3)   Adding of the consequents through the rules.
(4)   Converting the fuzzy response to a sharp value.

RESULTS AND DISCUSSION

To corroborate the performance of this model, a laptop was used, it was composed by Windows operative system, 6th Gen Intel (R) Core (TM) i5 processor, quad core, 8GB RAM, and an NVIDIA 840 with 2GB memory (GPU not accelerated). Each driver performed the open- closed-open eyes test once before getting into their vehicle, for a total of 20 sessions per driver.

The results are displayed in the graphical user interface. Then, different combinations were tried of window size and epoch length, to get the one that give the best results. Next, it is tested the eye opening and closing based on alpha measurements. For the FES system, it was tested its performance by comparing it with RNN, SVM and K-NN using training and testing each subject.

Result in the graphical interface

Figure 9 shows two levels of sleepiness found for the four most descriptive extracted features of the EEG signals. The upper part of the graph (blue signal) corresponds to the EEG signals without processing and in real time (a sampling frequency of 250 Hz), they were obtained from the derivative of Fp1 and Fp2. The middle part of the graph shows two signals, the first one in green corresponds to the entire signal captured during the test minute and the yellow signal corresponds to the signal after filtering. The lower part indicates the state of the driver, being "Drowsiness" or "Not Drowsy".
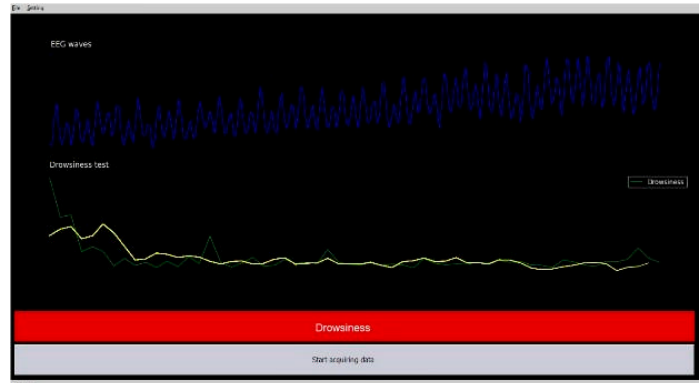
a)
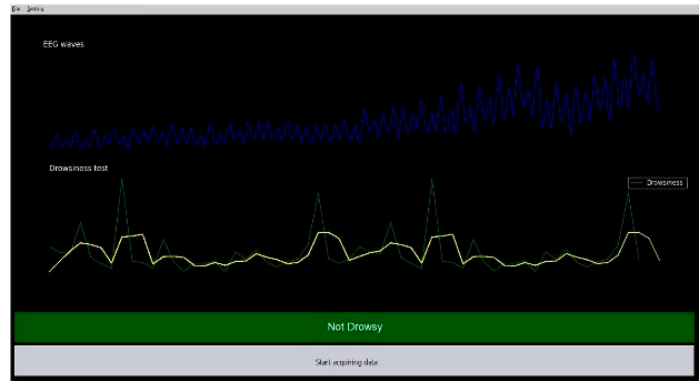
b)

FIGURE 9. Results in the graphical interface.

Different combinations of window size and epochs

The performance of the system was compared for different combinations of window size and sliding step size on the Welch periodogram. For this purpose, 120 samples of a single person with different configurations were used. Among the configurations that were tested, there was no overlap of sliding windows in the 0.25 s window size configuration with the 0.25 s sliding step. In all the other combinations, an overlap was considered. The total time coverage of each window was 2 s (epochs) for each configuration so the information contained in all configurations was the same. In Table 3, it can be seen that every window featuring overlap performed better than the window without any overlap.

In Table 3, it can be seen that the 0.5 s window with 0.125 s sliding step size was the best. Therefore, this combination was chosen to be our window setup for

extracting features from the EEG signal. Alpha waves start and end point detection performance.

Subject	Window = 0.25 Sliding = 0.1	Window = 0.4 Sliding = 0.125	Window = 0.5 Sliding = 0.125	Window = 0.5 Sliding = 0.25
1	81.67	83.33	87.50	85.00
2	79.17	80.00	85.83	80.83
3	75.00	77.50	85.00	81.67
4	77.50	78.33	84.17	79.17
5	76.67	75.83	85.00	84.17
6	79.17	80.00	85.83	83.33
7	75.00	79.17	82.50	81.67
8	81.67	80.83	81.67	82.50
9	78.33	78.33	85.83	85.00
10	76.67	77.50	85.00	80.83
Prom	78.08	79.08	**84.83**	82.42

As shown in Figure 8, the detection of start and end points relies only on Alpha waves; this generates a deviation at the exact moment. For this reason, the detection of these points was considered correct if they corresponded to the range of [I (s) ± 0.5s] and [F (s) ± 0.75s], a greater range was considered for the endpoint because in the attenuation-disappearance phenomenon, so it was more challenging to differentiate Alpha levels.

TABLE 4. **Detection performance #A and #D.**

N	#A	Start (%)	End (%)	#D	Start (%)	End (%)
1	62	75.81	72.58	58	81.03	77.59
2	65	81.54	73.85	55	81.82	80.00
3	71	84.51	74.65	49	83.67	81.63
4	70	75.71	72.86	50	80.00	82.00
5	63	77.78	82.54	57	85.96	78.95
6	69	78.26	72.46	51	82.35	80.39
7	72	80.56	83.33	48	77.08	79.17
8	66	77.27	74.24	54	79.63	81.48
9	59	81.36	76.27	61	78.69	77.05
10	61	81.97	80.33	59	84.75	71.19
P		79.48	76.31		81.50	78.94
SD		2.78	3.98		2.63	3.03

In Table 4, it is observed that the average of the percentages of successes of the start and end points is

79.48 % and 76.31 %, respectively, for drivers in state of alert. For drowsy drivers the average is 81.50 % and 78.94 %. These values confirm that the system adequately detects the start and end points of the eyes closed event using only EEG measurement.

Classifier comparison

To simplify the comparison of classifiers, only the samples that exceed the 25 detected values were taken, avoiding possible misrepresentations. We compared our FES classifier with SVM, KNN and RF using an independent assessment of each subject. Table 5 shows that in each evaluation, the model obtains the best accuracy of hits, being the highest detected 87.50 %. As indicated in Section 3.4.1, the KSS values of the subjects were used to determine if the person is in a state of alert or in a state of drowsiness, this determines the hit rate.

TABLE 5. **Accuracy (%) of SVM, KNN, RF and FES to classify conductor states.**

Subject	SVM (%)	KNN (%)	RF (%)	FES (%)
1	78.33	79.17	83.33	87.50
2	80.00	83.33	80.83	85.83
3	80.83	77.50	80.83	85.00
4	75.83	76.67	84.17	84.17
5	75.83	75.00	85.00	85.00
6	76.67	75.83	84.17	85.83
7	79.17	74.17	81.67	82.50
8	79.17	73.33	80.83	81.67
9	80.83	76.67	82.50	85.83
10	78.33	75.83	83.33	85.00
Prom	78.50	76.75	82.67	**84.83**
SD	1.78	2.70	1.48	**1.61**

Prevention hit rate

In Section 3.4.3 it was noted about the proof test that the system predicts the drowsy state of the driver. The tests consisted of determining if the driver during the journey showed signs of drowsiness (through the perception of the copilot and self-perception) and then comparing them with what the system had predicted. Table 6 shows the total hit rate of the prediction of drowsiness, due to there were 60 tests for each person.

TABLE 6. **System prediction hit rate.**

Subject	Number of drowsiness	Accuracy (%)
1	2	80.00
2	1	83.33
3	2	91.67
4	0	88.33
5	3	86.67
6	1	83.33
7	1	81.67
8	3	86.67
9	1	85.00
10	0	86.67

CONCLUSIONS

This document proposes a new system to detect driver drowsiness from EEG signals. This model aims to detect the change in alpha waves captured by the pair of electrodes located in the right frontal area (F2) and to detect the beginning and end of the samples during tests with eyes closed in order to detect the drowsy state of the driver before getting into the vehicle. The proposed model uses the Welch periodogram to extract the power of the alpha waves, a filter to improve the wave shape, and FES to classify the states of the conductors. The results have shown that our model can detect the driver's condition with an average accuracy of 84.8 %. These tests were compared with classifier models such as RNN, KNN, and SVM. The percentage of success obtained for the other learning methods was SVM = 78.5 %, KNN = 76.8 %, and RF = 82.6 %, making this model much superior to the others. Since this model only places two electrodes on the subject, it is practical for routine use in real-life scenarios; this has been proven in the preventive detection of drowsiness in drivers.

Future work will focus on strengthening the weakest points when detecting drowsiness. The implemented system works as a good base, but it can be noted that it has problems during the tests with the eyes open; future works will focus on filtering out the blinks that interfere with the alpha measurements. In addition, one more state will be added; there will be three states: alert, low drowsiness, and acute drowsiness. In addition, this system would complement a real-time detection system obtained from vehicle measurements.

ETHICAL STATEMENT

In this article, all of the subject were advised about the complete procedures and methods before the test. It was obtained the consent of each participant.

ACKNOWLEDGEMENTS

CONFLICT OF INTEREST

The authors declare that they have no known competing financial interests or personal relationships that could have appeared to influence the work reported in this paper.

AUTHOR CONTRIBUTIONS

R.A. conceptualization, methodology, data curation, software, visualization. B.A.C. data curation, software, visualization, methodology, validation. A.M.A. investigation, validation, methodology, writing original draft. E.S. project administration, methodology, conceptualization, writing original draft, review and editing. J.J.F.T.S. project

administration, methodology, supervision, writing review and editing. D.D.Y.A.C. methodology, writing review and editing, supervision. All authors reviewed and approved the final version of the manuscript.

REFERENCES

[1] World Health Organization, "Global status report on road safety 2018," WHO. France, 2018 Accessed: Dec. 21, 2023. [Online]. Available: https://www.who.int/publications/i/item/9789241565684

[2] Pan American Health Organization, World Health Organization, "Road Safety," PAHO/WHO. Accessed: Dec. 21, 2023. [Online]. Available: https://www.paho.org/en/topics/road-safety

[3] D. Carhuavilca, Perú: Natalidad, Mortalidad y Nupcialidad, 2019, Lima, Perú: Instituto Nacional de Informática y Estadística, 2020. [Online]. Available: https://www.inei.gob.pe/media/MenuRecursivo/publicaciones_digitales/Est/Lib1766/libro.pdf

[4] Policía Nacional del Perú, "Muertos por Accidentes de Tránsito 2006 - 2017," Ministerio de transportes y Comunicaciones. Accessed: Dec. 21, 2023. [Online]. Available: https://www.mtc.gob.pe/cnsv/documentos/muertosAccidenteTransito_2006-2017.pdf.

[5] E. Huerta. "La preocupante cifra de muertes por accidentes de tránsito en el Perú y sus principales causas." El Comercio Perú. https://elcomercio.pe/tecnologia/actualidad/preocupante-cifra-muertes-accidentes-transito-peru-principales-causas-ecpm-noticia-651076-noticia/ (accessed Dec. 21, 2023).

[6] J. Rey de Castro, "Drowsy drivers on the roads of Peru: findings and proposals," Rev. Med. Hered., vol. 22, no. 4, pp. 155-156, Oct. 2011. [Online]. Available: http://www.scielo.org.pe/scielo.php?script=sci_arttext&pid=S1018-130X2011000400001

[7] A. A. Putilov and O. G. Donskaya, "Construction and validation of the EEG analogues of the Karolinska sleepiness scale based on the Karolinska drowsiness test," Clin. Neurophysiol., vol. 124, no. 7, pp. 1346-1352, Jul. 2013, doi: https://doi.org/10.1016/j.clinph.2013.01.018

[8] V. Riethmeister, R. W. Matthews, D. Dawson, M. R. de Boer, S. Brouwer, and U. Bültmann, "Time-of-day and days-on-shift predict increased fatigue over two-week offshore day-shifts," Appl. Ergon., vol. 78, pp. 157-163, Jul. 2019, doi: https://doi.org/10.1016/j.apergo.2019.02.010

[9] A. Sahayadhas, K. Sundaraj, and M. Murugappan, "Detecting Driver Drowsiness Based on Sensors: A Review," Sensors, vol. 12, no. 12, pp. 16937-16953, Dec. 2012, doi: https://doi.org/10.3390/s121216937

[10] V. Bajaj, S. Taran, S. K. Khare, and A. Sengur, "Feature extraction method for classification of alertness and drowsiness states EEG signals," Appl. Acoust., vol. 163, art. no. 107224, Jun. 2020, doi: https://doi.org/10.1016/j.apacoust.2020.107224

[11] U. Budak, V. Bajaj, Y. Akbulut, O. Atila, and A. Sengur, "An Effective Hybrid Model for EEG-Based Drowsiness Detection," IEEE Sens. J., vol. 19, no. 17, pp. 7624-7631, Sep. 2019, doi: https://doi.org/10.1109/jsen.2019.2917850

[12] M. Fernandes, "Driver drowsiness detection using non-intrusive eletrocardiogram and steering wheel angle signals," M. S. thesis, Univ. Porto, Porto, Portugal, 2019. [Online]. Available: https://repositorio-aberto.up.pt/bitstream/10216/122936/2/358726.pdf

[13] S. Arefnezhad, S. Samiee, A. Eichberger, and A. Nahvi, "Driver Drowsiness Detection Based on Steering Wheel Data Applying Adaptive Neuro-Fuzzy Feature Selection," Sensors, vol. 19, no. 4, art. no. 943, Feb. 2019, doi: https://doi.org/10.3390/s19040943

[14] M. Chai, s.-w. Li, w.-c. Sun, m.-z. Guo, and m.-y. Huang, "Drowsiness monitoring based on steering wheel status," Transp. Res. D Transp. Environ., vol. 66, pp. 95-103, Jan. 2019, doi: https://doi.org/10.1016/j.trd.2018.07.007

[15] C. Fors, C. Ahlström, P. Sörner, J. Kovaceva, et al., "Camera-based sleepiness detection Final report of the project SleepEYE," Virtual Prototyping and Assessment by Simulation, 2011. Accessed: Aug. 23, 2023. [Online]. Available: https://www.diva-portal.org/smash/get/diva2:674103/FULLTEXT01.pdf

[16] Mohamed Hedi Baccour, Frauke Driewer, Enkelejda Kasneci, and W. Rosenstiel, "Camera-Based Eye Blink Detection Algorithm for Assessing Driver Drowsiness," Jun. 2019, doi: https://doi.org/10.1109/ivs.2019.8813871

[17] T. Azim, M. A. Jaffar, and A. M. Mirza, "Fully automated real time fatigue detection of drivers through Fuzzy Expert Systems," Appl. Soft Comput., vol. 18, pp. 25-38, May 2014, doi: https://doi.org/10.1016/j.asoc.2014.01.020

[18] V. Vijayan and E. Sherly, "Real time detection system of driver drowsiness based on representation learning using deep neural networks," J. Intell. Fuzzy Syst., vol. 36, no. 3, pp. 1977-1985, Mar. 2019, doi: https://doi.org/10.3233/jifs-169909

[19] B.-G. Lee, B.-L. Lee, and W.-Y. Chung, "Mobile Healthcare for Automatic Driving Sleep-Onset Detection Using Wavelet-Based EEG and Respiration Signals," Sensors, vol. 14, no. 10, pp. 17915-17936, Sep. 2014, doi: https://doi.org/10.3390/s141017915

[20] Y. Jiao, Y. Deng, Y. Luo, and B.-L. Lu, "Driver sleepiness detection from EEG and EOG signals using GAN and LSTM networks," Neurocomputing, vol. 408, pp. 100-111, Sep. 2020, doi: https://doi.org/10.1016/j.neucom.2019.05.108

[21] Y. Jiao and B.-L. Lu, "Detecting driver sleepiness from EEG alpha wave during daytime driving," in 2017 IEEE International Conference on Bioinformatics and Biomedicine (BIBM), Kansas City, MO, USA, 2017, pp. 728-731, doi: https://doi.org/10.1109/BIBM.2017.8217744

[22] Y. Jiao and B.-L. Lu, "An alpha wave pattern from attenuation to disappearance for predicting the entry into sleep during simulated driving," in 2017 8th International IEEE/EMBS Conference on Neural Engineering (NER), Shanghai, China, 2017, pp. 21-24, doi: https://doi.org/10.1109/NER.2017.8008282

[23] A. A. Putilov and O. G. Donskaya, "Alpha attenuation soon after closing the eyes as an objective indicator of sleepiness," Clin. Exp. Pharmacol. Physiol., vol. 41, no. 12, pp. 956-964, Dec. 2014, doi: https://doi.org/10.1111/1440-1681.12311

[24] S.-C. Ng and P. Raveendran, "EEG Peak Alpha Frequency as an Indicator for Physical Fatigue," in 11th Mediterranean Conference on Medical and Biomedical Engineering and Computing 2007. IFMBE Proceedings, vol 16. Springer, Heidelberg, Germany, 2007, pp. 517-520, doi: https://doi.org/10.1007/978-3-540-73044-6_132

[25]   S. Hanslmayr, J. Gross, W. Klimesch, and K. L. Shapiro, "The role of alpha oscillations in temporal attention," Brain Res. Rev., vol. 67, no. 1-2, pp. 331-343, Jun. 2011, doi: https://doi.org/10.1016/j.brainres-rev.2011.04.002

[26]   J. Katona, I. Farkas, T. Ujbanyi, P. Dukan, and A. Kovari, "Evaluation of the NeuroSky MindFlex EEG headset brain waves data," in 2014 IEEE 12th International Symposium on Applied Machine Intelligence and Informatics (SAMI), Herl'any, Slovakia, 2014, pp. 91-94, doi: https://doi.org/10.1109/SAMI.2014.6822382

[27]   M. Pathak and A. K. Jayanthy, "Designing of a single channel EEG acquisition system for detection of drowsiness," in 2017 International Conference on Wireless Communications, Signal Processing and Networking (WiSPNET), Chennai, India, 2017, pp. 1364-1368, doi: https://doi.org/10.1109/WiSPNET.2017.8299986

[28]   M. Pathak and A. K. Jayanthy, "Development of a Real- Time Single Channel Brain-Computer Interface System for Detection of Drowsiness," Biomed. Eng. Appl. Basis Commun., vol. 29, no. 3, art no. 1750019, Jun. 2017, doi: https://doi.org/10.4015/s1016237217500193

[29]   D. L. Schomer, "The Normal EEG in an Adult," in The Clinical Neurophysiology Primer, A. S. Blum, S. B. Rutkove, Eds., Totowa, NJ, USA: Humana Press eBooks, 2007, ch. 5, pp. 57-71, doi: https://doi.org/10.1007/978-1-59745-271-7_5

[30]   Y. Albadawi, M. Takruri, and M. Awad, "A Review of Recent Developments in Driver Drowsiness Detection Systems," Sensors, vol. 22, no. 5, art. no. 2069, Mar. 2022, doi: https://doi.org/10.3390/s22052069

[31]   G. Li and W.-Y. Chung, "Electroencephalogram-Based Approaches for Driver Drowsiness Detection and Management: A Review," Sensors, vol. 22, no. 3, art. no. 1100, Jan. 2022, doi: https://doi.org/10.3390/s22031100

[32]   S.-H. Hwang, M. Park, J. Kim, Y. Yun, and J. Son, "Driver Drowsiness Detection Using EEG Features," in HCI International 2018 - Posters' Extended Abstracts. HCI 2018. Communications in Computer and Information Science, vol. 852, Las Vegas, NV, USA, 2018, pp. 367-374, doi: https://doi.org/10.1007/978-3-319-92285-0_49

[33]   C. Dissanayaka, E. Ben-Simon, M. Gruberger, A. Maron-Katz, H. Sharon, T. Hendler, D. Cvetkovic, "Comparison between human awake, meditation and drowsiness EEG activities based on directed transfer function and MVDR coherence methods," Med. Biol. Eng. Comput., vol. 53, no. 7, pp. 599-607, Jul. 2015, doi: https://doi.org/10.1007/s11517-015-1272-0

[34]   R. Vallat, M. Eskinazi, A. Nicolas, and P. Ruby, "Sleep and dream habits in a sample of French college students who report no sleep disorders," J. Sleep Res., vol. 27, no. 5, art. no. e12659, Feb. 2018, doi: https://doi.org/10.1111/jsr.12659

[35]   E. Combrisson, R. Vallat, C. O'Reilly, M. Jas, et al., "Visbrain: A Multi-Purpose GPU-Accelerated Open-Source Suite for Multimodal Brain Data Visualization," Front. Neuroinform., vol. 13, art. no. 14, Mar. 2019, doi: https://doi.org/10.3389/fninf.2019.00014

[36]   P. A. M. Kanda, E. F. Oliveira, and F. J. Fraga, "EEG epochs with less alpha rhythm improve discrimination of mild Alzheimer's," Comput. Methods Programs Biomed., vol. 138, pp. 13-22, Jan. 2017, doi: https://doi.org/10.1016/j.cmpb.2016.09.023

[37]   J.-D. Wu and T.-R. Chen, "Development of a drowsiness warning system based on the fuzzy logic images analysis," Expert Syst. Appl., vol. 34, no. 2, pp. 1556-1561, Feb. 2008, doi: https://doi.org/10.1016/j.eswa.2007.01.019

Análisis Matemático no Lineal Relacionado a un Modelo de Insulina-Células Pancreáticas en Presencia de Epinefrina

Nonlinear Mathematical Analysis based on an Insulin-Pancreatic Cells Model in the Presence of Epinephrine

Diana Gamboa[1] ⓘ*, Paul J. Campos[1]* ⓘ ✉*.*

[1]Tecnológico Nacional de México/Instituto Tecnológico de Tijuana, Baja California - México

RESUMEN

En este trabajo se estudia un modelo de ecuaciones diferenciales ordinarias no lineales que describe la relación entre la masa de células β y la secreción de epinefrina. Se analiza el impacto del estrés asociado como causante de incremento de los niveles de glucosa en el organismo. El análisis matemático se fundamenta en la aplicación de la teoría de control no lineal para definir la capacidad de carga máxima para cada variable de estado, estableciendo un dominio invariante positivo acotado a través del método de Localización de Conjuntos Compactos Invariantes (LCCI). El objetivo es determinar los efectos asociados a la secreción de epinefrina en el aumento de los niveles de glucosa en sangre; por lo tanto, los resultados de este análisis ayudan a definir las condiciones necesarias y suficientes en las que la epinefrina eleva los niveles de insulina y glucosa en presencia de células β. El interés por estudiar este tipo de enfermedades se enfoca en la búsqueda de un tratamiento o un análisis que garantice un control completo de los niveles de glucosa. El desarrollo y análisis matemático de este trabajo fortalece la investigación vigente de diabetes mellitus insulinodependiente entorno a factores críticos de epinefrina que implican un incremento de glucosa en el organismo.

PALABRAS CLAVE: diabetes, modelo, células β, LCCI

ABSTRACT

In this work, a nonlinear model is studied based on ordinary differential equations that describe the relationship between the mass of β cells and the secretion of epinephrine. It analyzes the impact of stress associated with the cause of increased blood pressure and glucose levels in the body. The mathematical analysis is based on the appliance of the nonlinear control theory to define the maximum load capacity for each state variable, establishing a bounded positive invariant domain through the Localization of Compact Invariants Sets (LCIS) method. The objective is to determine the effects of epinephrine secretion on the increase of blood glucose levels; therefore, this analysis's results define the necessary and sufficient conditions in which epinephrine raises insulin and glucose levels in the presence of β cells. The interest in studying this type of disease focuses on searching for a treatment or an analysis that guarantees complete control of glucose levels. This work's development and mathematical analysis strengthen current research on insulin-dependent diabetes mellitus around critical epinephrine factors that imply an increase in glucose in the body.

KEYWORDS: diabetes, model, β cells, LCIS

Autor de correspondencia

DESTINATARIO: **Paúl J. Campos**

INSTITUCIÓN: **Tecnológico Nacional de México/Instituto Tecnológico de Tijuana**

DOMICILIO: **Tijuana, Blvd. Alberto Limón Padilla s/n, Mesa de Otay, 22454 Tijuana, B.C., México.**

CORREO ELECTRÓNICO: paul.campos@tectijuana.edu.mx

INTRODUCCIÓN

La diabetes mellitus (DM) es una enfermedad crónica derivada de la incapacidad del páncreas al no secretar suficiente insulina o la incapacidad del cuerpo para utilizarla eficazmente. La insulina es la hormona que regula la concentración de glucosa en la sangre (glucemia). La consecuencia común asociada a la DM no controlada es la hiperglucemia, es decir, altos niveles de glucemia. En el caso particular de la diabetes tipo 1 (DMT1) es el resultado de un ataque autoinmune a las células beta pancreáticas (células β) que secretan insulina[1][2].

Actualmente, el modelado matemático aplicado en el análisis de patologías humanas es una herramienta utilizada, en el área de la medicina, para mejorar la comprensión de un sistema fisiológico con el objetivo de prevenir futuras situaciones de enfermedades[3]. Sus revisiones aportan una descripción más detallada de esta enfermedad y son una herramienta que contribuye a su diagnóstico y prueba de tratamientos, gracias a las simulaciones basadas en estos[4]. A causa de esto, en las últimas décadas se han realizado esfuerzos para el diseño y análisis de modelos matemáticos que describan su dinámica.

Es conocido que la DM ha alcanzado cifras preocupantes a nivel mundial y al no tener cura, ha motivado al desarrollo de investigaciones sobre métodos para su diagnóstico, control y tratamiento. Sin embargo, no todos estos modelos cumplen con el principio de positividad, por lo que es necesario determinar si un modelo cumple con él para asegurar que el comportamiento del sistema siempre se mantendrá en los valores positivos para todo tiempo futuro, que generalmente ocurre en los sistemas fisiológicos (por ejemplo, no existen valores negativos de glucosa en sangre).

La actividad emocional, consecuencia a eventos de estrés, es considerada como uno de los factores asociados en la desestabilización del control metabólico, actuando sobre los niveles de glucemia a través de la movilización de las "hormonas del estrés" (como la epinefrina) e indirectamente por su impacto sobre las conductas de adherencia al tratamiento[5], la cual se considera común en pacientes con esta enfermedad y provoca que sus niveles de glucemia aumenten, haciéndola compleja de controlar. En[6], se reporta que la pandemia de enfermedad por coronavirus 2019 (COVID-19), ha impactado en DM con una mayor tasa de incidencia, así como formas de exacerbación de la hiperglucemia y sus complicaciones en pacientes. Aunado a ello, se reporta hiperglucemia inducida por estrés en muchos pacientes no diabéticos hospitalizados después de contraer COVID-19. Implicando que nuestro análisis matemático contribuye en continuar estudiando el comportamiento de la epinefrina en un modelo no lineal mediante un conjunto de ecuaciones diferenciales ordinarias.

Es importante destacar que recientemente en[7], se ha reportado un modelo que conduce a la predicción del nivel de glucemia, donde tales predicciones tienen el potencial de ser utilizadas como parte de sistemas de control las cuales pueden ser robustos para modelar imperfecciones y datos ruidosos. Lo interesante de este modelo es que su capacidad predictiva se compara con modelos enfocados a diabetes mellitus tipo 2 (DMT2). Así mismo, en[8] se reporta un análisis global enfocado a las biomatemáticas para continuar estudiando las hipótesis con las que algunos modelos de DM se definen con base a datos experimentales o in-silico. Es por ello, la inquietud de continuar estudiando los modelos con el que se predice DMT1 se convierte en un desafío vigente y, por ende, el análisis matemático mediante el método de Localización de Conjuntos Compactos Invariantes fortalece las hipótesis en el desarrollo de cada modelo que se ha propuesto en la literatura. Un avance reportado en[9], se discute un esquema de control activo para forzar que el régimen caótico de DMT1 siga un estado oscilatorio periódico, es decir, un equilibrio libre de desorden.

Por último, cabe destacar que el estudio de su comportamiento no lineal no ha sido reportado en la literatura y es donde impactará este análisis, el cual permite observar y estudiar la evolución del modelo a través del tiempo. Determinar la importancia de la influencia de la epinefrina dentro esta dinámica asociada a la DMT1; así como también determinar condiciones que sirvan como base para proponer y diseñar nuevos modelos matemáticos relacionados con la DMT1, considerando estos parámetros.

El estudio de la dinámica a largo plazo es de gran aportación dentro del campo de investigación ya que ayudan a encontrar o probar nuevas formas de diagnóstico y tratamiento de esta enfermedad. Comprueba si los modelos cumplen con el principio de positividad y determina las condiciones que permiten establecer un preámbulo matemático donde se evidencia la importancia de la epinefrina en esta dinámica asociada a la DMT1.

Modelo matemático glucosa-insulina

El antecedente del modelo de estudio es el propuesto por Topp *et al.*[10], que describe la dinámica de glucosa, insulina y masa de células β. El modelo principal de estudio es el propuesto por Mohammed *et al.*[2], es una modificación del modelo de[10] y describe la dinámica glucosa-insulina bajo la influencia de la epinefrina, el cual es representado por el siguiente sistema de ecuaciones diferenciales ordinarias:

$$\frac{dG}{dt} = R_0 + G_e - (E_{G0} + S_I I)G, \tag{1}$$

$$\frac{dI}{dt} = \frac{\beta \sigma G^2}{(\alpha + G^2)} - (\rho + k)I, \tag{2}$$

$$\frac{d\beta}{dt} = (-d_0 + r_1 G - r_2 G^2)\beta. \tag{3}$$

En este modelo se utilizan los mismos parámetros que los del modelo anterior, añadiendo el aumento de glucosa provocado por la secreción de epinefrina (G_e) y la eficiencia de la epinefrina en suprimir la secreción de

insulina (ρ), que consideran la influencia de la epinefrina. Estos parámetros se determinan con base en pruebas in vivo en sujetos sanos (hombres y mujeres). Durante la infusión de epinefrina las concentraciones de glucosa plasmática aumentan rápidamente y en 1 hora alcanzan un valor de meseta de 140 $\frac{mg}{dl}$. Mientras que una infusión de epinefrina con insulina en la sangre reduce el metabolismo de la glucosa un 41 %, es decir, la secreción de insulina por las células β se suprime y hay sensibilidad a la insulina[11][12].

Dadas estas implicaciones se asume que:

i. Solo el trauma, la excitación y el estrés son factores que desencadenan la secreción de epinefrina del riñón.
ii. La producción de glucosa del riñón inducida por la epinefrina es insignificante y se ignora.
iii. Se considera la a producción de glucosa del hígado inducida por la secreción de epinefrina proveniente del riñón.
iv. El nivel de insulina en sangre disminuirá por la supresión de epinefrina en la secreción de insulina.

En este modelo, las ecuaciones para cada dinámica (glucosa, insulina y masa de células β) se modelan con ecuaciones de balance de acuerdo a su comportamiento:

1. Concentración de glucemia en el momento $t\left(\frac{dG}{dt}\right)$. Se determina restando a la tasa de producción de glucosa su tasa de absorción, medida en $\frac{mgd}{dl}$.
2. Concentración de insulina en el momento $t\left(\frac{dI}{dt}\right)$. Se obtiene restando la tasa de aclaramiento de insulina de la tasa de secreción de insulina, medida en $\left(\frac{\mu Um}{dl}\right)$.
3. Masa de células β en el momento $t\left(\frac{d\beta}{dt}\right)$. Es el resultado de la tasa de formación de células β menos la tasa de pérdida de estas mismas, $\frac{mgdl}{dl}$.

De manera que este modelo predice que hay tres vías hacia la DM:

a. Hiperglucemia regulada. El punto fijo fisiológico se puede cambiar a un nivel hiperglucémico.

b. Bifurcación. El punto fisiológico y el punto de silla se pueden eliminar.

c. Hiperglucemia dinámica. Los defectos progresivos en la dinámica de la glucosa y/o la insulina pueden aumentar los niveles de glucosa a un ritmo inmediato que la adaptación de la masa de células β que disminuye los niveles de glucosa.

MATERIALES Y MÉTODOS

En esta sección se presentan los conocimientos necesarios para la aplicación del método de Localización de Conjuntos Compactos Invariantes (LCCI) y su aplicación para determinar el dominio de localización que contiene todos los conjuntos invariantes del sistema en estudio. Este método permite conocer el comportamiento en el corto y largo plazo de sistemas dinámicos descritos por Ecuaciones Diferenciales Ordinarias (EDOs) de primer orden[13]. En años recientes, ha sido aplicado en el estudio de diferentes sistemas dinámicos tales como sistemas biológicos que describen el desarrollo y evolución de enfermedades como el cáncer o la diabetes[14][15][16]. El método es estrictamente analítico, lo que implica que es posible encontrar la solución del problema sin la necesidad de resolver el sistema de EDOs por algún método numérico. Sin embargo, la solución numérica es utilizada para ilustrar los resultados matemáticos obtenidos, es decir, el dominio de localización y los conjuntos compactos invariantes del sistema.

Método LCCI

Inicialmente, se considera que el sistema no lineal puede ser descrito por

$$\dot{x} = F(x), \qquad (4)$$

donde $x \in R^n$, $F(x) = F(F_1(x),...,F_n(x))^T$ es un campo vectorial diferenciable. $h(x) \in C^\infty R^n$ es una función tal que h no es la primera integral de (4), es decir, su primera derivada es diferente de cero. La función h es

la función localizadora y dependiente de las variables del sistema. El objetivo de esta función es definir los supremos de cada una de las variables mediante ecuaciones y desigualdades. *S(h)* denota el conjunto $\{x \in R^n | L_F h(x)=0\}$; mientras, $L_F h(x)$ representa derivada Lie con respecto a *F*. Además, se asume que el ínfimo y el supremo quedan definidos por:

$$h_{inf} := inf\{h(x) | x \in S(h)\};$$
$$h_{sup} := sup\{h(x) | x \in S(h)\}.$$

Teorema 1,[17]. Cada conjunto compacto invariante Γ de (4) está contenido en el conjunto de localización

$$K(h)=\{h_{inf} \le h(x) \le h_{sup}\}.$$

Teorema 2,[17]. Considere $h_m(x), m=0,1,2,...$ una secuencia de funciones C^∞. Los conjuntos

$$K_0 = K(h_0), \; K_m = K_{m-1} \cap K_{m-1,m}, \; m>0,$$

con

$$K_{m-1,m} = \{x | h_{m,inf} \le h_m(x) \le h_{m,sup}\},$$

$$h_{m,sup} = S(h_m) \overset{sup}{\cap} K_{m-1} \; h_m(x),$$

$$h_{m,inf} = S(h_m) \overset{inf}{\cap} K_{m-1} \; h_m(x),$$

contienen todos los conjuntos compactos invariantes del sistema (4) y

$$K_0 \supseteq K_1 \supseteq \cdots \supseteq K_m \supseteq \cdots.$$

Positividad en sistemas no lineales

Entre la variedad de sistemas dinámicos, hay modelos que estrictamente sus potenciales soluciones deben ser positivas para ser catalogados como sistemas positivos, tal es el caso de los sistemas biológicos. Ahora, se considera un sistema dinámico descrito por:

$$\dot{x} = f(x), \qquad (5)$$

donde *f* es una función vectorial continua para un C^∞ y $x \in R^n$, es positivo si toda dinámica del sistema que

inicia en el primer ortante permanece en él, es decir, en $R^n_{+,0}$, todas sus dinámicas evaluadas a través del tiempo permanecen en este ortante. Para asegurar la positividad de un sistema dinámico, basta con revisar el Lema 1 para sistemas no lineales continuos e invariantes en el tiempo discreto.

Lema 1,[18]: Un sistema se llama positivo si y solo si R^n_+ es positivamente invariante, cumpliéndose la siguiente condición:

$$P \ \forall \ x \in \partial R^n_{+0} : x_i = 0 \ \rightarrow f_i(x) \geq 0. \qquad (6)$$

Es importante establecer que, para sistemas de índole biológico, es necesario que se cumpla el Lema 1 para aplicar funciones localizadoras lineales a través de LCCI, ya que funciones de orden superior podrían complicar el análisis matemático que se haga entorno a ambos modelos.

RESULTADOS Y DISCUSIÓN

En la Tabla 1, se muestra el tipo de estabilidad correspondiente a cada punto de equilibrio del modelo (1)-(3) después de haber aplicado el método indirecto de Lyapunov. La columna relacionada a Signos de $Re\lambda_i$, implica el signo correspondiente al valor propio obtenido por la ecuación característica.

TABLA 1. Estabilidad de los puntos de equilibrio.

	(G, I, β)	Signos de $Re\lambda_i$	Estabilidad alrededor del punto
P_1	100,11.94,358.67	$Re\lambda_1 = (-)$, $Re\lambda_2 = (-)$, $Re\lambda_3 = (-)$	Local asintóticamente estable
P_2	250, 3.58,47.27	$Re\lambda_1 = (+)$, $Re\lambda_2 = (-)$, $Re\lambda_3 = (-)$	Inestable
P_3	697.22,0,0	$Re\lambda_1 = (-)$, $Re\lambda_2 = (-)$, $Re\lambda_3 = (-)$	Local asintóticamente estable

La complejidad con el que se describe el modelo[2] es discutido solo con el análisis de los puntos de equilibrio

por lo que, la aplicación del método LCCI permite conocer las concentraciones máximas de G, I y β derivado de la influencia de la epinefrina para proponer algún tipo de controlador.

Aunado a ello, se realiza la prueba de positividad al modelo (1)-(3), es importante mencionar que en las ecuaciones (8) y (9) el valor de $G_* = \frac{dG}{dt}|_{G=0}$; satisfaciendo el Lema 1.

$$\frac{dG}{dt}\bigg|_{G=0} = R_0 + G_e - (E_{G0} + S_I I)(0) = R_0 + G_e, \qquad (7)$$

$$\frac{d\beta}{dt}\bigg|_{\beta=0} = (-d_0 + r_1 G_* - r_2 G_*^2)(0) = 0, \qquad (8)$$

$$\frac{dI}{dt}\bigg|_{I=0} = \frac{(0)\sigma G_*^2}{(\alpha + G_*^2)} - (\rho + k)(0) = 0. \qquad (9)$$

Ahora, se aplica el método LCCI proponiendo a la función localizadora $h_1 = G$, donde después de aplicar el Teorema 1 se obtiene el siguiente conjunto de localización:

$$K_1 = \left\{ G \leq h_1|_{S(h_1)} := \frac{R_0 + G_e}{E_{G0}} \right\}; \qquad (10)$$

definiendo un $G_{mín} = 0$ y un $G_{máx} \leq \frac{R_0 + G_e}{E_{G0}}$. Posteriormente se propone una segunda función localizadora $h_2 = q_1 G + q_2 \beta$, el cual mediante la aplicación del Teorema 2 se obtiene el conjunto de localización definido como:

$$K_2 = \left\{ q_1 G + q_2 \beta \leq h_2|_{S(h_2)} \cap K_1 \right\}; \qquad (11)$$

donde $h_2|_{S(h_2)} \cap K_1 = q_1 G_{máx} + \frac{q_1(R_0 + G_e)}{d_0}$, implicando que $\beta_{mín} = 0$ y $\beta_{máx} \leq q_1 \left(\frac{R_0 + G_e}{E_{G0}} \right) + \frac{q_1(R_0 + G_e)}{d_0}$.

Es importante mencionar que dentro de la función se encuentra los parámetros libres q_1 y q_2, siendo ambos parámetros positivos y puede tomar cualquier valor. Finalmente, se propone la última función localizadora $h_3 = I$, debido a que se cuenta con $G_{máx}$ y $\beta_{máx}$, esto facilita definir, mediante el Teorema 2, una región

acotada para I, la cual queda definida por el siguiente conjunto:

$$K_3 = \left\{ I \leq h_3|_{S(h_3)} \cap K_2 \cap K_1 := \frac{\beta_{max}\sigma G_{máx}^2}{\alpha + (\rho + k)} \right\}, \quad (12)$$

identificando como $I_{mín} = 0$ y un $I_{máx} \leq \frac{\beta_{máx}\sigma G_{máx}^2}{a + (\rho + k)}$.

Por lo tanto, derivado de la aplicación del método de LCCI, se establece el siguiente teorema:

Teorema 3. La localización de todos los conjuntos compactos invariantes se obtiene a través de funciones localizadoras dependientes de las variables de estado del sistema, denotado por (1)-(3), definiendo el dominio de interés del conjunto $K = \{K_1 \cap K_2 \cap K_3\}$, donde $K = G_{máx} \cap I_{máx} \cap \beta_{máx}$ debido a las funciones localizadoras h_i para $i = 1,2,3$. Donde la región de localización se satisface bajo la restricción de $\mathbf{R}_{+,0}^3$. Dado que $\mathbf{R}_{+,0}^3 = G(t) \geq 0, I(t) \geq 0, \beta(t) \geq 0$.

FIGURA 1. **Comportamiento de las trayectorias hacia el punto de equilibrio P$_1$, cuando se considera la condición inicial para *G*(0) = 200, *I*(0) = 4.5, *β*(0) = 65.**

Simulaciones numéricas

Considerando al punto de equilibrio P$_1$ de la Tabla 1, se observa en la Figura 1 que todas las trayectorias convergen a dicho punto cuando se considera la

condición inicial para $G(0) = 200$, $I(0) = 4.5$, $\beta(0) = 65$; además, se puede ver como sus trayectorias convergen al punto de equilibrio P$_1$, validando que se encuentra en el ortante positivo y es asintóticamente estable en forma local, de acuerdo con el método indirecto de Lyapunov. En la Tabla 2, se muestra el valor numérico relacionado a cada parámetro en el modelo (1)-(3). Para el desarrollo de la etapa de simulación se aplica el comando de ODE45 de MatLab para la comprobación de resultados, el cual representa el uso del algoritmo Runge-Kutta de cuarto y quinto orden, utilizando un paso de integración de 0.001.

Ahora, para pasar a la validación de los resultados del método de LCCI. En la Figura 2 se muestra el dominio de localización $K = \{K_1 \cap K_2 \cap K_3\}$ cuando se cumple la condición $d_0 + r_2 G_2 > r_1 G$, de acuerdo con los valores establecidos en la Tabla 2. Además, se presenta la primera vertiente del modelo, donde se considera $G = G_{mín}$ en la concentración máxima de β, es decir $\beta_{máx} \leq q_1\left(\frac{R_0 + G_e}{E_{G0}}\right) + \frac{q_1(R_0 + G_e)}{d_0}$.
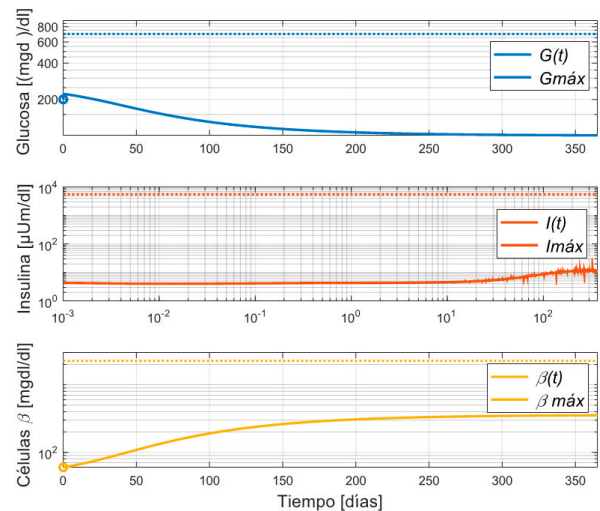
FIGURA 2. **Dominio de localización para cada variable de estado cuya trayectoria se encuentra contenida, es decir, se muestra el dominio de localización del modelo (1)-(3) implicando que se tiene un *G$_{máx}$*, *I$_{máx}$* y *β$_{máx}$*; satisfaciendo el Teorema 3 mediante el Teorema 1 y Teorema 2.**

Parámetro	Descripción	Valor	Unidad
R_0	Tasa neta de producción de glucosa a $G = 0$	864	$\dfrac{mgd}{dl}$
E_{G0}	Eficacia total de la glucosa a $I = 0$	1.44	d^{-1}
S_I	Sensibilidad total a la insulina	0.72	$\dfrac{ml\mu}{dU}$
σ	Tasa máxima de secreción de insulina por las células β	43.2	$\dfrac{\mu Um}{dl}$
α	Punto de inflexión de la función sigmoidea	20,000	$\dfrac{mg^2 dl}{l^2}$
k	Tasa de aclaramiento de I para músculos, hígado y riñones	432	d^{-1}
d_0	Tasa de muerte natural de células β	0.06	d^{-1}
r_1	Rango de tolerancia a la glucosa de las células β	0.00084	$\dfrac{mdl}{dg}$
r_2	Rango de tolerancia a la glucosa de las células β	0.0000021	$\dfrac{mgl^2}{dg^2}$
G_e	Aumento de glucosa debido a la secreción de epinefrina	140	$\dfrac{mgd}{dl}$
ρ	Eficacia de la epinefrina en suprimir la secreción de I	41	%

Utilizando las mismas condiciones iniciales que en la Figura 1, se muestran las trayectorias de $G(t)$, $I(t)$ y $\beta(t)$, que se encuentran por debajo de los valores obtenidos para cada concentración máxima que en este caso son $G_{máx} \leq 697.22$, $I_{máx} \leq 42326.15$ y $\beta_{máx} \leq 17430.55$. Así mismo, en el la Figura 3 se muestra que todas las trayectorias se encuentra en el ortante positivo y es asintóticamente estable de forma local; además, se observa el dominio de localización que contienen a las trayectorias del modelo (1)-(3), satisfaciendo el Teorema 3 cuando se considera el punto de equilibrio P_3.
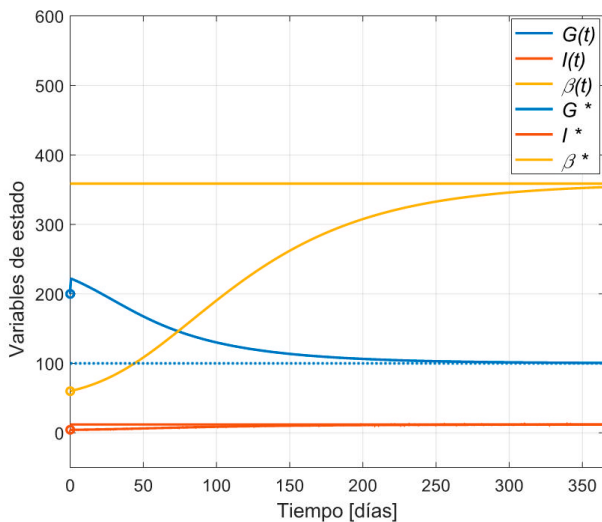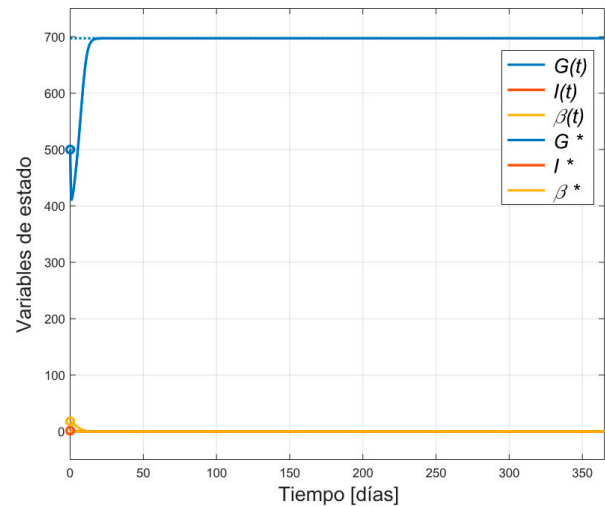

FIGURA 3. **Comportamiento de las trayectorias hacia el punto de equilibrio P_3, cuando se considera la condición inicial para $G(0) = 500$, $I(0) = 1.5$, $\beta(0) = 18$.**

CONCLUSIONES

El modelo analizado en este estudio contiene tres puntos de equilibrio en el ortante positivo, los cuales son influenciados por el aumento de glucosa debido a la secreción de epinefrina (Ge) y la eficacia de la epinefrina en suprimir la secreción de insulina (ρ); a través de las funciones localizadoras se obtienen las condiciones de su dominio de localización definido por $K = \{K_1 \cap K_2 \cap K_3\}$. Este tiene dos vertientes para la condición de $\beta_{máx}$ en presencia de epinefrina. Donde las condiciones de este modelo se ven influenciadas por los parámetros Ge y ρ, por lo que se muestra un aumento de sus valores con respecto a los establecidos en el modelo antecesor[6].

Es importante mencionar que la ecuación que corresponde a la masa de células β ($d\beta$) tiene cambios de signo y es igual para ambos modelos, porque representa la muerte de células β y su replicación (considerando la reducción cuando hay hiperglucemia) mediante un polinomio que no incluye la influencia de la epinefrina. Esta característica particular provoca que haya limitaciones al proponer y seleccionar la función localizadora h_2, esto debido a que la mayoría llevan a un resultado donde la condición de $\beta_{máx}$ es negativa, que biológicamente no es posible.

De acuerdo a lo establecido en el marco teórico del modelo[2], un suministro de epinefrina (causado por activación emocional) produce un incremento en la concentración de glucosa y disminuye la secreción de insulina por las células β. Sin embargo, al obtener los puntos de equilibrio y las condiciones de su dominio de localización de este modelo (sus concentraciones máximas de G, I y β) se demuestra que hay un aumento en los niveles de tres variables en comparación con los obtenidos del modelo de Topp donde, se esperaría que los valores de I fueran menores.

Por último, para llevar a cabo las simulaciones numéricas se consideran condiciones iniciales que son cercanas a sus puntos de equilibrio. Se observa que el comportamiento de las variables con respecto al tiempo siempre converge al mismo punto de equilibrio, el cual se considera asintóticamente estable en forma local (P_1 o P_3) con esas condiciones y las trayectorias son similares entre modelos por lo que, la epinefrina no provoca grandes cambios en esto. Sin embargo, la influencia de la epinefrina en esta dinámica provoca un aumento en el valor de los puntos de equilibrio y las concentraciones máximas de G, I y β, como puede ser observado en las Figuras 1-2.

Como trabajo a futuro se pretende analizar otra variante del modelo, considerando la propuesta en[19]. Además, plantear otros valores positivos para los parámetros q_1 y q_2 de la función localizadora h_2, los cuales se consideran como $q_1 = q_2 = 1$ y determinar su influencia en los niveles máximos de cada concentración. Adicionalmente, se buscará analizar los modelos considerando la presencia de una entrada de control en la variable de insulina (I), para determinar si existe la posibilidad de diseñar una ley de control considerando el parámetro de epinefrina. Este trabajo de investigación se encuentra distante de implementar hipotéticamente un páncreas artificial mediante una discusión matemática, sin embargo, las implicaciones matemáticas obtenidas contribuyen para el desarrollo de algún entrenamiento computacional[20], el cual permita diseñar una ley de control considerando el parámetro de epinefrina. Así mismo, se establece un preámbulo matemático el cual permite ser una referencia para el simulador UVA/Padova[21]; analizando el comportamiento de la epinefrina considerando a un conjunto de células pancreáticas.

AGRADECIMIENTOS

CONTRIBUCIÓN DE LOS AUTORES

D. G. conceptualización, análisis formal del modelo, estado del arte, escritura y edición del borrador del manuscrito. P. J. C. validación, organización de información, edición, revisión y correcciones del manuscrito.

REFERENCIAS

[1] A. Basto-Abreu, N. López-Olmedo, R. Rojas-Martínez, C. A. Aguilar-Salinas, *et al.*, "Prevalencia de prediabetes y diabetes en México: Ensanut 2022," Salud Publica Mex, vol. 65, pp. s163-s168, jun. 2023, doi: **https://doi.org/10.21149/14832**

[2] I. I. Mohammed, I. Adamu, S. J. Barka, "Mathematical model for the dynamics of glucose, insulin and β-cell mass under the effect of trauma, excitement and stress," Model. Numer. Simul. Mater. Sci., vol. 9, no. 4, pp. 71-96, oct. 2019, doi: **https://doi.org/10.4236/mnsms.2019.94005**

[3] O. A. Montesinos-López, C. M. Hernández-Suarez, "Modelos matemáticos para enfermedades infecciosas," Salud Publica Mex., vol. 49, no. 3, pp. 218-226, jul. 2007. [En línea]. Disponible en: **https://www.scielo.org.mx/scielo.php?script=sci_arttext&pid=S0036-36342007000300007**

[4] E. F. Panqueba Moreno, J. M. Ruiz Vera, "Control óptimo de la glucosa en la sangre mediante infusión continua de insulina," Ciencia Desarro., vol. 13, no. 2, pp. 49-67, jul. 2022, doi: **https://doi.org/10.19053/01217488.v13.n2.2022.14173**

[5] F. X. Méndez-Carrillo, M. Beléndez-Vázquez, "Variables emocionales implicadas en el control de la diabetes: estrategias de intervención," An. Psicol., vol. 10, no. 2, pp. 189-198, 1994. [En línea]. Disponible: **https://revistas.um.es/analesps/article/view/29671**

[6] M. Zahedi, S. Kordrostami, M. Kalantarhormozi, M. Bagheri, "A Review of Hyperglycemia in COVID-19," Cureus, vol. 15, no. 4, pp. 1-7, 2023, doi: **https://doi.org/10.7759/cureus.37487**

[7] M. Sirlanci, M. E. Levine, C. C. Low Wang, D. J. Albers, A. M. Stuart, "A simple modeling framework for prediction in the human glucose-insulin system," Chaos, vol. 33, no. 7, art. no. 073150, jul. 2023, doi: **https://doi.org/10.1063/5.0146808**

[8] S. V. K. R. Rajeswari, P. Vijayakumar, "Mathematical Approaches in the Study of Diabetes Mellitus," in Computer Vision and Robotics. Algorithms for Intelligent Systems, Lucknow, India, 2023, pp. 229-248, doi: **https://doi.org/10.1007/978-981-19-7892-0_18**

[9] J. M. Munoz-Pacheco, C. Posadas-Castillo, E. Zambrano-Serrano, "The effect of a non-local fractional operator in an asymmetrical glucose-insulin regulatory system: Analysis, synchronization and electronic implementation," Symmetry, vol. 12, no. 9, art. no. 1395, 2023, doi: **https://doi.org/10.3390/sym12091395**

[10] B. Topp, K. Promislow, G. DeVries, R. M. Miura, D. T. Finegood, "A model of β-cell mass, insulin, and glucose kinetics: pathways to diabetes," J. Theor. Biol., vol. 206, no. 4, pp. 605-619, oct. 2000, doi: **https://doi.org/10.1006/jtbi.2000.2150**

[11] D. Laurent, K. F. Petersen, R. R. Russell, G. W. Cline, G. I. Shulman, "Effect of epinephrine on muscle glycogenolysis and insulin-stimulated muscle glycogen synthesis in human," Am. J. Physiol., vol. 274, no. 1, pp. 130-138, 1998, doi: **https://doi.org/10.1152/ajpendo.1998.274.1.E130**

[12] D. C. Deibert, R. A. Defronzo, "Epinephrine-induced insulin resistance in man," J. Clin. Invest., vol. 65, no. 3, pp. 717-721, 1980, doi: **https://doi.org/10.1172/JCI109718**

[13] A. P. Krishchenko, "Localization of Invariant Compact Sets of Dynamical Systems," Differ. Equ., vol. 41, no. 12, pp. 1669-1676, 2005, doi: **https://doi.org/10.1007/s10625-006-0003-6**

[14] D. Gamboa, C. E. Vázquez, P. J. Campos, "Nonlinear Analysis for a Type-1 Diabetes Model with Focus on T-Cells and Pancreatic β-Cells Behavior," Math. Comput. Appl., vol. 25, no. 2, pp. 23, 2020, doi: **https://doi.org/10.3390/mca25020023**

[15] D. Gamboa, C. E. Vázquez-López, R. Gutierrez, P. J. Campos, "Nonlinear Analysis of the C-Peptide Variable Related to Type 1-Diabetes Mellitus," Symmetry, vol. 13, no. 7, pp. 1238, 2021, doi: **https://doi.org/10.3390/sym13071238**

[16] D. Gamboa, L. N. Coria, P. A. Valle, "Ultimate Bounds for a Diabetes Mathematical Model Considering Glucose Homeostasis," Axioms, vol. 11, no. 7, art. no. 320, 2022, doi: **https://doi.org/10.3390/axioms11070320**

[17] A. P. Krishchenko, K. E. Starkov, "Localization of compact invariant sets of the Lorenz system," Phys. Lett. A, vol. 353, no. 5, pp. 383-388, 2006, doi: **https://doi.org/10.1016/j.physleta.2005.12.104**

[18] K. E. Starkov, "On dynamic tumor eradication conditions under combined chemical/anti-angiogenic therapies," Phys. Lett. A, vol. 382, no. 6, pp. 387-393, 2018, doi: **https://doi.org/10.1016/j.physleta.2017.12.025**

[19] K. Saranya, T. Iswarya, V. Mohan, K. E. Sathappan, L. Rajendran, "Mathematical modeling of Glucose, Insulin, β-Cell Mass: Homotopy Perturbation Method Approach," Eur. J. Mol. Clin. Med., vol. 07, no. 02, pp. 3513-3530, 2020. [En línea]. Disponible en: **https://ejmcm.com/uploads/paper/ca3ad85a4a3175b4f8ac48ac1f80300c.pdf**

[20] P. G. Jacobs, P. Herrero, A. Facchinetti, J. Vehi, *et al.*, "Artificial intelligence and machine learning for improving glycemic control in diabetes: best practices, pitfalls and opportunities," IEEE Rev. Biomed. Eng., pp. 19-41, 2023, doi: **https://doi.org/10.1109/RBME.2023.3331297**

[21] C. Cobelli, B. Kovatchev, "Developing the UVA/Padova Type 1 Diabetes Simulator: Modeling, Validation, Refinements, and Utility," J. Diabetes Sci. Technol., vol. 17, no. 6, pp. 1493-1505, 2023, doi: **https://doi.org/10.1177/19322968231195081**

Use of Biomedical Engineering for Rehabilitation of Patients with Disability Caused by Guillain-Barré Syndrome: a Systematic Review

Uso de la Ingeniería Biomédica para Rehabilitación de Pacientes con Discapacidad Causada por el Síndrome de Guillain-Barré: Una Revisión Sistemática

Andrés Burjand Torres-Reyes [1] (iD), Ivette Reyes-Hernández [1] (iD), Omar Arturo Domínguez-Ramírez [1] (iD) (✉)
Ana María Tellez-Lopez[1] (iD)

[1]Universidad Autónoma del Estado de Hidalgo, Hidalgo - México

ABSTRACT

This systematic review aims to assess the extent to which biomedical engineering has been applied in the rehabilitation of patients suffering from Guillain-Barré Syndrome (GBS), given the scarcity of information on this topic. We conducted a thorough analysis of research articles, conference abstracts, and case reports published between 2000 and 2023, specifically from ScienceDirect, PubMed, IEEE Xplore, Springer, and Dimensions. 19 articles were extensively discussed, complemented by an additional 40 information sources providing supplementary information. Each paper underwent a meticulous review process by the four authors, where each separately examined the title and abstract of the papers and subsequently provided a thorough examination of the full text; when conflicts arose, a clear consensus was reached through discussion. The analysis of the articles revealed a notable improvement in upper and lower limb function of GBS patients that was facilitated by both custom-made and commercial devices. Likewise, a small handful of other devices have been used (e.g., to improve urinary retention issues). There is a clear opportunity for new research, innovation and applications.

KEYWORDS: Biomedical engineering, Guillain-Barré Syndrome, neurorehabilitation, rehabilitation device

RESUMEN

Esta revisión sistemática tiene como objetivo evaluar hasta qué punto se ha aplicado la ingeniería biomédica en la rehabilitación de pacientes que padecen el Síndrome de Guillain-Barré (SGB), dada la escasez de información sobre este tema. Realizamos un análisis exhaustivo de artículos de investigación, resúmenes de conferencias e informes de casos publicados entre 2000 y 2023, específicamente de ScienceDirect, PubMed, IEEE Xplore, Springer y Dimensions. Se discutieron ampliamente 19 artículos, complementados con 40 fuentes de información adicionales. Cada artículo pasó por un meticuloso proceso de revisión por parte de los cuatro autores, donde cada uno examinó por separado el título y el resumen de los artículos y posteriormente proporcionó un examen exhaustivo del texto completo; cuando surgieron conflictos, se alcanzó un consenso mediante la discusión. El análisis de los artículos reveló una mejora notable en la función de las extremidades superiores e inferiores de los pacientes con SGB que fue facilitada por dispositivos tanto hechos a medida como comerciales. Asimismo, se han creado un pequeño puñado de otros dispositivos, (por ejemplo, para mejorar los problemas de retención urinaria). Existe una clara oportunidad para nueva investigación, innovación y aplicaciones.

PALABRAS CLAVE: dispositivo de rehabilitación, Ingeniería Biomédica, Síndrome de Guillain-Barré, neurorrehabilitación

Corresponding Author

TO: **Omar Arturo Domínguez-Ramírez**

INSTITUTION: **Universidad Autónoma del Estado de Hidalgo**

ADDRESS: **Carretera Pachuca-Tulancingo Km. 4.5, Colonia Carboneras, Mineral de la Reforma, Hidalgo, C.P. 42184, México**

EMAIL: **omar@uaeh.edu.mx**

INTRODUCTION

Rationale

Guillain-Barré Syndrome (GBS) is a prevalent cause of acute flaccid paralysis, distinguished by symmetrical weakness of the limbs, and hyporeflexia or areflexia [1][2][3][4]. Reports of GBS date back to the second half of the 19th century, and it has been formally investigated since 1916 [3]. Infection or other immune-related stimulation that causes an atypical autoimmune response that targets peripheral nerves and their spinal roots is often what precedes it [2][5]; more than 90 % of patients reach the peak of the disease severity between 2 and 4 weeks since the sickness debuts [6]. There are multiple clinically distinguishable subtypes of GBS: Acute inflammatory demyelinating polyradiculoneuropathy (AIDP), the most common; Miller- Fisher Syndrome (MFS); Acute motor axonal neuropathy (AMAN); Acute motor sensory axonal neuropathy (AMSAN); Bickerstaff's Encephalitis (EB); and Pharyngeal-cervical- brachial weakness [1][6][7][8].

The symptoms of GBS vary depending on the subtype. Taking AIDP, for example, the aberrant immune response consists mainly in the degradation of the patient's myelin [9], this reports in paresthesia in feet and fingertips followed by symmetrical or slightly asymmetrical weakness in lower limbs that can ascend to the upper limbs in a matter of hours or days, and even affect the respiratory system muscles in severe cases [1][6][10][11].

GBS treatment generally combines multidisciplinary supportive medical care and immunotherapy. Recognized as the most effective treatments: Intravenous Immunoglobulin (IVIg) and plasma exchange are the most common and have proven to be very effective, especially if they are started within the first 2 weeks of the disease's debut [1][12]. Although the majority of cases report a complete or partial recovery of the patients, with very few resulting in death, many of the affected individuals obtain a residual deficit that impacts their living conditions. For instance, 20 % of GBS patients still require assistance walking six months after their sickness first manifested. Reduced muscular strength, sensory indications, weariness, and discomfort are the most typical remaining deficiencies [1][13][14].

Currently, the GBS rehabilitation process is based primarily in a multidisciplinary set of interventions, conducted mainly by neurologists and rehabilitation physicians. The main goal is to give the patient back a partial or complete autonomy and the ability to carry out normal life activities. According to the requirements of the particular patient, this may also include nursing care, nutritionist guidance, psychotherapy, speech therapy, and social rehabilitation in addition to physical or occupational therapy and exercise regimens. One of the main problems is that since multidisciplinary rehabilitation varies markedly between regions, it is challenging to design research trials to properly assess the effectiveness of the rehabilitation [10][11].

Another common rehabilitation approach for GBS is exercise [15]. For example, in a Dutch study, 20 GBS patients who complaint mainly of fatigue had an intervention consisting of three 45-minute sessions weekly for 12 weeks, the target was to increase heart rate from 65 % to 90 % of maximal heart rate, and during that period the workload was gradually increased. As a consequence, there was less fatigue, more isokinetic muscular strength, and a higher peak oxygen uptake [10][15][16].

Neuromuscular electrical stimulation has been a remarkable ally in GBS rehabilitation as well, especially for patients with a delicate state of health or an acute paralysis [10]. Without the patient's involvement, muscle contractions can be induced via neuromuscular electrical stimulation (NMES). In the acute stage of GBS, until patients have adequately recuperated to start a multidisciplinary rehabilitation effort, this may be an alternate treatment approach that can minimize inactivation and denervation waste [10][17].

Besides these approaches for GBS rehabilitation, there are some cases where biomedical engineering is applied in neurorehabilitation for this disease, however, these cases not only are scarce compared to the use of traditional rehabilitation but they are also little studied, hence the need for a systematic review for the analysis of the current state of the art.

Objective

This systematic review targets to respond the question "How has biomedical engineering been used for the rehabilitation of patients with disability caused by Guillain-Barré?" and to provide a broad perspective on the knowledge that is presently available on the subject. It seeks to give a solid platform for decision-makers, therapists and future investigations for the development of better neurorehabilitation methods based on biomedical engineering in GBS.

MATERIALS AND METHODS

Review design and search strategy

This systematic review was developed in concordance with the Preferred Reporting Items for Systematic Reviews and Meta- Analyses (PRISMA) 2020 statement guidelines [18], over three months: from April to June of 2023. Five databases were used in total: ScienceDirect, PubMed, IEEE Xplore, Springer and Dimensions. The guiding question for the review design and execution was: "How biomedical engineering has been used for the rehabilitation of patients with disability caused by Guillain-Barré?".

The investigation was performed using a search equation combining Boolean operators and focused on three key terms, and was stated as follows: ("Guillain Barré" OR "Acute inflammatory demyelinating polyradiculoneuropathy" OR "Miller-Fisher Syndrome" OR "Acute motor sensory axonal neuropathy" OR "Acute motor axonal neuropathy") AND (rehabilitation OR recovery) AND ("biomedical engineering" OR "electronic device" OR "haptic device" OR "neuromodula-

tion" OR "virtual environment" OR "telemedicine" OR "artificial intelligence" OR "internet of things" OR "wearable device" OR "robot" OR "biomedical transducer"). The key terms related to biomedical engineering were selected by using the IEEE Taxonomy.

The overall procedure for recognizing relevant articles was: (I) literature search in designated databases applying eligibility criteria; (II) export of results in reference files and import to specialized software for literature reviews (Rayyan); (III) removal of duplicates; (IV) selection of articles by title and abstract; (V) selection of articles by full-text analysis; (VI) detection of any additional relevant papers using the snowball technique.

This academic work is exempt from Institutional Review Board clearance because it is a systematic review.

Eligibility Criteria

Inclusion criteria:
•Research articles, conference abstracts and case reports released in full text between 2000 and 2023 in English.
•Articles published in peer-reviewed journals.
•Articles about rehabilitation of patients with disability caused by Guillain-Barré Syndrome using biomedical engineering.

Exclusion criteria:
•Review articles, mini-reviews, systematic reviews, books, editorials, encyclopedia, discussions and correspondence.

Selection

After the database search, each article was subject to a manual filtration process by analyzing the title and abstract, followed by a full-text selection. Every article was scrutinized independently by the four authors, and when conflict arose, consensus was achieved through discussion.

The selection of papers, in both processes, was conducted considering the eligibility criteria and the focus of the research question.

Data extraction

Data were obtained from eligible papers using a standardized format based on the PRISMA guidelines where a variety of key summarizing points of information were collected; this was carried out by the three reviewers. The variables determined useful to extract from each article were: Author(s), publication date, country (or region where the research was conducted), objective, patients, brief description of the biomedical engineering device, methodology, results and conclusions. The result of this extraction is exposed in Table 1.

Quality assessment of the included articles

To assess the quality of the articles it was used the "Checklist for assessing the quality of quantitative studies" of the "Standard Quality Assessment Criteria for Evaluating Primary Research Papers from a Variety of Fields", developed by Kmet, Lee and Cook in collaboration with the Alberta Heritage Foundation for Medical Research [19]. This checklist consists of 14 items stated as follows: I1: Question/objective sufficiently described. I2: Study design evident and appropriate. I3: Method of subject/comparison group selection or source of information/input variables described and appropriate. I4: Subject (and comparison group, if applicable) characteristics sufficiently described. I5: If interventional and random allocation was possible, was it described? I6: If interventional and blinding of investigators was possible, was it reported? I7: If interventional and blinding of subjects was possible, was it reported? I8: Outcome and (if applicable) exposure measure(s) well defined and robust to measurement/misclassification bias. Means of assessment reported. I9: Sample size appropriate. I10: Analytic methods described/justified and appropriate. I11: Some estimate of variance is reported for the main results. I12: Controlled for confounding. I13: Results reported in sufficient detail. I14: Conclusions supported by the

results. This checklist consists of 14 items. All the papers with 80% or more of positive results were included.

RESULTS AND DISCUSSION

Search results

The database search using the Boolean equation yielded a total of 24,691 papers, with most articles found in Dimensions (23,818). However, after applying filtration based on the inclusion and exclusion criteria, only 2,237 remained. Of this total, 179 were duplicates, and the rest underwent analysis based on title and abstract, resulting in 154 papers. The next step involved a thorough examination of the full text of these articles to determine their usefulness for the review. Additionally, the snowball technique was employed by reviewing the references. Following this process, 19 articles were selected for inclusion in the systematic review. These selected articles were used to summarize the information using the pre-defined focus variables (refer to Table 1). The PRISMA flow diagram in Figure 1 illustrates the selection steps and results, providing reasons for excluding 135 out of the 154 articles.

Quality and Reliability of Results

The included studies' quality was analyzed using the Checklist for assessing the quality of quantitative studies and the conclusions are reflected in Table 2. Figure 2 exhibits how many of the 19 articles are JCR and the number of articles that correspond to Quartile 1, 2, 3 or 4.

Summarized results obtained from the articles

The analyzed 19 studies have been described in Table 1 reporting the chosen variables: Author(s), publication date, country (or region where the research was conducted), objective, patients, a brief description of the biomedical engineering device, methodology, results, and conclusions.
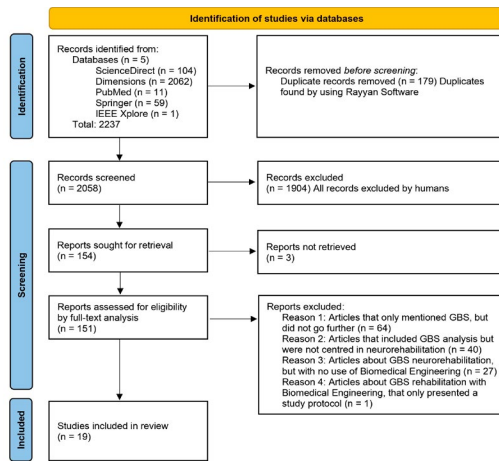
FIGURE 1. PRISMA flow diagram for the steps followed to obtain the selection of eligible papers [18].
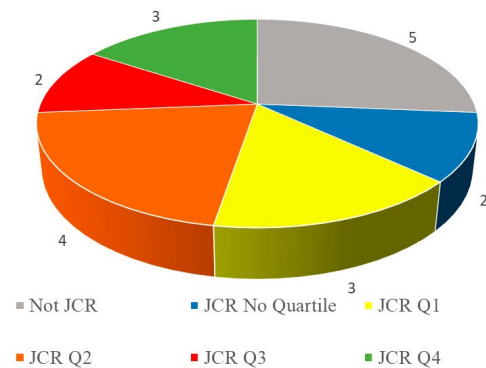
FIGURE 2. Pie chart of the JCR quartiles the journals of the presented articles belong to.

Global distribution of the studies

The presented studies took place in 11 countries (Figure 3), although, in many cases, researchers of the same study came from different Universities, regions and even from different countries. The place where more studies were conducted was Zürich, Switzerland, with a total of 4.
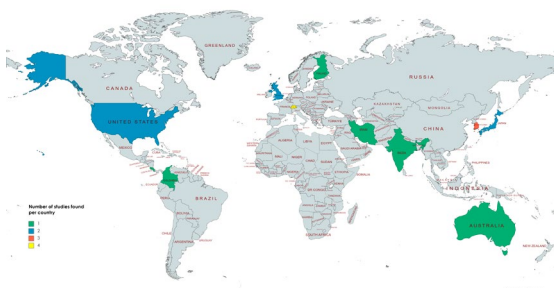
FIGURE 3. Map of the countries where the studies took place.

Discussion

The need to organize information on GBS and its treatments is necessary for progress and future advances. This systematic review started with the of how biomedical engineering has been utilized towards the rehabilitation of patients with Guillain-Barré and the path to answer it start with a search equation divided into three parts: 1.- The disease and its most common subtypes (GBS), 2.- the key objective in relation to this disease (to rehabilitate) and 3.- the instruments to achieve it via biomedical technologies. A minor detail worth mentioning is that one of the used databases, Science Direct, has a limit of Boolean operators, but by repeating the search while rotating the terms the same result was achieved as if it did not have this restriction. It is plausible to criticize this search equation for being slightly general, however, the researchers have determined that there is not enough information about this topic, thus warranting a reasonably general search equation that translates into more results and meticulous screening.

Regarding search results, it is interesting how few eligible studies were obtained, despite the 22-year span that was examined. This could indicate, contextualized within this systematic review, a lack of development of this field and, therefore, a significant area of future study.

Concerning the reliability of the obtained articles, 14 of the journals are included in the Journal Citation Reports [39], half of them in quartiles 1 and 2, which is a recognized standard for research quality. This indicates that the articles probably contain reliable information, but it does not mean they are not subject to possible bias. The use of the Checklist developed by Kmet, Lee and Cook also revealed the excellent quality of the articles.

Only 5 articles provided complete information on the sex, age, height and weight of the patients [20][21][22][23][24].

Considering articles that provided data on the sex of the GBS patients, there were in total 13 male [20][21][22][23][24][25][26][27][28][29][30] and 2 female patients [31][33] examined throughout these investigations. Analyzing the articles that provided data about patient's ages, the age ranged from 7 to 86 years old, with the mean being 39.5 years.

The main area targeted by the studies was the lower limbs, eleven studies [20][21][22][23][24][26][27][28][30][33][34] worked with biomedical devices that helped patients' rehabilitation in this area. Six studies focused on the upper limbs [25][29][32][35][36][37]. Céspedes *et al.* [38] worked on a Socially Assistive Robot using a NAO platform, and even though the subjects were focused on lower-limb rehabilitation, the purpose of the platform is to be an assistant therapist that makes observations and gives feedback to the patient. Wosnitzer *et al.* [31] used neuromodulation to attend urinary retention aiming the study at the sacral nerves. The area that more studies targeted was the lower limbs, which is consistent with the data that the most common disability amongst GBS patients is weakness or partial or complete paralysis in legs [5][7]. Most studies only included male GBS patients, solely two women were mentioned as subjects. This observation aligns with the fact that, unlike other auto-immune diseases, GBS is significantly more frequent in men than in women [11][40].

Of the 19 studies, 12 took place in countries that, according to the United Nations' "World Economic Situation and Prospects 2022" [41] are developed economies: Switzerland, Japan, United States of America (USA), Australia, Finland and United Kingdom (UK), the first one being the one where more investigations were conducted: four. The remaining 7 took place in countries with developing economies, all of which hosted one study, except for South Korea, where 3 took place. A possible connection between the number of studies for each continent and the density of incidences of GBS cases could be theorized, nonetheless, the data does not reveal one: The continents with more studies were Asia and Europe, each with 7, however,

the statistics show that in these regions the range of incidences per 100,000 habitants is 0.44-3.25 and 0.84-1.91, respectively. In South America, where only 2 researches were found, the range is 5.6-7.63 per 100,000 habitants [41]. Probably the real reason behind the differences in the number of studies are population and economic development: In Asia lives more than half of the planet's population [42], Japan is one of the world's leading economies and India, South Korea and Iran are thriving developing economies [41] that excel in technology and science; Europe's population is almost twice of that of South America [42], and Finland, UK and Switzerland are three formidable developed economies with high per capita income [41].

The variety excels in the presented studies in terms of the biomedical engineering devices utilized. Ten of the devices were custom-made systems, tested in the same article [20][21][22][24][25][29][32][35][36][37]. The other seven devices were acquired commercially [23][26][27][28][30][31][33][34][38]. Two of these devices were used in different studies: Morning Walk was the protagonist in two papers [33][34], and Lokomat was the main device in two studies as well [26][28]. However, it was also employed to test the NAO platform as a therapy assistance robot in a third study [38].

There were a total of four devices based on haptics and virtual reality, with one focusing on lower limb rehabilitation [20] and the other three concentrating on upper limb rehabilitation [29][32][36]. All of them paid close attention to the issue of patient motivation during therapy, particularly the PITS [29], which centered on pediatric rehabilitation. The developers applied principles of serious game development, as the main objective and the entire experience are designed to aid in rehabilitation while still maintaining motivation through an enjoyable gaming experience. The positive results obtained in the studies demonstrate the usefulness of specific-purpose video games in rehabilitation, a concept supported by research such as the one conducted by Ong *et al.* [43].

TABLE 1. Analyzed articles summarized. Note: Height is expressed in centimeters and weight in kilograms.

Reference	Author(s) and year	Goal	Patient(s)	Brief description of the biomedical engineering system	Methodology	Results	Conclusions
[20]	Albiol-Pérez S., Forcano-García M., Muñoz-Tomás M., Manzano-Fernández P., Solsona-Hernández S., Mashat M. A., Gil-Gómez J. A. 2014.	Try out a virtual motor rehabilitation program to boost patient compliance and enhance therapeutic outcomes.	**Patient one:** Male, (Subtype) MFS, (Age) 54, (Height) 174.9, (Weight) 75.5, (Time since hospitalization) 5 months. **Patient two:** Male, (Age) 33, (Height) 168.8, (Weight) 94, (Time since hospitalization) 4 months.	**Active Balance Rehabilitation (ABAR):** Various virtual settings emphasizing weight transference and specific motions. It includes two difficulty levels and six interactive games. The budget-friendly hardware comprises a 47-inch TV, a PC, a WBB, and a Bluetooth dongle.	Twenty sessions, thrice weekly: 30 minutes for conventional rehab, 30 minutes for VMR (Virtual Motor Rehabilitation) with ABAR. Static balance work involves lateral and forward-backward weight shifts. Dynamic balance work includes single-leg stance and sit-to-stand movements. Patients began with cognitive and functional tests, along with static and dynamic balance assessments; these tests were repeated at the final and follow-up stages.	**Patient one** demonstrates autonomous ambulation under therapist supervision, ascending and descending stairs, and traversing slopes, with notable enhancements in shoulder muscle mass and joint range. Persistent upper limb motor coordination disorders are observed. **Patient two** attains independent ambulation, negotiating stairs and slopes, displaying augmented muscle strength in the left ankle. Despite progress, persistent hypoesthesia is noted in fingertips, foot soles, and heels.	VMR presents a groundbreaking contribution to GBS patient rehabilitation, demonstrating suitability and effectiveness. However, a notable limitation is the diminished sample size. Clinical experts advocate the exploration of additional modules to augment the dynamic recovery process.
[21]	Fang Y., Lerner Z.. 2021.	**(1)** To compare the influence of bilateral ankle exoskeleton support with assistance limited to the paretic limb on walking performance. **(2)** To validate the effectiveness of a real-time ankle-moment-adaptive exoskeleton control system for assisting hemiparetic gait.	* (1 GBS out of 3 subjects) GBS patient: Male, (Age) 65, (Weight) 93.5, (Height) 173, (Time since injury) 5 years. Disability scale: 2. Primarily unilateral gait deficit due to hemiparesis.	An unattached ankle exoskeleton weighing 2.6 kg, powered by a 2 Ah Li-ion battery. It delivers plantar and dorsiflexor ankle support through brushless DC motors (Maxon) situated in a waist assembly, utilizing Bowden cable transmission. The system incorporates a custom PCB housing motor driver, a microcontroller, signal processing components, and a Bluetooth transceiver.	Each session comprises initial acclimatization and a rest period exceeding 20 minutes. Formal data collection involves three 6-minute randomized walking scenarios: baseline walking with shoes lacking the mechanism, walking with exoskeleton support limited to the paretic limb, and bilateral walking with the device supporting both sides. Participants subsequently undergo 6-minute walk test trials in each circumstance within a 25-meter corridor.	GBS patients exhibited a preference for exoskeletal assistance limited to the paretic limb on the treadmill, with no discernible preference on solid ground. The adaptive system demonstrated efficacy in facilitating walking. In enhancing clinically pertinent treadmill and over-ground walking performance, bilateral support frequently exhibited greater reliability than unilateral assistance.	Three individuals exhibiting hemiparetic gait underwent validation of the ankle-moment-adaptive exoskeleton controller. The results underscored the safety and efficacy of both bilateral and paretic-limb-only support in enhancing overall ankle function, overground walking speed, and treadmill performance.
[25]	Lee K., Park J., Beom J., Park H. 2018	To create and assess a passive shoulder joint tracking system that accounts for gravity and enables three-DOF shoulder joint movement.	* (1 GBS out of 19 subjects, 8 healthy) One male GBS patient.	**Shoulder Joint Tracker:** Primarily comprises a horizontal tracker featuring a two-link mechanism and a vertically oriented tracker supported by a compressive spring composed of interconnected small spring segments.	The tracker underwent evaluation through two key shoulder movements—flexion/extension and abduction/adduction—via a three-DOF motion capture experiment utilizing the J-Wrex and CPM rehabilitation systems. The experiments were conducted in three setups: unrestricted motion without any device, motion aided by the device alongside the tracker, and motion assisted solely by the existing device.	The tracker exhibited high efficacy in tracking arm movements. Analysis of the Glenohumeral (GH) joint's Range of Motion (ROM) focused on determining the arm elevation ROM common to all three conditions. The range of motion in the inferior–superior direction was more extensive in both healthy individuals and patients compared to the transversal direction. Although the ROM in the absence of the tracker was generally minimal, it was nearly identical for both the unrestricted and tracker-assisted conditions.	GH joint tracking performance was experimentally validated. The tracking module, by achieving increased range of motion with reduced power consumption for the same rehabilitation tasks, has the potential to enhance the comfort and efficacy of shoulder rehabilitation.
[35]	Kauhanen L., Jylänki P., Lehtonen J., Rantanen P., Alaranta H., Sams M. 2007.	Developing a Brain-Computer Interface (BCI) enabling tetraplegic individuals to operate it within a brief thirty-minute timeframe.	* (1 GBS out of 6 subjects) Subject S2: (Age) 59, (Time since injury) 1.5 years	**TKK-BCI system:** The client obtained EEG signals via TCP/IP, with the server collecting them in 20-ms data packets. Upon accumulating sufficient packets for feature extraction, MATLAB was employed for analysis. Post-categorization of the data, the client received the results and provided user feedback.	Subjects used EEG signals to guide a circle from the screen center to specific locations on each side by performing rapid movements with their right or left hands. Movements included fist closure, finger raising, and pinching. Participants were instructed to choose a specific movement and maintain it throughout the trial (S2 chose fist closure).	S2 was able to perform 10 correct games vs 1 mistake. The other subjects had a ratio correct/incorrect of: 15/0, 8/1, 3/0, 1/2, 9/5.	Participant S2 successfully acquired the ability to use a BCI during a series of five to seven training sessions, each lasting four minutes.

[33]	Choi S., Kim S. W., Jeon H. R., Lee J. S., Kim D. Y. 2019.	To evaluate the viability and effectiveness of utilizing Robot-Assisted Gait Training (RAGT)	* (7 GBS out of 189 subjects) 7 GBS patients (Ages) Between 31.6 and 71.6 years,	**Morning Walk®:** is an end-effector robot featuring a saddle seat for body support. Its autonomous end-effector footplates	RAGT consisted of three phases: (1) a screening trial involving 5 minutes each of walking in "flat surface," "stair-up," and "stair-down" modes, (2) an initial assessment where physiatrists stratified patients	In the Hard group, one GBS patient discontinued training due to saddle discomfort, and the remaining patients in the Possible group completed all sessions. None of the patients in the Hard	This study indicates that individuals with various neurological conditions, including GBS, can safely and effectively utilize an end-effector-type automated gait machine with saddle support.
		employing the Morning Walk®, an end-effector robot with footplate and saddle seat support, for the improvement of functional capabilities.	Inclusion criteria: Patients who could sustain an upright seated position without external assistance, despite having a spinal cord damage classified as grade C or D. Exclusion criteria: patients <120 cm in height and with >120 kg of body mass.	replicate motion behavior in the longitudinal plane, guiding the feet to recreate natural gait patterns.	into prediction groups (Hard, Difficult, and Possible) based on the expected capacity to complete RAGT, and (3) the main treatment involving RAGT conducted five times a week for thirty minutes per session, with successful completion requiring 24 sessions.	group completed RAGT, while 66.7% of the Difficult group successfully finished, with only three abandoning. In the Possible group, only 4.2% (7 out of 168) patients were unable to complete RAGT.	
[26]	Meyer-Heim A., Borggraefe I., Ammann-Reiffer C., Berweck S., Sennhauser F. H., Colombo G., Knecht B., Heinen F. 2007.	To evaluate the feasibility of employing robotic-assisted treadmill training as a therapeutic intervention for children with central gait impairment.	* (2 GBS out of 26 subjects) 2 male GBS patients of 7 and 10 years. Inclusion criteria: impairment of the central gait caused by inherited or acquired brain or spinal disorders. The femur needed to be at least 21 cm long.	**Driven Gait Orthosis (DGO) Lokomat:** Comprising two leg orthoses, adjustable features include the span of the hip orthosis, upper and lower leg lengths of the DGO, and the position and dimensions of the leg braces. Both adult and pediatric versions were utilized.	In-patient group training for GBS patients consisted of two to five weekly 45-minute DGO sessions, totaling 20 sessions. The training included various therapeutic modalities such as occupational therapy, speech and language therapy, neuropsychology, orthopedagogy, circuit training, and preschool activities. Occupational therapy sessions covered balance training, joint mobility and stretching, COGT, and functional exercises.	24 patients successfully underwent DGO training. Among the in-patient group, 13 out of 15 children demonstrated enhanced gait speed. Of the thirteen children capable of performing the 6-Meter Walking Test, 11 exhibited improvements in walking distance. In terms of the Functional Ambulation Categories (FACs), six out of sixteen children showed enhanced walking ability, nine remained stable, and one regressed to a previous category.	The clinical rehabilitation regimen for children, implemented in both inpatient and outpatient settings, efficiently incorporated DGO training. Throughout the training period, the vast majority of children consistently exhibited a heightened motivation to participate in the DGO program.
[36]	Takahashi Y, Terada T, Inoue K, Ito Y, Ikeda Y, Lee H. 2007.	to seamlessly integrate motion and sensory interventions to sustain a quantitative assessment of the degree of disorder in the patient.	* (2 GBS out of 133 subjects, 126 healthy).	**Haptic Device System Rehabilitation:** Involving a haptic device equipped with two servomotors featuring reduction gears, link rods, a grip, and a flat panel, this system also integrates a display and a computer. The link rods establish a linkage between the grip and servomotors.	Patients can perform two-dimensional upper limb motions by manipulating their grip on the surface of the flat panel. In the WAVE game, patients strive to maintain the cursor within circles while navigating along a line. Adjustments can be made to the height and cycle of the wave. The system records the grip's location and velocity when subjected to diverse forces, including load, assistance, viscosity, and friction. The wave cycle is set to two during these experiments.	Patients exhibited reduced effectiveness in movement, struggling to maintain a consistent grip speed as it frequently dropped to zero. Nevertheless, an improvement in performance was observed when applying viscosity force.	Experimental results suggest the potential utility of this approach for effective patient training, providing data for evaluating dysfunction severity and training program efficacy. Moreover, it can sustain patients' engagement throughout the recovery process.
[22]	Tanida S, Kikuchi T, Kakehashi T, Otsuki K, Ozawa T, Fujikawa T. 2009	To prove the effectiveness of an Intelligently Controllable Ankle Foot Orthosis (I-AFO) for a GBS patient.	One GBS subject: Male, (Age) 34, (Height) 183, (Weight) 83.1. The subject had difficulties moving their lower limbs voluntarily, particularly their ankle and toe joints on both sides.	**I-AFO:** An attachable laptop equipped with a versatile card (A/D and D/A) serves as a controller, providing the reference signal for regulating braking torque through amplified electric current. Input signals from a potentiometer and foot switches are conveyed to the controller via the A/D card.	Gait studies were conducted on a level surface, with results recorded using a response force plate and a three-dimensional movement analysis device. The participant underwent walking trials under three conditions: (1) barefoot walk, (2) walk with I-AFO, and (3) walk with plastic orthosis (P-AFO walk). Each test was performed at three distinct walking speeds: normal (1.30 seconds, 92 steps per minute), fast (1.03 seconds, 116 steps per minute), and slow (1.72 seconds, 69 steps per minute).	In the I-AFO walk, there was a noticeable increase in the flexural angle of the hip joint during the swing phase compared to the barefoot walk. Both the barefoot and P-AFO walks exhibited a distinct elevation in the knee joint angle at the onset of the stance phase. Despite dorsiflexion observed in both P-AFO and barefoot walks, the I-AFO walk demonstrated clear plantarflexion during the initial portion of the stance phase. In contrast to the other walking conditions, the rapid increase following foot contact with the floor surface diminished in the I-AFO walk.	The noticeable improvements led to suggestions on the effectiveness of the I-AFO's ankle joint control.

					freedom was applied to compute momentum in the dynamic model.		
[37]	Nehrujee A, Andrew H, Reethajane tsurekha, Patricia A, Samuelka maleshku mar S, Prakash H. 2021.	To evaluate the usability of PLUTO: robot with one Degree of Freedom (DoF) that can train many joints simultaneously.	(1 GBS patient out of 45 subjects, 30 healthy).	**PLUg and Train rObot (PLUTO):** A portable, lightweight, and versatile hand rehabilitation robot utilizes a single actuator with an open/free output shaft. This design enables training for various wrist and hand functions, allowing easy coupling with alternative passive single-DOF mechanisms.	To evaluate the outcome, the authors employed a System Usability Scale (SUS) as the standard for categorizing system usability. Additionally, a User Experience Questionnaire (UEQ) assessed usability across six subscales: perspicuity, attractiveness, novelty, stimulation, efficiency, and dependability. The training with the robot was gamified using three performance-adaptive games.	With an average score of 73.84 among the 45 participants, the system demonstrated acceptable usability (SUS > 70, t = 1.81, p = 0.038). According to UEQ findings, both patients and doctors evaluated all six subscales positively, with no negative scores observed in either group.	The system's immediate efficacy is outstanding. Subsequent research is required to evaluate the feasibility of implementing minimally supervised treatment, along with its long-term (beyond two weeks) usability and effectiveness.
[27]	Tuckey J., Greenwood R. 2004	To assess the GBS patient's response to treadmill training using Partial Body Weight Support (PBWS).	One male GBS patient: (Age) 44, (Height) 188.9, (Time since injury) 4 years.	**Biodex Unweighting Support System:** Enables calibration of the supported bodyweight proportion, utilizing a conventional rehabilitation treadmill.	During the hospitalization, the patient engaged in 4-5 weekly 45-minute physical therapy sessions, pursued a daily independent progressive muscular strength training program, and joined 4-5 physical therapy groups. The utilization of the PBWS system was incorporated into his therapy sessions.	The PBWS system contributed to the patient's notable improvement in treadmill walking distance, progressing from 3 meters to 100 meters. On the floor, within a week, the walking distance increased from 15 meters to 40 meters.	This study demonstrates the effectiveness of a PBWS system, functioning as a safety tool for high-risk weight-bearing exercises and gait retraining.
[38]	Céspedes N, Múnera M, Gómez C, Cifuentes CA. 2020	To assess the Socially Assistive Robot's (SAR) efficacy in neurorehabilitation.	* (1 GBS out of 4 subjects) One GBS patient.	**NAO:** A 58 cm humanoid robot with 25 DOF, 7 tactile sensors, 4 microphones, speakers, two 2D cameras, and voice recognition in 20 languages, featuring open-source programmable code.	Programmed routines include cervical posture feedback, thoracic posture feedback, heart rate alert, Borg scale inquiry fulfilled by the robot, and motivational feedback routines. The robot provides feedback to either the patient or the therapist in all routines. Eight 45-minute Lokomat sessions were completed.	Under the robot condition, all patients exhibited enhanced posture. The GBS patient's poor cervical posture time decreased from 22% to 5.15%, and poor thoracic posture time reduced from 2.66% to 2.00%. All therapists agreed that the robot was a valuable tool for providing feedback to patients and reducing workload.	The study revealed the positive and well-received influence of the robot on companionship, social contact, and cervical and thoracic postural behavior.
[28]	Bolliger M, Banz R, Dietz V, Lünenburger L. 2008.	To test a novel measuring technique's ability to quantify isometric muscle force in the DGO Lokomat.	(1 GBS out of 14 subjects) One male GBS patient (P13): (Age) 53, (Time since injury) 6 months	**Driven Gait Orthosis (DGO) Lokomat: (Described in article 6)**	The DGO Lokomat combines a dynamic body weight support device and a treadmill. In the sagittal plane, the DGO directs the patient's leg trajectory, utilizing linear back-drivable actuators within an exoskeleton framework to move the knee and hip joints. Actual joint angles are measured by potentiometers, while force transducers gauge linear forces in each actuator.	To assess inter- and intra-rater reliability, a total of 672 measurements were taken, comprising 84 for each joint and movement direction. Intra-rater reliability was lower compared to inter-rater reliability. Utilizing the average of two trials instead of a single measurement increased the reliability when calculating Intraclass Correlation Coefficients.	The DGO Lokomat provided precise results when assessing the maximum voluntary muscular force of hip and knee flexors and extensors in individuals with neurological movement disorders (NMD).
[34]	Rhee SY, Jeon H, Kim SW, Lee JS. 2020.	To assess the impact of gait training on GBS patients with a robotic end-effector type device.	15 GBS patients. Inclusion criteria: (1) 19 years or older, (2) first GBS diagnosis. (Mean age) 55.7 ± 15.3. (Mean time since injury) 3.9 ± 3.6 months.	**Morning Walk®: (Described in article 5).**	Subjects underwent 24 thirty-minute sessions of gait training supported by Morning Walk®. Evaluation of participants included the Modified Barthel Index Score (MBI) for activities of daily living, the Medical Research Council (MRC) scale for muscle strength, the Functional Ambulation Categories (FAC) for functional gait, the Rivermead Mobility Index (RMI) for functional abilities, and the 2-minute walk test (2MWT) for endurance of walking distance.	After Morning Walk®-assisted gait training, all outcome measures demonstrated improvements compared to baseline data. There were significant enhancements in ankle, knee, and hip muscular power, as well as improvements in FAC, MBI, 2MWT, and RMI.	After Morning Walk®-assisted gait training, individuals with GBS exhibited notable improvements in daily living activities, gait endurance, and lower limb motor power.

[24]	Chrif F, Van Hedel HJA, Vivian M, Nef T, Hunt KJ. 2022.	To assess the usability and technical viability of an interactive leg-press training robot designed to help children with neuromuscular deficits improve their leg muscle strength and control.	* (1 GBS out of 5 patients) One male GBS patient: (Age) 14.8, (Height) 165, (Weight) 65.5.	**Interactive leg press training device:** A seat module that can be adjusted, separate footplates connected to two pneumatic linear actuators by lever mechanisms, and an LCD screen that faces the user. Two exergames were developed in Unity for the training environment: Space Shooter and Ping-Pong.	Supervised by two therapists, patients underwent a single training session with the therapeutic apparatus. Before each session, therapists received an equipment introduction. Sessions lasted 40-45 minutes, incorporating active resistance training where patients maintained desired position profiles against resistive forces applied to the footplates. Exergames, conducted in active resistance mode, were part of the training.	All patients found the interactive device instruction satisfactory. Therapists gave a SUS score of 61.2 ± 18.4. In active resistance training, every patient completed the exercise without any adverse effects. During exergames, high motivation and engagement were observed, with all patients successfully navigating the games.	Users have embraced and deemed the pediatric system practical. Experimental results quantitatively affirm the effectiveness of the proposed training modes, yielding satisfactory numerical outcomes.
[32]	Laver K, Lim F, Reynolds K, George S, Ratcliffe J, Sim S, *et al.* 2012.	To assess whether a grocery shopping simulator based on virtual reality is useful for neurological rehabilitation.	(1 GBS out of 15 patients) One female GBS patient: (Age) 86. Patients who met the eligibility requirements were undergoing therapy for a neurological ailment and had the necessary cognitive, emotional, physical, and visual abilities to try out the simulator.	**Virtual Reality Grocery Shopping Simulator:** Designed to be versatile, realistic, and flexible, the hardware includes a large touch screen displaying the supermarket surroundings and a specially designed shopping cart handle. The virtual supermarket comprises three aisles displaying food products and their corresponding pricing, along with a manned checkout area.	The session commenced with an introduction, followed by a practical demonstration. Participants then had practice time before undertaking a predetermined task within a specific timeframe. The task involved starting at the supermarket entrance, selecting four items from a shopping list, and proceeding to the checkout. This test was repeated with consenting participants to assess learning and potential improvement in speed over time. Subsequently, participants answered a questionnaire to gauge their level of interest and enjoyment.	Out of the participants, 14 believed the program would be beneficial for recovery, with only 6 directly considering it helpful for rehabilitation. Regarding the software's ease of use, nine participants found it easy to learn, and twelve individuals described it as straightforward, although four found it somewhat frustrating to use.	The shopping simulator demonstrated utility for individuals undergoing neurological rehabilitation. Further investigation is required to validate the program.
[29]	Wille D, Eng K, Holper L, Chevrier E, Hauser Y, Kiper D, *et al.* 2009.	To assess how well a Pediatric Interactive Treatment System (PITS) based on virtual reality may help children with motor impairments improve their arm and hand function.	(1 GBS out of 5 patients) One male GBS patient with both arms affected: (Age) 13 years, 10 months.	**Paediatric Interactive Therapy System (PITS):** Comprising a height-adjustable custom table on wheels, a speaker-equipped display, a personal computer, and tailor-made data gloves for measuring forearm 3D orientation and finger flexion/extension, it includes a vibration motor for haptic feedback.	The Melbourne Assessment (MA), Box and Block Test (BBT), and Nine Hole Peg Test (NHPT) were used as outcome measures, administered before and after treatment. Additionally, patients rated their level of enjoyment on a subjective 0–10 scale (0 = no fun at all; 10 = lots of fun) after each session.	The GBS patient was excluded from the group evaluation in the Melbourne Assessment due to the lack of a pre-assessment. However, in both the Box and Block Test (BBT) and Nine Hole Peg Test (NHPT), both arms of the GBS patient exhibited improvement. Overall, all five patients demonstrated improved results in each test compared to their pre-therapy sessions.	Successfully integrating PITS into the clinical rehabilitation program, despite occasional technical challenges affecting motivation, all children remained highly motivated due to engaging gaming challenges, unpredictability, indirect competitiveness through the high-score function, and immediate feedback on their motor progress.
[30]	Bulley P.	To test The Podiatron as a rehabilitation tool for a patient with GBS.	One male GBS patient: (Age) 58 years, (Time since injury) 10 months.	**The Podiatron:** A motorized wobbling board with adjustable pitch, featuring handrails and a control panel, designed specifically for enhancing and mobilizing the back, hips, knees, and ankles.	The podiatron was incorporated alongside the patient's regular physiotherapy. Sessions, held twice a day for 10 minutes at Level 1 (a 5° incline), gradually increased to maximum speed over the initial 30 seconds. Initially supervised to ensure body alignment, the patient later self-monitored using a mirror. This visual compensation addressed reduced somatosensory input, promoting extension and stimulating the vestibulospinal tract.	The patient exhibited improvement in all assessments following Podiatron use: 10-m walk (15.45 s to 14.11 s, 8.67% improvement); "up and go" (25.40 s to 22.07 s, 13.13% improvement); Confidence in walking (2.5 to 4.5, 44.44% improvement); Surface area of elevated left foot (17.68 cm2 to 6.52 cm2, 63.12% improvement); Surface area of elevated right foot (88.8 cm2 to 6.28 cm2, 92.93% improvement).	The implementation of the Podiatron expanded the surface area of the patient's feet for enhanced support. While progress seemed stagnant initially, two months later, substantial improvement in functional ability was observed, although not immediately evident in the first-week assessment.

TABLE 2. **Checklist for assessing the quality of quantitative studies. "2" = Yes, "1" = Partially, "0" = No, "-" = Does not apply**

	ITEMS														
Studies	1	2	3	4	5	6	7	8	9	10	11	12	13	14	Total
[20]	2	2	2	2	2	-	-	2	1	2	-	-	2	2	19/20
[21]	2	2	2	2	2	-	-	2	1	2	-	-	2	2	19/20
[22]	1	2	2	2	2	-	-	1	2	2	-	-	2	2	18/20
[23]	1	1	2	2	2	-	-	2	1	2	-	-	1	2	16/20
[24]	1	2	2	2	2	-	-	2	2	2	-	-	2	2	19/20
[25]	1	2	2	2	2	-	-	2	2	2	-	-	2	2	19/20
[26]	2	2	2	1	2	-	-	1	2	2	-	-	2	2	18/20
[27]	1	2	2	1	2	-	-	2	2	2	-	-	2	2	18/20
[28]	2	2	2	1	1	-	-	2	2	2	-	-	2	2	18/20
[29]	1	1	1	2	2	-	-	2	2	2	-	-	2	2	17/20
[30]	0	1	2	1	2	-	-	2	2	2	-	-	2	2	16/20
[31]	1	1	2	1	2	-	-	1	2	2	-	-	2	2	16/20
[32]	1	2	2	1	2	-	-	2	2	2	-	-	2	1	17/20
[33]	2	2	2	1	2	-	-	2	2	2	-	-	2	2	19/20
[34]	1	2	2	1	2	-	-	2	2	2	-	-	2	0	16/20
[35]	2	2	2	1	2	-	-	2	2	2	-	-	2	2	19/20
[36]	1	2	2	1	1	-	-	2	2	2	-	-	2	2	17/20
[37]	1	2	2	0	2	-	-	2	2	2	-	-	2	2	17/20
[38]	1	2	2	0	2	-	-	2	2	2	-	-	2	2	17/20

Three devices were orthoses: two of them were wearables designed for the ankle-foot area [21][22]. Contrary to most orthoses, these devices had integrated electronic systems that improved the patients' ability to move their feet. The third one is the Lokomat [26][28], which functions as an integrated system providing body weight support and rehabilitating gait by driving both legs. The Biodex Unweighting Support System [27] only provides weight support but is adjustable, aiding in gait rehabilitation. The Morning Walk devicen[33][34] had great relevance in gait rehabilitation. Even though, in some cases, the saddle caused discomfort, the use of the end-effector footplates has proven to be beneficial for the patients.

It is worth mentioning that four of the studies addressed limb-related issues indirectly. Jamshidi *et al.*[23] developed a computerized model using the SimMechanics toolbox to simulate human gait, aiming to contribute to the improvement of leg orthosis.

Céspedes *et al.* [38] designed their experiment around patients using the Lokomat for gait rehabilitation, with the main focus on developing an automated assistant for rehabilitation. Kauhanen *et al.* [35] addressed upper limb rehabilitation, targeting tetraplegic patients. The EEG device 'TTK-BCI' provided screen feedback based on left-hand or right-hand movement attempts. Lastly, Lee *et al.* [25] created a passive shoulder joint tracker that can be integrated into various rehabilitation mechanisms to aid in upper limb rehabilitation. An outlier in the investigations was conducted by Wosnitzer *et al.* [31]; they did not focus on arm or leg rehabilitation but successfully applied sacral nerve neuromodulation to treat urinary retention.

Almost every GBS patient treated showed positive rehabilitation results; one of the few exceptions occurred in the study conducted by Choi *et al.* [33], where one patient was unable to complete the process due to discomfort with the saddle. The biomedical

engineering devices proved to be useful, although, in most cases, further analysis and validation are required, especially in the long term.

A wide variety of parameters, scales, and methods were used to measure the patients' evolution during research directly dedicated to rehabilitation. The most commonly used tests [20][26][28][30] included the 10-meter walk test, which is essentially a speed evaluation measuring the time it takes for the patient to walk 10 meters [43][44][45][46]. The 'timed up and go test' also calculates speed but involves additional activities such as standing up, turning around, and sitting down [45][46][47]. A related test designed to estimate endurance is the 6-minute walk test [21][26][28], which records the distance the patient walks in 6 minutes [48][49][50].

The Medical Research Council Scale for Muscle Strength was also applied [27][33][34]. This scale focuses on muscle strength, encompassing 6 muscle systems in total [51][52][53]. However, since these studies were focused on the lower limbs, only 3 systems were considered: hip flexors, knee extensors, and foot dorsiflexors. Typically, therapists used the Functional Ambulation Categories [26][33][34] in conjunction with this form of examination.

Besides velocity and endurance, equilibrium is a crucial parameter to observe. For this purpose, the Berg Balance Scale [21], Tinetti test, and Unipedal stance time were employed [20]. These methods were useful in assessing patients' improvement, and all objectively revealed a correlation between the use of biomedical devices and the subjects' progression.

Multiple studies reveal the importance of motivation and comfortability during the neurorehabilitation process [54][55][56][57][58]. In order to take in consideration this topic, both the physical and psychological acceptance of the devices were taken in consideration in the studies, two of them used scales like the Suitability Evaluation Questionnaire [20] or the User Experience

Questionnaire [37], but most authors reported subjective observations made by the therapists. In the bulk of the studies, the authors observed that the improvement of the patient's autonomy and motor abilities had a remarkable incidence in their motivation and psychological well-being.

The usability of biomedical devices was tested in two studies by means of the System Usability Scale [24][37], which is a highly reliable tool for measuring the usability of a system or device. While this scale can be somewhat subjective, it is also very versatile [58][59]. However, in most research, authors opted for custom-made scales.

Living with the disabilities caused by GBS can be a significant challenge, as basic day-to-day activities become much harder to execute. Both patients and caregivers are psychologically affected, and their quality of life is reduced. This impact can be even more challenging for those who don't have good economic conditions.

Biomedical engineering devices are being used as auxiliary technologies that serve as extensions of human capacities. They enhance traditional rehabilitation methods, and the benefits for the patients multiply. There is a vast range of possibilities with this equipment, from wearables capable of providing firmness to steps to haptic devices that train fine motor abilities. Additionally, there are very complex mechanical systems that can take a patient from not being able to walk 4 meters to almost complete independence.

We must highlight the importance of studying the long-term effects of these rehabilitation methods. There should be more follow-up studies to understand the consequences in the long term and how well patients have evolved, in order to pursue a holistic comprehension of the benefits of these devices.

CONCLUSIONS

This systematic review has answered the question 'How has biomedical engineering been used for the rehabilitation of patients with disabilities caused by Guillain-Barré?' and, at the same time, has made contributions to the field. The targeted areas for rehabilitation were identified, revealing where current devices tend to focus. The review illustrated the global distribution of studies using this approach for GBS rehabilitation and provided an analysis of the probable reasons why some continents have more studies than others. The biomedical engineering devices were described, and a general analysis was provided, considering whether they were custom-made or commercially acquired, and classifying them based on the engineering principle they operate on (haptics, orthosis, unweighting support systems, etc.). Another contribution is a brief description of the scales used to assess the status development of patients before and after rehabilitation with the devices. All of these contributions, along with the main objective of the investigation, help to create a solid platform for future research in this field.

We can conclude that, even though most studies lack an understanding of long-term effects, biomedical engineering devices are a useful ally in the rehabilitation process, serving both as the main therapy and as an auxiliary one. There are opportunities for new research based on the foundations provided by the pioneers in these studies. The authors would like to encourage biomedical engineers, therapists, and physicians to explore this avenue.

ACKNOWLEDGEMENTS

LIMITATIONS OF THE ARTICLE

One of the main problems encountered is that many of the studies did not have the GBS patients as the center of the investigation, this made it difficult, and sometimes impossible to obtain specific information on their development. Another general limitation is that most studies included a very reduced number of patients, and the great majority were samples from a single rehabilitation center, which caused a lack of heterogeneity.

FUNDING

DECLARATION OF COMPETING INTERESTS

All authors declare there are no conflicts of interests.

AUTHOR CONTRIBUTIONS

A. B. T. R. Conceptualization, data curation, formal analysis, investigation, methodology, project administration, writing original draft, writing review and editing, visualization, resources. I. R. H. Conceptualization, methodology, supervision, validation, writing review and editing. O. A. D. R. Conceptualization, project administration, supervision, validation, investigation, funding acquisition, writing review and editing. A. M. T. L. Methodology, validation, resources, supervision, writing review and editing.

REFERENCES

[1]   B. van den Berg, C. Walgaard, J. Drenthen, C. Fokke, B. C. Jacobs, and P. A. Van Doorn, "Guillain-Barré syndrome: Pathogenesis, diagnosis, treatment and prognosis," Nat. Rev. Neurol., vol. 10, no. 8, pp. 469-482, 2014, doi: **https://doi.org/10.1038/nrneurol.2014.121**

[2]   H. J. Willison, B. C. Jacobs, and P. A. van Doorn, "Guillain- Barré syndrome," Lancet, vol. 388, no. 10045, pp. 717-727, Aug. 2016, doi: **https://doi.org/10.1016/s0140-6736(16)00339-1**

[3]   A. Créange, "Guillain-Barré syndrome: 100 years on," Rev. Neurol., vol. 172, no. 12, pp. 770-774, Dec. 2016, doi: **https://doi.org/10.1016/j.neurol.2016.10.011**

[4]   N. Shahrizaila, H. C. Lehmann, and S. Kuwabara, "Guillain-Barré syndrome," Lancet, vol. 397, no. 10280, pp. 1214-1228, Mar. 2021, doi: **https://doi.org/10.1016/s0140-6736(21)00517-1**

[5]   A. Mirian, M. W. Nicolle, and A. Budhram, "Guillain- Barré syndrome," Can. Med. Assoc. J., vol. 193, no. 11, pp. E378-E378, Mar. 2021, doi: **https://doi.org/10.1503/cmaj.202710**

[6]   J. Expósito, L. Carrera, D. Natera, G. Nolasco, A. Nascimento, and C. Ortez, "Síndrome de Guillain-Barré y otras neuropatías autoinmunes: tratamiento actual," Med., vol. 82, no. 3, pp. 82-88, 2022. [Online]. Available: **https://www.medicinabuenosaires.com/revistas/vol82-22/s3/82s3.pdf**

[7]   M. M. Dimachkie and R. J. Barohn, "Guillain-Barré Syndrome and Variants," Neurol. Clin., vol. 31, no. 2, pp. 491-510, May 2013, doi: **https://doi.org/10.1016/j.ncl.2013.01.005**

[8]   S. R. Sudulagunta, M. B. Sodalagunta, M. Sepehrar, H. Khorram, et al., "Guillain-Barré syndrome: clinical profile and management," Ger. Med. Sci., vol. 13, art. no. Doc16, Sep. 2015, doi: **https://doi.org/10.3205/000220**

[9]   M. R. Ashrafi, A. Mohammadalipoor, A. R. Naeini, M. Amanat, et al., "Clinical Characteristics and Electrodiagnostic Features of Guillain-Barré Syndrome Among the Pediatric Population," J. Child. Neurol., vol. 35, no. 7, pp. 448-455, Jun. 2020, doi: **https://doi.org/10.1177/0883073820905157**

[10] T. Harbo and H. Andersen, "Neuromuscular effects and rehabilitation in Guillain-Barré syndrome," in Zika Virus Impact, Diagnosis, Control, and Models, C. R. Martin, V. R. Preedy, C. J. Hollins Martin, R. Rafendram, Eds., Oxford, United Kingdom: Elsevier, 2021, ch. 2, pp. 143- 149, doi: **https://doi.org/10.1016/B978-0-12-820267-8.00013-3**

[11] F. Khan and B. Amatya, "Rehabilitation interventions in patients with acute demyelinating inflammatory polyneuropathy: a systematic review," Eur. J. Phys. Rehabil. Med., vol. 48, no. 3, pp. 507-522, Sep. 2012. [Online]. Available: **https://www.minervamedica.it/en/journals/europa-medicophysica/article.php?cod=R33Y2012N03A0507**

[12] P. A. van Doorn, L. Ruts, and B. C. Jacobs, "Clinical features, pathogenesis, and treatment of Guillain-Barré syndrome," Lancet Neurol., vol. 7, no. 10, pp. 939-950, Oct. 2008, doi: **https://doi.org/10.1016/s1474-4422(08)70215-1**

[13] B. R. Wakerley and N. Yuki, "Pharyngeal-cervical-brachial variant of Guillain-Barre syndrome," J. Neurol. Neurosurg. Psychiatry, vol. 85, no. 3, pp. 339-344, Mar.2014, doi: **https://doi.org/10.1136/jnnp-2013-305397**

[14] B. S. Schoenberg, "Epidemiology of Guillain-Barré syndrome," Adv. Neurol., vol. 19, pp. 249-60, 1978.

[15] N. S. Arsenault, P.-O. Vincent, Y. B. H. Shen, R. Bastien, A. Sweeney, "Influence of exercise on patients with Guillain-Barré syndrome: A systematic review," Physiother. Can., vol. 68, no. 4, pp. 367-376, 2016, doi: **https://doi.org/10.3138/ptc.2015-58**

[16] J. B. Bussmann, M. P. Garssen, P. A. van Doom, and H. J. Stam, "Analysing the favourable effects of physical exercise: Relationships between physical fitness, fatigue and functioning in Guillain-Barré syndrome and chronic inflammatory demyelinating polyneuropathy," J. Rehabil. Med., vol. 39, no. 2, pp. 121-125, Mar. 2007, doi: **https://doi.org/10.2340/16501977-0007**

[17] S. Jones, W. D. Man, W. Gao, I. J. Higginson, A. Wilcock, and M. Maddocks, "Neuromuscular electrical stimulation for muscle weakness in adults with advanced disease," Cochrane Database of Syst. Rev., vol. 2016, no. 10, art. no. CD009419, Oct. 2016, doi: **https://doi.org/10.1002/14651858.cd009419.pub3**

[18] M. J. Page, D. Moher, P. M. Bossuyt, I. Boutron, et al., "PRISMA 2020 explanation and elaboration: updated guidance and exemplars for reporting systematic reviews," BMJ, vol. 372, art. no. n160, Mar. 2021, doi: **https://doi.org/10.1136/bmj.n160**

[19] L. M. Kmet, R. C. Lee, and L. S. Cook, Standard Quality Assessment Criteria for Evaluating Primary Research Papers from a Variety of Fields. Alberta Heritage Foundation for Medical Research, 2004, doi: **https://doi.org/10.7939/R37M04F16**

[20] S. Albiol-Pérez, M. Forcano-García, M. T. Muñoz-Tomás, P. Manzano-Fernández, S. Solsona-Hernández, M. A. Mashat, J. A. Gil-Gómezet, "A novel virtual motor rehabilitation system for guillain-barré syndrome: Two single case studies," Methods Inf. Med., vol. 54, no. 2, pp. 127-134, 2015, doi: **https://doi.org/10.3414/me14-02-0002**

[21] Y. Fang and Z. F. Lerner, "Bilateral vs. Paretic-Limb-Only Ankle Exoskeleton Assistance for Improving Hemiparetic Gait: A Case Series," IEEE Robot Autom. Lett., vol. 7, no. 2, pp. 1246-1253, Apr. 2022, doi: **https://doi.org/10.1109/lra.2021.3139540**

[22] S. Tanida, T. Kikuchi, T. Kakehashi, K. Otsuki, et al., "Intelligently controllable Ankle Foot Orthosis (I- AFO) and its application for a patient of Guillain-Barre syndrome," in 009 IEEE International Conference on Rehabilitation Robotics, Kyoto, Japan, 2009, pp. 857-862, doi: **https://doi.org/10.1109/ICORR.2009.5209590**

[23] N. Jamshidi, M. Rostami, S. Najarian, M. B. Menhaj, M. Saadatnia, and S. Firooz, "Modelling of human walking to optimise the function of ankle-foot orthosis in Guillan- Barré patients with drop foot," Singapore Med. J., vol. 50, no. 4, pp. 412-417, Apr. 2009. [Online]. Available: **http://smj.sma.org.sg/5004/5004a13.pdf**

[24] F. Chrif, H. J. A. van Hedel, M. Vivian, T. Nef, and K. J. Hunt, "Usability evaluation of an interactive leg press training robot for children with neuromuscular impairments," Technol. Health Care, vol. 30, no. 5, pp. 1183- 1197, Mar. 2022, doi: **https://doi.org/10.3233%2FTHC-213629**

[25] K.-S. Lee, J.-H. Park, J. Beom, and H.-S. Park, "Design and evaluation of passive shoulder joint tracking module for upper-limb rehabilitation robots," Front. Neurorobot., vol. 12, art. no. 38, Jul. 2018, doi: **https://doi.org/10.3389/fnbot.2018.00038**

[26] A. Meyer-Heim, I. Borggraefe, C. Ammann-Reiffer, St. Berweck, et al., "Feasibility of robotic-assisted locomotor training in children with central gait impairment," Dev. Med. Child Neurol., vol. 49, no. 12, pp. 900-906, Dec. 2007, doi: **https://doi.org/10.1111/j.1469-8749.2007.00900.x**

[27]   J. Tuckey and Greenwood R., "Rehabilitation after severe Guillain-Barré syndrome - the use of partial body weight support," Physiother. Res. Int., vol. 9, no. 2, pp. 96-103, 2004, doi: https://doi.org/10.1002/pri.306

[28]   M. Bolliger, R. Banz, V. Dietz, and L. Lünenburger, "Standardized voluntary force measurement in a lower extremity rehabilitation robot," J. Neuroeng. Rehabil., vol. 5, art. no. 5, Oct. 2008, doi: https://doi.org/10.1186/1743-0003-5-23

[29]   D. Wille, K. Eng, L. Holper, E. Chevrier, et al., "Virtual reality-based paediatric interactive therapy system (PITS) for improvement of arm and hand function in children with motor impairment a pilot study," Dev. Neurorehabil., vol. 12, no. 1, pp. 44-52, Feb. 2009, doi: https://doi.org/10.1080/17518420902773117

[30]   P. Bulley, "The podiatron: an adjunct to physiotherapy treatment for Guillain-Barré syndrome?," Physiother. Res. Int., vol. 8, no. 4, pp. 210-215, Nov. 2003, doi: https://doi.org/10.1002/pri.291

[31]   M. S. Wosnitzer, R. Walsh, and M. P. Rutman, "The use of sacral neuromodulation for the treatment of non- obstructive urinary retention secondary to Guillain-Barré syndrome" Int. Urogynecol. J. Pelvic Floor Dysfunct., vol. 20, no. 9, pp. 1145- 1147, Sep. 2009, doi: https://doi.org/10.1007/s00192-009-0826-9

[32]   K. Laver, F. Lim, K. Reynolds, S. George, J. Ratcliffe, S. Sim, M. Crotty, "Virtual Reality Grocery Shopping Simulator: Development and Usability in Neurological Rehabilitation," Presence, vol. 21, no. 1, pp. 183-191, Feb. 2012, doi: https://doi.org/10.1162/PRES_a_00098

[33]   S. Choi, S. W. Kim, H. R. Jeon, J. S. Lee, D. Y. Kim, and J. W. Lee, "Feasibility of Robot-Assisted Gait Training with an End-Effector Type Device for Various Neurologic Disorders" Brain Neurorehabil., vol. 13, no. 1, art. no. e6, Nov. 2019, doi: https://doi.org/10.12786/bn.2020.13.e6

[34]   S. Y. Rhee, H. Jeon, S. W. Kim, and J. S. Lee, "The effect of an end-effector type of robot-assisted gait training on patients with Guillain-Barre syndrome: a cross-sectional study," F1000Res, vol. 9, art. no. 1465, 2020, doi: https://doi.org/10.12688/f1000research.26246.1

[35]   L. Kauhanen, P. Jylänki, J. Lehtonen, P. Rantanen, H. Alaranta, and M. Sams, "EEG-based brain-computer interface for tetraplegics," Comput. Intell. Neurosci., vol. 2007, art. no. 23864, 2007, doi: https://doi.org/10.1155%2F2007%2F23864

[36]   Y. Takahashi, T. Terada, K. Inoue, Y. Ito, Y. Ikeda, H. Lee, T. Komeda, "Haptic Device System for Upper Limb Motor and Cognitive Function Rehabilitation: Grip Movement Comparison between Normal Subjects and Stroke Patients" in 2007 IEEE 10th International Conference on Rehabilitation Robotics, Noordwijk, Netherlands, 2007, pp. 736-741, doi: https://doi.org/10.1109/ICORR.2007.4428507

[37]   A. Nehrujee, H. Andrew, Reethajanetsurekha, A. Patricia, et al., "Plug-and-train robot (pluto) for hand rehabilitation: Design and preliminary evaluation," IEEE Access, vol. 9, pp. 134957-134971, 2021, doi: https://doi.org/10.1109/ACCESS.2021.3115580

[38]   N. Céspedes, M. Múnera, C. Gómez, and C. A. Cifuentes, "Social Human-Robot Interaction for Gait Rehabilitation," IEEE Trans. Neural Syst. Rehabil. Eng., vol. 28, no. 6, pp. 1299-1307, Jun. 2020, doi: https://doi.org/10.1109/TNSRE.2020.2987428

[39]   Clarivate. "Journal Citation Reports." Clarivate. https://clarivate.com/products/scientific-and-academic-research/research-analytics-evaluation-and-management-solutions/journal-citation-reports/ (accessed 2023).

[40]   J. J. Sejvar, A. L. Baughman, M. Wise, and O. W. Morgan, "Population incidence of Guillain-Barré syndrome: A systematic review and meta-analysis," Neuroepidemiology, vol. 36, no. 2. pp. 123-133, Apr. 2011, doi: https://doi.org/10.1159/000324710

[41]   United Nations, "World Economic Situation and Prospects 2022," United Nations. 2022. Accessed: May 23, 2023. [Online]. Available: https://www.un.org/development/desa/dpad/publication/world-economic-situation-and-prospects-2022/

[42]   United Nations, "World Population Prospects 2022: Summary of Results," New York, 2022. United Nations. 2022. Accessed: 2023. [Online]. Available: https://www.un.org/development/desa/pd/content/World-Population-Prospects-2022

[43]   D. S. M. Ong, M. Z. Weibin, and R. Vallabhajosyula, "Serious games as rehabilitation tools in neurological conditions: A comprehensive review," Technol.Health Care, vol. 29, no. 1, pp. 15-31, Jan. 2021, doi: https://doi.org/10.3233/thc-202333

[44]   A. Jackson, C. T. Carnel, J. F. Ditunno, M. S. Read, et al., "Outcome Measures for Gait and Ambulation in the Spinal Cord Injury Population," J. Spinal Cord. Med., vol. 31, no. 5, pp. 487-499, Jan. 2008, doi: https://doi.org/10.1080/10790268.2008.11753644

[45]   O. Beauchet, B. Fantino, G. Allali, S. W. Muir, M. Montero- Odasso, and C. Annweiler, "Timed up and go test and risk of falls in older adults: A systematic review," J. Nutr. Health Aging., vol. 15, no. 10, pp. 933-938, Dec. 2011, doi: https://doi.org/10.1007/s12603-011-0062-0

[46]   E. Barry, R. Galvin, C. Keogh, F. Horgan, and T. Fahey, "Is the Timed Up and Go test a useful predictor of risk of falls in community dwelling older adults: a systematic review and meta- analysis," BMC Geriatr., vol. 14, no. 1, art. no. 14, Dec. 2014, doi: https://doi.org/10.1186/1471-2318-14-14

[47]   R. P. Kleyweg, F. G. A. van der Meché, and P. I. Schmitz, "Interobserver agreement in the assessment of muscle strength and functional abilities in Guillain-Barré syndrome," Muscle Nerve, vol. 14, no. 11, pp. 1103-1109, Nov. 1991, doi: https://doi.org/10.1002/mus.880141111

[48]   G. Scivoletto, F. Tamburella, L. Laurenza, C. Foti, J. F. Ditunno, and M. Molinari, "Validity and reliability of the 10-m walk test and the 6-min walk test in spinal cord injury patients," Spinal Cord., vol. 49, no. 6, pp. 736-740, Jun. 2011, doi: https://doi.org/10.1038/sc.2010.180

[49]   H. J. A. van Hedel, M. Wirz, and V. Dietz, "Standardized assessment of walking capacity after spinal cord injury: the European network approach," Neurol. Res., vol. 30, no. 1, pp. 61-73, Feb. 2008, doi: https://doi.org/10.1179/016164107x230775

[50]   K. Bennell, F. Dobson, and R. Hinman, "Measures of physical performance assessments: Self-Paced Walk Test (SPWT), Stair Climb Test (SCT), Six-Minute Walk Test (6MWT), Chair Stand Test (CST), Timed Up & Go (TUG), Sock Test, Lift and Carry Test (LCT), and Car Task," Arthritis Care Res. (Hoboken), vol. 63, no. S11, pp. S350-S370, Nov. 2011, doi: https://doi.org/10.1002/acr.20538

[51]   S. T. Larson and J. Wilbur, "Muscle Weakness in Adults: Evaluation and Differential Diagnosis," Am. Fam. Physician, vol. 101, no. 2, pp. 95-108, Jan. 2020. [Online]. Available: https://www.aafp.org/pubs/afp/issues/2020/0115/p95.html

[52]   T. Paternostro-Sluga, M. Grim-Stieger, M. Posch, O. Schuhfried, et al., "Reliability and validity of the Medical Research Council (MRC) scale and a modified scale for testing muscle strength in patients with radial palsy," J. Rehabil. Med., vol. 40, no. 8, pp. 665-671, Aug. 2008, doi: https://doi.org/10.2340/16501977-0235

[53] N. Maclean and P. Pound, "A critical review of the concept of patient motivation in the literature on physical rehabilitation," Soc. Sci. Med., vol. 50, no. 4, pp. 495-506, Feb. 2000, doi: https://doi.org/10.1016/s0277-9536(99)00334-2

[54] A. Kusec, D. Velikonja, C. DeMatteo, and J. E. Harris, "Motivation in rehabilitation and acquired brain injury: can theory help us understand it?," Disabil. Rehabil., vol. 41, no. 19, pp. 2343-2349, Sep. 2019, doi: https://doi.org/10.1080/09638288.2018.1467504

[55] P. Meyns, T. Roman de Mettelinge, J. van der Spank, M. Coussens, and H. Van Waelvelde, "Motivation in pediatric motor rehabilitation: A systematic search of the literature using the self-determination theory as a conceptual framework," Dev. Neurorehabil., vol. 21, no. 6, pp. 371-390, Aug. 2018, doi: https://doi.org/10.1080/17518423.2017.1295286

[56] Y. Nishiwaki, M. Nakamura, and M. Nihei, "A novel method of evaluating changes in intrinsic motivation during cognitive rehabilitation," in 2021 43rd Annual International Conference of the IEEE Engineering in Medicine & Biology Society (EMBC), Mexico, 2021, pp. 2095-2099, doi: https://doi.org/10.1109/EMBC46164.2021.9630738

[57] G. Verrienti, C. Raccagni, G. Lombardozzi, D. De Bartolo, and M. Iosa, "Motivation as a Measurable Outcome in Stroke Rehabilitation: A Systematic Review of the Literature," Int. J. Environ. Res. Public Health, vol. 20, no. 5, art. no. 4187, Feb. 2023, doi: https://doi.org/10.3390/ijerph20054187

[58] Z. Zhou, J. Li, H. Wang, Z. Luan, Y. Li, and X. Peng, "Upper limb rehabilitation system based on virtual reality for breast cancer patients: Development and usability study," PLoS One, vol. 16, no. 12, art. no. e0261220, Dec. 2021, doi: https://doi.org/10.1371/journal.pone.0261220

[59] E. L. Friesen, "Measuring AT Usability with the Modified System Usability Scale (SUS)," Stud. Health Technol. Inform., vol. 242, pp. 137-143, 2017. [Online]. Available: https://ebooks.iospress.nl/publication/47262

Study of the Length of time Window in Emotion Recognition based on EEG Signals

Estudio de la Longitud de Ventana de Tiempo en el Reconocimiento de Emociones Basado en Señales EEG

Alejandro Jarillo Silva[1] (iD), *Víctor Alberto Gómez Pérez[1]* (iD), *Omar Arturo Domínguez Ramírez[2]* (iD)(✉).

[1]Universidad de la Sierra Sur, Oaxaca - México

[2]Universidad Autónoma del Estado de Hidalgo, Hidalgo - México

ABSTRACT

The objective of this research is to present a comparative analysis using various lengths of time windows (TW) during emotion recognition, employing machine learning techniques and the portable wireless sensing device EPOC+. In this study, entropy will be utilized as a feature to evaluate the performance of different classifier models across various TW lengths, based on a dataset of EEG signals extracted from individuals during emotional stimulation. Two types of analyses were conducted: between-subjects and within-subjects. Performance measures such as accuracy, area under the curve, and Cohen's Kappa coefficient were compared among five supervised classifier models: K-Nearest Neighbors (KNN), Support Vector Machine (SVM), Logistic Regression (LR), Random Forest (RF), and Decision Trees (DT). The results indicate that, in both analyses, all five models exhibit higher performance in TW ranging from 2 to 15 seconds, with the 10 seconds TW particularly standing out for between-subjects analysis and the 5-second TW for within-subjects; furthermore, TW exceeding 20 seconds are not recommended. These findings provide valuable guidance for selecting TW in EEG signal analysis when studying emotions.

KEYWORDS: electroencephalogram, emotion recognition, machine learning, time window length

RESUMEN

El objetivo de esta investigación es presentar un análisis comparativo empleando diversas longitudes de ventanas de tiempo (VT) durante el reconocimiento de emociones, utilizando técnicas de aprendizaje automático y el dispositivo de sensado inalámbrico portátil EPOC+. En este estudio, se utilizará la entropía como característica para evaluar el rendimiento de diferentes modelos clasificadores en diferentes longitudes de VT, basándose en un conjunto de datos de señales EEG extraídas de individuos durante la estimulación de emociones. Se llevaron a cabo dos tipos de análisis: entre sujetos e intra-sujetos. Se compararon las medidas de rendimiento, tales como la exactitud, el área bajo la curva y el coeficiente de Cohen's Kappa, de cinco modelos clasificadores supervisados: K-Nearest Neighbors (KNN), Support Vector Machine (SVM), Logistic Regression (LR), Random Forest (RF) y Decision Trees (DT). Los resultados indican que, en ambos análisis, los cinco modelos presentan un mayor rendimiento en VT de 2 a 15 segundos, destacándose especialmente la VT de 10 segundos para el análisis entre los sujetos y 5 segundos intra-sujetos; además, no se recomienda utilizar VT superiores a 20 segundos. Estos hallazgos ofrecen una orientación valiosa para la elección de las VT en el análisis de señales EEG al estudiar las emociones.

PALABRAS CLAVE: aprendizaje automático, electroencefalograma, longitud de ventana de tiempo, reconocimiento de emociones

Corresponding author

TO: Omar Arturo Domínguez Ramírez

INSTITUTION: Univerdad Autónoma del Estado de Hidalgo

ADDRESS: Kilómetro 4.5 carretera Pachuca-Tulancingo en la Colonia Carboneras, Mineral de la Reforma, Hidalgo.

EMAIL: omar@uaeh.edu.mx

INTRODUCTION

Human emotions have an impact on day-to-day actions and decisions. They are important aspects of communication and human emotional intelligence, in other words, the capacity to understand and manage emotions is crucial for the success of personal interactions[1]. There are areas of opportunity in technological innovation in the study of emotions, for example, affective computing, which has the objective of equipping machines with emotional intelligence to improve human-computer interactions (HCI)[2]. Another area is human-robot interaction (HRI), which aims to make robots capable of interpreting and expressing emotions similar to those of human beings and thereby modulate relevant aspects of the interaction[3]. Thus, the possible applications of an interface capable of evaluating human emotional states are numerous, ranging from medical diagnoses, rehabilitation processes, and digital commerce to new teaching methods.

In HCI, non-invasive, reliable and accessible portable sensors play an important role in the study of emotions. This is because in many work environments the use of modern technologies has increased considerably, with the objective of improving the interaction between the user and the technologies. However, many of these systems impose high demands on cognitive states, which can lead to the arousal of a person's negative emotions[4]. One of the most effective approaches to emotion recognition is based on the use of physiological signals. Among the numerous physiological signals, it has been reported that brain signals are found to be directly related with human emotions[5][6][7]. Favorable results have been reported when evaluating different classification algorithms, this during the application of diverse feature extraction techniques through electroencephalographic (EEG) signals[8][9][10].

The estimation of emotions in real-time involves processing a continuous stream of biosignals with the lowest latency possible. Research in system development for emotional state detection is mainly focused on recognition methodology[11]. On the other hand, the field of BCI systems using EEG signals is constantly evolving. For example, in[12], an algorithm for attention detection during mathematical reasoning is proposed. In addition, in[13], an analysis of EEG signals is performed using diverse classification techniques, achieving significant results in motion detection. Another relevant contribution is presented in[14], with the introduction of a new neural network model designed for classification with a limited amount of motor imagery data. In[15], a methodology based on EEG signals is presented to detect the level of attention in children, applying a multilayer perception neural network model. Finally, in[16], a methodology based on motor imagery for a BCI system is presented, using convolutional neural networks. These papers highlight the diversity of approaches in current research on emotional estimation and the development of BCI systems using brain signals.

However, segmentation plays an important role in achieving real-time or continuous monitoring of emotional states (that is to say, the selection of the time window), which has received little attention and requires further research. The majority of works reported utilize different time windows (TW) as inputs for model training[6][7]. The consequences of employing different TW could influence the trained model to be unsuitable for application in real-time emotion recognition because the knowledge learned from the model is related to the sampled features for subsequent detection. In addition, combining different TW in the same analysis would cause the trained model to be inconsistent due to the changing characteristics of EEG signals in temporal sequences[17].

In order to avoid this problem, analyses at different TW lengths of temporal sequences have been developed using EEG signals. For example, Lin *et al.*, report in their research a TW of 1 second to calculate the

spectrogram of an EEG, in order to investigate the relationship between emotional states and brain activities, with an accuracy of 82.29 % in their model *et al.*[18]. On the other hand, Zheng *et al.* report a TW of 4 seconds without overlap in order to extract combined EEG features with eye tracking with the objective of carrying out emotional recognition tasks with an accuracy in their model of 71.77 %[19]. Zhuang *et al.* used a TW of 5s for feature extraction and emotion recognition based on empirical mode decomposition with an accuracy of 69 % in their model[20]. It is noted that different TW lengths have been used in EEG signal processing, but the appropriate length measurement for the detection of emotions is not established. Ouvan *et al.* carried out a study of the size of TW with the experiment-level batch normalization method in feature processing, in their findings they report that the best performing TW length was 2 seconds[21]. Healey *et al.* present a study of emotions (emotion recognition) with windows of 60, 180 and 300 seconds, but they do not report the performance of each TW[22]. Gioreski *et al.* report a laboratory study for stress detection with TW between 30 and 360 seconds, and in their findings indicate the window of 300 seconds presents better performance[23]. However, few studies have examined the effect of wavelength on the performance of classifier models during emotion recognition.

Among the most-used parameters for measuring a classifier model's performance are accuracy (ACC), defined as the fraction of predictions that the model classifies correctly, the precision or positive predictive value (PPV) that is the percentage of correct classifications of the model within the predictions of positive emotions, completeness or sensitivity (Recall) which is defined as the proportion of emotions that were correctly identified as having a condition, true positive, over the total number of emotions that are actually positive[24]. Other research employs the Area Under the Curve (AUC) of Receiver Operating Characteristic (ROC) in order to evaluate the performance of classifier algorithms[5][25]. Another parameter used is specificity, which measures the number of subjects who were correctly identified as having a negative emotion over the total number of subjects who actually present a negative emotion. However, for balanced studies that have on average almost the same amount of data for all categories (different emotions) the performance measures are ACC, AUC and Cohen's Kappa coefficient[8][10][12][26][27].

Another potential drawback in the study of emotions arises when variables are analyzed and reported at the group level rather than being used to evaluate the emotions in an individual. This is to say, the associations between physiological variables and emotions found through a group-level analysis may not generalize the case for evaluating emotions in an individual, as they cannot be sufficiently robust to reliably assess the emotional state at a given time for an individual[28].

Therefore, there is a gap in defining the size of the TW that will induce the best performance from the sorting algorithm for recognizing emotions. Furthermore, it has not been clearly established if the study of data must be made on an individual or on a group level. Accordingly, the aim of this research is to evaluate classification performance in detecting emotions via EEG signals at the group and individual levels by conducting a systematic comparison of TW values below 30 seconds. The performance metrics selected for this evaluation are ACC, AUC and Cohen's Kappa coefficient.

This article is divided in the following structure: first, an Introduction is provided that establishes the contextual framework of the research. The second section addresses the Materials and Methods, detailing the proposed approach to conduct the study. Next, in the third section, the Results and Discussions are presented, highlighting the observations and analysis derived from the research. Finally, the last section covers the Conclusions, summarizing the key findings and their implications.

MATERIALS AND METHODS

In order to carry out this study of emotion recognition, the data set is employed from[29]. For this data set, controlled experiments were designed to induce positive, negative, and neutral emotions from video clips. Participants ranged in age from 19 to 35 years (mean age 24.3). There were 8 women and 17 men.

To carry out the performance study of classification models with different TW the flow presented in Figure 1 is implemented.

The dataset contains the signals of 25 subjects from 14 electrodes of the EEG device. Every signal was broken down into alpha, beta, gamma and delta frequency bands. In this study, MATLAB 2017a libraries were used for the preprocessing of data, feature extraction and analysis of the classification algorithms. The workstation consists of a PC with an i7 processor, 8GB of RAM and 4GB of Nvidia GeForce.

Acquisition of EEG Data

The EEG sensing device used was the Emotiv EPOC+, which has 14 channels: AF3, F7, F3, FC5, T7, P7, O1, O2, P8, T8, FC6, F4, F8, AF4, plus two references: Common Mode Sense (CMS) and Driven Right Leg (DRL) in P3 and P4 (see Figure 2). This device has been widely used in different research related to emotions and the study of pathologies[30][31][32]. The data obtained directly from the file of every subject were the preprocessed theta (4-8 Hz), alpha (8-12 Hz), low beta (12-16 Hz), high beta (16-25 Hz) and gamma (25-45 Hz) band signals.

Data Segmentation

The main objective of this study was to evaluate and compare the performance of different classifiers for emotion recognition with different TW shorter than 30 seconds. In Table 1 the lengths of TW considered is presented as well as the number of blocks obtained. Therefore, the format of the

features in each trial was defined as (14x5x300); 14 representing the number of electrodes, 5 representing the frequency bands and 300 being the number of features extracted from the corresponding trial. In total 10 different TW lengths were examined in order to investigate the effect on the performance of classifier models in the study of emotions employing EEG sensors at a between-subject and within-subject level.

FIGURE 1. **The proposed framework for emotion classification.**
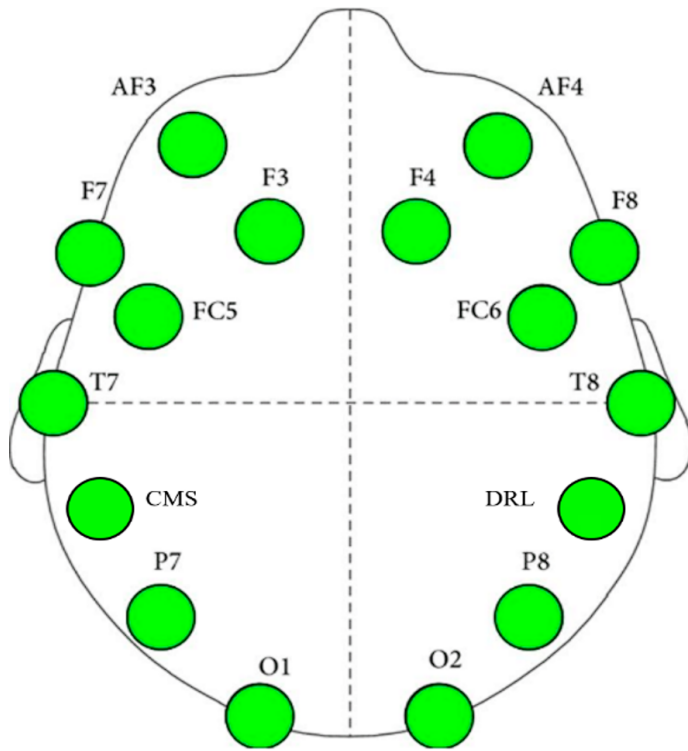
FIGURE 2. Emotiv device and electrode position system 10-20 modified.

Data Segmentation

The main objective of this study was to evaluate and compare the performance of different classifiers for emotion recognition with different TW shorter than 30 seconds. In Table 1 the lengths of TW considered is presented as well as the number of blocks obtained. Therefore, the format of the features in each trial was defined as (14x5x300); 14 representing the number of electrodes, 5 representing the frequency bands and 300 being the number of features extracted from the corresponding trial. In total 10 different TW lengths were examined in order to investigate the effect on the performance of classifier models in the study of emotions employing EEG sensors at a between-subject and within-subject level.
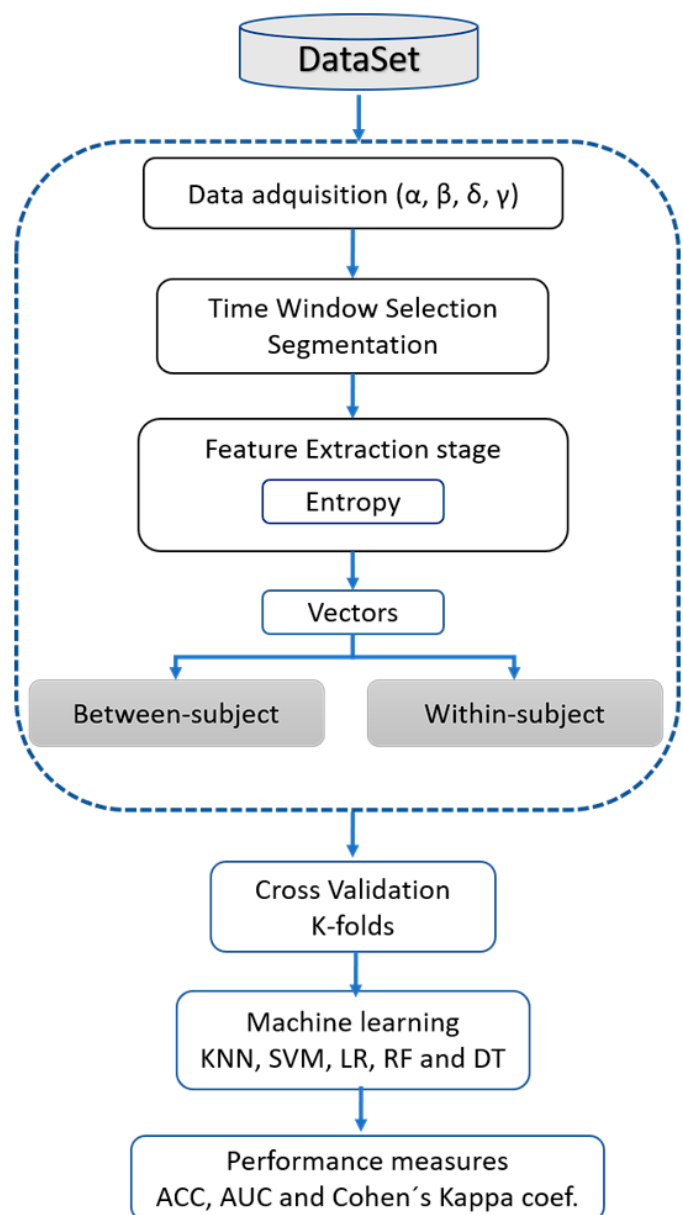
Feature Extraction

Since EEG signals are complex due to nonlinearity and randomness of time series data the calculation of time series entropy is incorporated[32][33]. The TW is modified

separately in each analysis and the entropy is calculated as a characteristic. Several entropy functions exist; however, the Log Energy function stands out for its excellent performance in the analysis of EEG signals. This is due to its remarkable sensitivity to energy changes, lower susceptibility to high-frequency noise and rapid amplitude variations, and its ability to characterize the complexity associated with the sub-bands of EEG signals[34][35]. This entropy function is based on the wavelet theory. There are different types of entropy, in this study we use Log energy. This type of entropy is based in wavelet theory where we assume a signal x=[x1 x2 x3 ... xn] and a probability distribution function P(x_i) where i is the index of the signal's elements, then the entropy is defined as[36]:

$$H(x) = \sum_{i=1}^{n} log(P(x_i)^2) \qquad (1)$$

under the convention that log(0)=0. For this study the five frequency bands of every electrode were processed and the log energy entropy characteristic was extracted.

TABLE 1. Details of the TW information in each trial. N corresponds to the number of features.

Parameters		Format of Features (14x5xN)
TW length (s)	TW Number	
1	300	(14x5x300)
2	150	(14x5x150)
3	100	(14x5x100)
4	75	(14x5x75)
5	60	(14x5x60)
10	30	(14x5x30)
15	20	(14x5x20)
20	15	(14x5x15)
30	10	(14x5x10)

The emotional state analysis is carried out on an individual and group level. On the group level the classification models with different TW are evaluated. For the performance evaluation of the models on an individual level, statistical tests are performed to determine whether there is a statistically significant difference in classification performance between

different window lengths and between different classification algorithms.

Classification Analysis

In order to carry out the training and evaluation of the models, the k-fold cross-validation technique is used with a value of k=5, where k is number of folders into which the data are separated. The classifier models compared in this study were K-Nearest Neighbors (KNN), Support Vector Machine (SVM), Logistic Regression (LR), Decision Tree (DT) and Random Forest (RF). The use of supervised classifiers was chosen because of their ability to achieve more accurate and specific learning, as they are trained to establish direct connections between known patterns and labels. Moreover, these classifiers are widely used in the study of emotions, according to the literature[10][37][38][39][40][41]. For the classification analysis the Machine Learning Toolbox 11.1 module from Matlab was used. The configuration parameters for every model are listed in Table 2.

TABLE 2. Parameter configuration in the Machine Learning Toolbox 11.1 module

Parameter Setting	
Classifier	Parameter
Fine KNN	n_neighbors=1, metric=euclidean, distance=equal
SVM	kernel function= linear, kernel scale=automatic, box constraint level=1 multiclass method= one-vs-one
LR	None
RF	None
DT	Maximum number of splits=4 Split criterion= Ginís diversity index

RESULTS AND DISCUSSION

Between-subject Study

The performance results for the models on the between-subject level are shown in Table 3. The ACC, AUC and Cohen's Kappa coefficient of each model are

presented as performance metrics. The results indicate that, regardless of the classifier model used, the TW that enhance their performances are between 2 and 15 seconds, with the 10s TWs standing out. The KNN model achieves the highest level of ACC, reaching 87.7 % in the 10 seconds TW, while the DT model exhibits the worst performance at 62.1 % in the 20 seconds TW. In terms of AUC, the best-performing model is RF with 0.93 for TW of 2 to 5 seconds, while the DT model shows the worst performance with 0.61 using a 20 seconds TW. Finally, the model with the best Cohen's Kappa coefficient is the KNN with 0.75 in the 10 seconds TW, and the DT model obtains the lowest result with 0.21 in the 30 seconds TW.

TABLE 3. Recognition results at the between-subject level (ACC, AUC and Cohen's Kappa coefficient)

ACC-ACC-Cohen´s Kappa coefficient				
TW	KNN	SVM	LR	RF	DT
1	83.3- 0.83- 0.66	64.1- 0.69- 0.28	63.7- 0.69- 0.27	83.6- 0.92- 0.67	63.4- 0.66- 0.27
2	83.3- 0.83- 0.67	65.1- 0.71- 0.30	64.7- 0.71- 0.30	84.3- **0.93**- 0.68	63.4- 0.66- 0.27
3	84.8- 0.85- 0.70	65.9- 0.72- 0.31	65.2- 0.72- 0.30	84.8- **0.93**- 0.69	62.8- 0.65- 0.28
4	85.4- 0.85- 0.71	66.1- 0.72- 0.32	65.7- 0.72- 0.31	84.4- 0.92- 0.69	63.6- 0.66- 0.28
5	86.5- 0.86- 0.72	66.9- **0.73**- 0.33	**66.5**- **0.73**- 0.31	**84.6**- **0.93**- **0.70**	**63.9**- 0.66- 0.25
10	**87.7**- **0.88**- **0.75**	**67.2**- **0.73**- 0.35	65.8- **0.73**- 0.33	83.4- 0.87- 0.65	63.8- **0.67**- **0.29**
15	86.7- 0.87- 0.74	66- 0.72- 0.30	64.1- 0.72- 0.31	80.6- 0.89- 0.63	62.9- **0.67**- 0.25
20	84.3- 0.84- 0.69	63.2- 0.7- 0.29	64- 0.7- 0.29	78.8- 0.85- 0.58	61.2- 0.62- 0.27
30	80- 0.8- 0.54	59- 0.64- 0.17	64.4- 0.69- 0.23	73.8- 0.62- 0.44	62- 0.73- 0.21

The results indicate that, in general terms, the performance of the models tends to decrease significantly for TW greater than 20 seconds.

ACC-ACC-Cohen´s Kappa coefficient					
TW	KNN	SVM	LR	RF	DT
1	82.4- 0.82- 0.65	83.48- 0.90- 0.67	81.3- 0.89- 0.66	86.95- 0.938 0.74	78.83 0.82 0.58
2	82.36- 0.82- 0.64	84.5- 0.91- 0.69	81.4- 0.88- 0.75	87.7- 0.94- 0.75	80.43- 0.83- 0.61
3	83.0- 0.83- 0.67	84.6- 0.91- 0.70	81.4- 0.84- 0.62	86.9- 0.83- 0.74	81.20- 0.814- 0.62
4	83.6- 0.83- 0.682	85.4- 0.91- 0.682	**82.3- 0.85- 0.610**	87.26- 0.938 0.745	80.99 0.832 0.620
5	85.6- 0.85- 0.69	**85 – 0.91- 0.707**	81.1- 0.85- 0.629	**87.24- 0.936 0.745**	**82.2- 0.832 0.636**
10	**85.8- 0.86- 0.715**	83.8- 0.91- 0.702	61.9- 0.62- 0.209	85.47 0.93 0.709	79.17- 0.8 0.583
15	86.1- 0.86- 0.704	81.42- 0.88- 0.654	67.6- 0.69- 0.35	82.99- 0.88- 0.659	74.14- 0.748- 0.483
20	82.7- 0.82- 0.664	79.97- 0.85- 0.611	71.4- 0.75- 0.458	81.37- 0.872- 0.627	70.89- 0.718- 0.423
30	79.5- 0.79- 0.642	72.7- 0.76- 0.395	67.7- 0.71- 0.368	72.39- 0.77- 0.447	67.88- 0.679- 0.358

Within-subject Results

Emotion recognition results within subject variability are shown in Table 4. It is observed that the KNN model achieves its best performances in temporal TW ranging from 5 to 15 seconds, with the optimal result obtained in the 10 seconds TW. On the other hand, the SVM model shows better performances in TW from 2 to 10 seconds, with the 5 seconds TW being the most outstanding in terms of ACC, AUC, and Cohen's Kappa coefficient. The LR model performs better in TW from 1 to 5 seconds, presenting its best result in the 4 seconds TW. For the RF model, its best performance is found in TW from 1 to 10 seconds, although the 4 seconds TW stands out the most. Finally, the DT model exhibits better performance in TW from 2 to 10 seconds, achieving the best result in the 5 seconds TW.

These results demonstrate that, regardless of the model chosen from these five, the TW that promote better performance in terms of ACC, AUC, and Cohen's Kappa coefficient are between 2 and 15 seconds. Moreover, the 10-second TW appears to be the most suitable for this type of configuration.

Accuracy				
	ACC		AUC	
TW length (s)	X^2	P-value	X^2	P-value
1	38.93	<0.001	78.17	<0.001
2	36.69	<0.001	68.70	<0.001
3	25.491	<0.001	66.80	<0.001
4	29.0	<0.001	67.01	<0.001
5	21.285	<0.001	55.83	<0.001
10	58.42	<0.001	77.66	<0.001
15	33.543	<0.001	31.717	<0.001
20	31.5	<0.001	42.65	<0.001
30	23.04	<0.001	19.87	<0.001

In order to identify possible significant disparities between ACC and AUC values associated with different threshold values (TW), Friedman nonparametric statistical tests were performed for repeated measurements of a single factor. This test was chosen based on its robustness to violations of normality and its lower sensitivity to outliers compared to parametric tests, such as ANOVA. The results of these tests are presented in Table 5, considering a significance level of 0.05 for the evaluation of statistical significance.

It is observed that in all TW, there are significant differences between the models. This indicates that not only does the length of the TW interfere with performance, but the chosen model also plays a role.

The Table 6 presents the results of the Friedman non-parametric hypothesis test for multiple TW sizes and Wilcoxon test for the TW pairs generated by the KNN model.

TABLE 6. **KNN model results between the ACC for different TWs.**

Results		
Null Hyphotesis	W	P-value
$\mu_5 = \mu_{10} = \mu_{15} = \mu_{20}$	5.795	0.122
$\mu_1 = \mu_2 = \mu_3 = \mu_4$	3.603	0.308
$\mu_5 \leq \mu_3$	300	<0.001
$\mu_{20} \leq \mu_{30}$	209	0.016

When comparing the equality of the mean of ACC in TW of 5, 10, 15, and 20 seconds, it is not possible to reject the null hypothesis. In the case of testing the equality hypothesis between TW of 1, 2, 3, and 4 seconds, it is also not possible to reject the difference. However, the TW of 5 seconds presents better performance than that of 3 seconds, and that of 20 seconds presents better performance than that of 30 seconds, as there is no significant difference between the TW of 5, 10, 15, and 20 seconds it can be considered that these are the ones that present better performance in terms of ACC for emotion detection.

TABLE 7. **Results of the SVM model between the ACC for different TW.**

Results		
Null Hyphotesis	W	P-value
$\mu_5 = \mu_{10} = \mu_{15} = \mu_{20}$	2.776	0.427
$\mu_1 = \mu_2 = \mu_3$	4.0607	0.131
$\mu_5 = \mu_4$	134.5	0.668
$\mu_{20} \leq \mu_{30}$	173	<0.001

The comparison of means of ACC of the SVM models for different TW is presented in Table 7. It is observed that the mean ACC of 20 seconds is higher than the 30 seconds, and that there is no significant statistical difference between the TW of 5, 10, 15 and 20 seconds

TABLE 8. **Results of the LR model between the ACC for different TW.**

Results		
Null Hyphotesis	W	P-value
$\mu_{15} = \mu_{10} = \mu_{30}$	4.151	0.126
$\mu_1 = \mu_2 = \mu_3 = \mu_4 = \mu_5$	8.190	0.052
$\mu_5 \leq \mu_{10}$	2.0	<0.001

Table 8 shows the results of the comparisons of the ACC means of the LR model between different TW. It is observed that TW less than or equal to 5 seconds present a better performance in emotion detection.
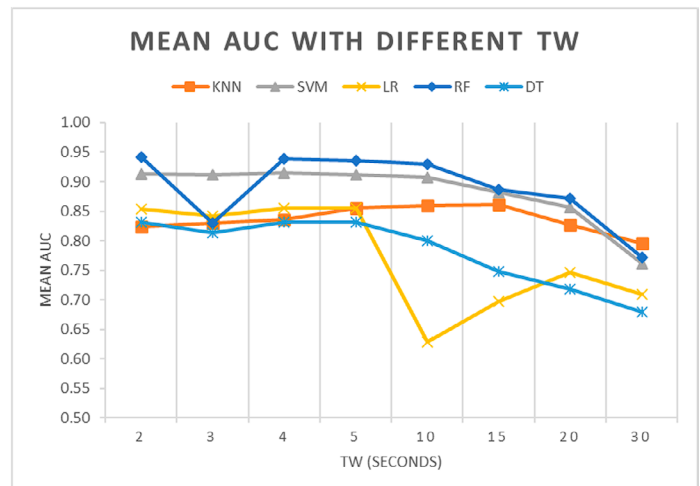

FIGURE 3. **Mean AUC performance with different TW and classification models.**

Figure 3 shows the performance results of the AUC averages of the five models. The best performing classifier is the SVM even though it was decreasing at 10, 15, 20 and 30 seconds TW. However, the RF model has the highest levels of AUC. The KNN model shows a growth in the AUC from TW 4 to 15 seconds. Finally, as the TW length

increases, the three classifiers tend to decrease their performance in terms of AUC.

CONCLUSIONS

In this study, the performance of three emotion classification models is evaluated, considering different TW sizes in data segmentation and two experimental setups. The first configuration involved the participation of 25 subjects in a between-subjects design. The results indicate that the window size significantly influences the performance of the classifiers. For example, the KNN model shows optimal results in TW sizes between 4 and 15 seconds, while the SVM, LR, RF and DT models excel in 4 to 10 seconds TW. In conclusion, for a between-subjects configuration, TWs of 4 to 15 seconds are recommended.

In the within-subject configuration the highest performance results are presented in TWs between 4 and 15 seconds for the KNN model with an ACC between 83.6 % and 86.12 %, respectively. However, for the SVM model the TW with the highest performance are between 2 and 10 seconds with an average AUC of 0.91. It is also observed that using the KNN model the performance results in terms of ACC and AUC do not differ significantly between the between-subject and within-subject configurations. However, for the LR and SVM models there is a significant difference when comparing the configurations: both models present better performance in the within-subjects configuration.

In general terms, it can be concluded that, in the study of emotions using EEG signals, regardless of the experimental setup or the classifier model employed, the TW that exhibit optimal performance in the classifiers, measured in terms of ACC, AUC and Cohen´s Kappa coefficient, are in the range of 2 to 15 seconds. Ultimately, it is observed that, by increasing the duration of the TW above 20 seconds, all three models experience a decrease in performance. Likewise, the use of TW equal to or longer than 20 seconds is not recommended for emotion recognition.

On the other hand, future research will focus on addressing the limitations identified in this study. This work includes: a) conducting additional analysis with a larger sample of participants, b) exploring a comparative analysis between supervised and unsupervised classification methods, and c) considering multiple features of entropy, such as Threshold Entropy and Shannon Entropy.

ACKNOWLEDGEMENTS

AUTHOR CONTRIBUTIONS

A. J. S. Conceptualization (literature review, problem definition, theoretical framework selection, planning of instruments and tools), data curation, formal analysis, investigation, methodology (data analysis planning), project administration, writing original draft, writing review and editing, visualization, and resources. V. A. G. P. Conceptualization (literature review, review of alternative methodologies), methodology (methodology adjustments and peer review), supervision, validation, writing review, and editing. O. A. D. R. Conceptualization (feasibility analysis and preliminary methodological design), project administration, supervision, validation, investigation, funding acquisition, writing review, and editing.

REFERENCES

[1]   P. Salovey and J. D. Mayer, "Emotional intelligence. Imagination, cognition and personality," Imagin. Cogn. Pers., vol. 9, no. 3, pp. 185-211, 1990, doi: **https://psycnet.apa.org/doi/10.2190/DUGG-P24E-52WK-6CDG**

[2]   R. W. Picard, "Affective Computing for HCI", in 8th International Conference on Human-Computer Interaction) on Human-Computer Interaction: Ergonomics and User Interfaces-Volume I - Volume I, 1999, pp. 829-833, doi: **https://dl.acm.org/doi/abs/10.5555/647943.742338**

[3]   R. Stock-Homburg, "Survey of emotions in human–robot interactions: Perspectives from robotic psychology on 20 years of research," Int. J. Soc. Robotics, vol. 14, no. 2, pp. 389-411, Mar. 2022, doi: **https://doi.org/10.1007/s12369-021-00778-6**

[4]   M. S. Young, K. A. Brookhuis, C. D. Wickens and P. A. Hancock, "State of science: Mental workload in ergonomics," Ergonomics, vol. 58, no. 1, Dec. 2014, doi: **https://doi.org/10.1080/00140139.2014.956151**

[5]   J. X. Chen, P. W. Zhang, Z. J. Mao, Y. F. Huang, D. M. Jiang, and Y. N. Zhang, "Accurate EEG-Based Emotion Recognition on Combined Features Using Deep Convolutional Neural Networks," IEEE Access, vol. 7, pp. 44317-44328, Jun. 2019, doi: **https://doi.org/10.1109/ACCESS.2019.2908285**

[6]   C. Qing, R. Qiao, X. Xu, and Y. Cheng, "Interpretable Emotion Recognition Using EEG Signals," IEEE Access, vol. 7, pp. 94160-94170, Jul. 2019, doi: **https://doi.org/10.1109/ACCESS.2019.2928691**

[7]   M. M. Duville, Y. Pérez, R. Hugues-Gudiño, N. E. Naal-Ruiz, L. M. Alonso-Valerdi, D. I. Ibarra-Zarate, "Systematic Review: Emotion Recognition Based on Electrophysiological Patterns for Emotion Regulation Detection," Appl. Sci., vol. 13, no. 12, art. no. 6896, Feb. 2023, doi: **https://doi.org/10.3390/app13126896**

[8]   C. Pan, C. Shi, H. Mu, J. Li, and X. Gao, "EEG-Based Emotion Recognition Using Logistic Regression with Gaussian Kernel and Laplacian Prior and Investigation of Critical Frequency Bands," Appl. Sci., vol. 9, no. 2, art. no. 1619, Apr. 2019, doi: **https://doi.org/10.3390/app10051619**

[9]   D. Wu, "Online and Offline Domain Adaptation for Reducing BCI Calibration Effort," IEEE Trans. Hum.-Mach. Syst., vol. 47, no. 4, pp. 550-563, Aug. 2017, doi: **https://doi.org/10.1109/THMS.2016.2608931**

[10]   G. Li, D. Ouyang, Y. Yuan, W. Li, Z. Guo, X. Qu, P. Green, "An EEG Data Processing Approach for Emotion Recognition," IEEE Sens. J., vol. 22, no. 11, pp. 10751-10763, Jun. 2022, doi: **https://doi.org/10.1109/JSEN.2022.3168572**

[11]   P. Schmidt, A. Reiss, R. Dürichen, and K. Van Laerhoven, "Wearable-Based Affect Recognition—A Review," Sensors, vol. 19, no. 19, art. no. 4079, Sep. 2019, doi: **https://doi.org/10.3390/s19194079**

[12]   J. J. Esqueda Elizondo, L. Jiménez Beristáin, A. Serrano Trujillo, M. Zavala Arce, et al., "Using Machine Learning Algorithms on Electroencephalographic Signals to Assess Engineering Students' Focus While Solving Math Exercises," Rev. Mex. Ing. Biom., vol. 44, no. 4, pp. 23-37, Nov. 2023, doi: **https://doi.org/10.17488/RMIB.44.4.2**

[13]   F. J. Ramírez-Arias, E. E. García-Guerrero, E. Tlelo-Cuautle, et al., "Evaluation of machine learning algorithms for classification of EEG signals," Technologies, vol. 10, no 4, art. no. 79, Jun. 2022, doi: **https://doi.org/10.3390/technologies10040079**

[14]   M. Zheng and Y. Lin, "A deep transfer learning network with two classifiers based on sample selection for motor imagery brain-computer interface," Biomed. Signal Process. Control, vol. 89, art. no. 105786, Mar. 2024, doi: **https://doi.org/10.1016/j.bspc.2023.105786**

[15]   J. J. Esqueda-Elizondo, R. Juárez-Ramírez, O. R. López-Bonilla, E. E. García-Guerrero, et al., "Attention measurement of an autism spectrum disorder user using EEG signals: A case study," Math. Comput. Appl., vol. 27, no. 2, art. no. 21, Mar. 2022, doi: **https://doi.org/10.3390/mca27020021**

[16]   Y. Qin, B. Li, W. Wang, X. Shi, H. Wang, and X. Wang, "ETCNet: An EEG-based motor imagery classification model combining efficient channel attention and temporal convolutional network," Brain Res., vol. 1823, art. no. 148673, Nov. 2023, doi: **https://doi.org/10.1016/j.brainres.2023.148673**

[17]   J. Li, S. Qiu, C. Du, Y. Wang, and H. He, "Domain Adaptation for EEG Emotion Recognition Based on Latent Representation Similarity," IEEE Trans, Cogn. Dev. Syst., vol. 12, no. 2, pp. 344-353, Jun. 2020, doi: **https://doi.org/10.1109/TCDS.2019.2949306**

[18]   Y. -P. Lin, C.-H. Wang, T.P. Jung, T.-L. Wu, S.-K. Jeng, J.-R. Duann, J.-H. Chen, "EEG-Based Emotion Recognition in Music Listening", IEEE Trans. Biomed. Eng., vol. 57, no. 7, pp. 1798-1806 Jul. 2010, doi: **https://doi.org/10.1109/tbme.2010.2048568**

[19]   W.-L. Zheng, B.-N. Dong, and B.-L. Lu, "Multimodal emotion recognition using EEG and eye tracking data," in 2014 36th Annual International Conference of the IEEE Engineering in Medicine and Biology Society, Chicago, IL, USA, 2014, pp. 5040-5043, doi: **https://doi.org/10.1109/EMBC.2014.6944757**

[20]   N. Zhuang, Y. Zeng, L. Tong, C. Zhang, H. Zhang, and B. Yan, "Emotion recognition from EEG signals using multidimensional information in EMD domain," Biomed Res. Int., vol. 2017, art. no. 8317357, 2017, doi: **https://doi.org/10.1155/2017/8317357**

[21]   D. Ouyang, Y. Yuan, G. Li, and Z. Guo, "The Effect of Time Window Length on EEG-Based Emotion Recognition," Sensors, vol. 22, no. 13, art. no. 4939, Jun. 2022, doi: **https://doi.org/10.3390/s22134939**

[22]   J. Healey, L. Nachman, S. Subramanian, J. Shahabdeen, and M. Morris, "Out of the Lab and into the Fray: Towards Modeling Emotion in Everyday Life," in 8th International Conference, Pervasive 2010, P. Floréen, A. Krüger, M. Spasojevic, Eds., Helsinki, Finland 2010, doi: **https://doi.org/10.1007/978-3-642-12654-3_10**

[23]   M. Gjoreski, M. Luštrek, M. Gams, and H. Gjoreski, "Monitoring stress with a wrist device using context," J. Biomed. Inform., vol. 73, pp. 159-170, Sep. 2017, doi: **https://doi.org/10.1016/j.jbi.2017.08.006**

[24]   R. Alhalaseh and S. Alasasfeh, "Machine-Learning-Based Emotion Recognition System Using EEG Signals," Computers, vol 9, no 4, art. no. 95, 2020, doi: **https://doi.org/10.3390/computers9040095**

[25]   K. S. Kamble and J. Sengupta, "Ensemble Machine Learning-Based Affective Computing for Emotion Recognition Using Dual-Decomposed EEG Signals," IEEE Sens. J., vol. 22, no. 3, pp. 2496-2507, Feb. 2022, doi: **https://doi.org/10.1109/JSEN.2021.3135953**

[26]   X. Li, D. Song, P. Zhang, Y. Zhang, Y. Hou, and B. Hu, "Exploring EEG Features in Cross-Subject Emotion Recognition," Front. Neurosci., vol 12, art. no. 162, Mar. 2018, doi: **https://doi.org/10.3389/fnins.2018.00162**

[27]   B. Tripathi and R. K. Sharma, "EEG-Based Emotion Classification in Financial Trading Using Deep Learning: Effects of Risk Control Measures," Sensors, vol. 23, no. 7, art. no. 3474, Mar. 2023, doi: **https://doi.org/10.3390/s23073474**

[28]   M. D. Rinderknecht, O. Lambercy, and R. Gassert, "Enhancing simulations with intra-subject variability for improved psychophysical assessments," PLoS One, vol. 13, no. 12, art. no. e0209839, Dec. 2018, doi: **https://doi.org/10.1371/journal.pone.0209839**

[29]   A. Jarillo-Silva, V. A. Gomez-Perez, E. A Escotto-Cordova, and O. A. Domínguez-Ramírez, "Emotion Classification form EEG signals using wearable sensors:pilot test," ECORFAN Journal-Bolivia, vol. 7, no. 12, pp. 1-9, Sep. 2020. [Online]. Available: **https://www.ecorfan.org/bolivia/journal/vol7num12/ECORFAN_Journal_Bolivia_V7_N12.pdf**

[30]   K. Kotowski, K. Stapo, J. Leski, and M. Kotas, "Validation of Emotiv EPOC+ for extracting ERP correlates of emotional face processing," Biocybern. Biomed. Eng., vol. 38, no 4, pp. 773-781, 2018, doi: **https://doi.org/10.1016/j.bbe.2018.06.006**

[31]   F. Mulla, E. Eya, E. Ibrahim, A. Alhaddad, R. Qahwaji, and R. Abd-Alhameed, "Neurological assessment of music therapy on the brain using Emotiv Epoc," in 2017 Internet Technologies and Applications (ITA), Wrexham, UK, 2017, pp. 259-263, doi: **https://doi.org/10.1109/ITECHA.2017.8101950**

[32]   N. Browarska, A. Kawala-Sterniuk, J. Zygarlicki, M. Podpora, M. Pelc, R. Martinek, and E. J. Gorzelańczyk, "Comparison of smoothing filters influence on quality of data recorded with the emotiv epoc flex brain–computer interface headset during audio stimulation," Brain Sci., vol. 11, no. 1, art. no. 98, Jan. 2021, doi: **https://doi.org/10.3390/brainsci11010098**

[33]   P. R. Patel and R. N. Annavarapu, "EEG-based human emotion recognition using entropy as a feature extraction measure," Brain Inf., vol 8, art. no. 20, Oct. 2021, doi: **https://doi.org/10.1186/s40708-021-00141-5**

[34]   P. Krishnan and S. Yaacob, "Drowsiness detection using band power and log energy entropy features based on EEG signals," Int. J. Innov. Technol. Explor. Eng, vol 8, no. 10, pp. 830-836, Aug. 2019, doi: **https://doi.org/10.35940/ijitee.j9025.0881019**

[35]   A. B Das and M. I. H. Bhuiyan, "Discrimination and classification of focal and non-focal EEG signals using entropy-based features in the EMD-DWT domain," Biomed. Signal Process. Control, vol. 29, pp. 11-21, Aug. 2016, doi: **https://doi.org/10.1016/j.bspc.2016.05.004**

[36]   R. Djemal, K. AlSharabi, S. Ibrahim, and A. Alsuwailem, "EEG-Based Computer Aided Diagnosis of Autism Spectrum Disorder Using Wavelet, Entropy, and ANN," BioMed Res. Int., vol. 2017, no 1, art. no. 9816591, 2017, doi: **https://doi.org/10.1155/2017/9816591**

[37]   S. Koelstra, C. Muhl, M. Soleymani, J.-S. Lee, et al., "DEAP: A Database for Emotion Analysis; Using Physiological Signals," IEEE Trans. Affect. Comput., vol. 3, no. 1, pp. 18-31, 2012, doi: **https://doi.org/10.1109/T-AFFC.2011.15**

[38]   A. Bablani, D. Reddy Edla, and S. Dodia, "Classification of EEG Data using k-Nearest Neighbor approach for Concealed Information Test," Procedia Comput. Sci., vol. 143, pp. 242-249, 2018, doi: **https://doi.org/10.1016/j.procs.2018.10.392**

[39]   D.-W. Chen, R. Miao, W.-Q. Yang, Y. Liang, H.-H. Chen, L. Huang, C.-J. Deng, N. Han, "A feature extraction method based on differential entropy and linear discriminant analysis for emotion recognition," Sensors, vol. 19, no. 7, art. no. 1631, Oct. 2019, doi: **https://doi.org/10.3390/s19071631**

[40]   S. Babeetha and S. S. Sridhar, "EEG Signal Feature Extraction Using Principal Component Analysis and Power Spectral Entropy for Multiclass Emotion Prediction," in Fourth International Conference on Image Processing and Capsule Networks, Bangkok, Thailand, 2023, pp. 435-448, doi: **https://doi.org/10.1007/978-981-99-7093-3_29**

[41]   V. Doma and M. Pirouz, "A comparative analysis of machine learning methods for emotion recognition using EEG and peripheral physiological signals," J. Big Data, vol. 7, art. no. 18, Mar. 2020, doi: **https://doi.org/10.1186/s40537-020-00289-7**